UNIVERSIDADE DE SÃO PAULO

FACULDADE DE MEDICINA DE RIBEIRÃO PRETO

THAMYRIS SANTOS SILVA

Estresse na adolescência induz alterações comportamentais e desbalanço excitatório/inibitório no hipocampo ventral: envolvimento da desregulação redox e disfunção mitocondrial

Ribeirão Preto

2023

THAMYRIS SANTOS SILVA

Estresse na adolescência induz alterações comportamentais e desbalanço excitatório/inibitório no hipocampo ventral: envolvimento da desregulação redox e disfunção mitocondrial

Versão Original

Tese apresentada ao Programa de Pós-Graduação em Ciências Biológicas da Faculdade de Medicina de Ribeirão Preto da Universidade de São Paulo, como requisito parcial para a obtenção do grau de Doutor em Ciências.

Área de concentração: Farmacologia

Orientador: Prof. Dr. Felipe Villela Gomes

Ribeirão Preto

2023

Nome: SILVA, Thamyris Santos

Título: Estresse na adolescência induz alterações comportamentais e desbalanço excitatório/inibitório no hipocampo ventral: envolvimento da desregulação redox e disfunção mitocondrial

Tese apresentada à Faculdade de Medicina de Ribeirão Preto da Universidade de São Paulo para obtenção do título de Doutor em Ciências.

Aprovado em: _____ / _____ / _____

Banca examinadora

Prof. Dr. _____

Instituição: _____

Julgamento: _____

Profa. Dra. _____

Instituição: _____

Julgamento: _____

Prof. Dr. _____

Instituição: _____

Julgamento: _____

ADOLESCENT STRESS INDUCES BEHAVIORAL CHANGES AND HIPPOCAMPAL EXCITATORY/INHIBITORY IMBALANCE:

involvement of redox dysregulation and mitochondrial dysfunction

Thamyris Santos Silva

ACKNOWLEDGEMENTS

This thesis would never have succeeded without the help of a great many people whom I would like to thank.

First, I would like to thank my direct supervisor, Professor **Felipe Gomes**. This Ph.D. has been a great adventure, with many ups and, of course, many downs, and I feel very blessed to have a patient supervisor by my side. You always remained curious about science and prompted me to answer our scientific questions, which definitely kept me motivated throughout these 4 years. I really appreciate how much effort you have put into my personal development. You always stimulated us to present at conferences and to go abroad during our Ph.D., always helping it work. Despite some difficulties with COVID pandemic, I'm proud of what we have accomplished and developed. It was a great experience to work on this project and to help you to set up the Gomes lab. Thank you, Felipe, for being such a positive and stimulating supervisor. I'm sure we will keep in touch and see each other in the future!

I would like to thank the people that made my time at Ribeirão Preto unforgettable: **Dri, Rayanne, Débora Uber, Laura Gomez, Giu Bertozi, Ícaro, Isadora and Nicole.** It was such a blessing to go through this together with you. I also would like to thank my undergrad students: **Lara and Beatriz.** Working with each of you was a pleasure, and I wish you all the best for your future careers! Also, I wish the **Gomes Lab (current and former members)** all the best with your projects and hope you will enjoy working here as much as I did! I'm super thankful to have been part of this lab and will miss you all!

Dear Professor **Carmen Sandi,** I'm very grateful I got the opportunity to experience such innovative and exciting science. It really helped me to develop further as a scientist. Thank you for opening the doors of your lab and supporting diversity in Neuroscience. You are an amazing scientist and an inspiring woman, with whom I would like to continue learning and getting experiences. I also want to thank you for your advice and support in my Ph.D. You always knew to ask the right questions, gave a broader perspective, and as my PhD progressed, your input was very valuable for completing my scientific education. Finally, I also would like to thank you for the time

you took to talk about the continuation after my Ph.D. I hope to see you soon in Switzerland!

Being a visiting Ph.D. student in **Sandi's Lab** was a true milestone in my life. I have so much enjoyed all the days with you guys, **Giulia, Laurine, Cami, Jojo, Dogu, Silvie, Nico, Emilia, Cate, Elias, Apoline, Haissa, Loredana, Arthur, Eva, Sri, Olívia, Simone, Silvia and others.** We had a lot of great coffees, lunches, happy hours, swimming in the lake, climbing, and skiing together! Thank you all for making me feel so welcome and were always willing to help! In particular, **Doğukan,** thank you very much for contributing to my thesis and teaching me bioinformatic analyses. It was a pleasure to be part of the team, and it was great learning about brain metabolism and more during my immersion in Sandi's Lab!

This thesis would never have been here without the help of many collaborations: Professor **Francisco Guimãraes and members from his lab**, thank you for welcoming me to your lab and providing technical and practical important contributions to this thesis and our collaborations. Professor **Luciane Alberici and members from her lab,** thank you for your input on the mitochondrial aspects of this thesis.

Dear **committee**, I highly appreciate your time reading and questioning my work. I am looking forward to the discussion during my defense.

I will be eternally grateful to my parents, **Silvia and Celson,** who worked hard to offer me the opportunity to study. For sure, knowledge is the best inheritance I could ever receive from you. Without your help finishing this thesis on time and simultaneously moving out of Brazil and emigrating to Switzerland would not have succeeded. Dear **Dad**, your interest in knowledge is never diluted, which kept me going on my scientific path! Dear **Mom**, your caring was so nice in the completion phase! I could not wish for a more loving and caring parent. Thank you very, very much for everything!

Finally, I would like to thank my beloved husband, **Caio Lopes**. Thank you for always being by my side, being my confidant, advisor, and best friend. Thank you for not allowing me to give up or question my abilities. Also, for helping me to be a better and more patient person. I thank you for every moment that we shared on this path. Thank you so much for making this dream come true together with me.

To all those who, in some way, were part of this achievement, my gratitude is expressed here.

"I cannot, therefore, consider the organism without its environment."

-Peter D. Mitchell, winner of the 1978 Nobel Prize for Chemistry for the Chemiosmotic theory

ABSTRACT

SILVA. T. S. **Adolescent stress induces behavioral changes and hippocampal excitatory/inhibitory imbalance: involvement of redox dysregulation and mitochondrial dysfunction.** 2023. Thesis (Graduate Program in Biological Science, Pharmacology) – Ribeirão Preto Medical School, University of São Paulo, Ribeirão Preto.

The developing adolescent brain is highly susceptible to social experiences and environmental insults, influencing how personality traits emerge. We previously found that adolescent stress leads to long-lasting behavioral changes and excitatory/inhibitory (E/I) balance dysregulation in the ventral hippocampus (vHip) associated with neurodevelopmental disorders, such as schizophrenia and bipolar disorder. The neurobiological mechanisms of psychiatric disorders have been linked with oxidative damage and reduced antioxidant capacity in the brain. However, the impact of severe stressors during adolescence, a critical neurodevelopmental period, on mitochondrial function, redox balance, and their functional consequences are not completely understood. We hypothesized that mitochondrial respiratory function and redox homeostasis in the vHip are affected by adolescent stress, leading to behavioral and electrophysiological changes associated with neuropsychiatric disorders. First, we performed a behavioral characterization during late adolescence (postnatal day, PND 47 – 50), including naïve animals and animals exposed to stress from PND 31 until 40 (10 days of footshock and 3 restraint sessions) by assessing sociability (social interaction test) and cognition function (novel-object recognition test). Then, we uncovered changes in E/I balance by analyzing the activity of glutamate pyramidal neurons, and the number of parvalbumin (PV)-containing GABAergic interneurons and their possible association with oxidative stress. To address the dynamic impact of stress on mitochondrial redox homeostasis, we performed high-resolution respirometry, DHE staining, MitoSox™ and AmplexRed® assays one (PND 41) and ten days (PND 51) after stress protocol. Also, we evaluated glutathione (GSH) and glutathione disulfide (GSSG) levels at PND 51. Finally, we assess the genome-wide transcriptomic signature of vHip of stressed animals by performing a bulk RNA-sequencing following the behavioral tests. One week after stress, adolescent-stressed animals exhibited: (1) loss of sociability and cognitive impairment; (2) enhanced vHip pyramidal neuron activity; and (3) reduction in the number of PV-positive cells and their associated perineuronal nets. These changes were associated with an increased marker of oxidative stress in the vHip, in which was co-localized with PV interneurons. By performing high-resolution respirometry analysis, we found that stress impacted mitochondrial uncoupled efficiency (PND 41) and the phosphorylation capacity (PND 51). In addition, stressed animals displayed long-lasting redox dysregulation in the vHip, as revealed by molecular analysis. GSSG levels were increased in the vHip and serum of stressed animals and negatively correlated with social and cognitive

performance, indicating that GSH was previously oxidized by ROS in stress conditions, and may affect behavioral phenotype. In another cohort of animals, we identified three cluster subgroups by performing principal component analysis of behavioral assessment: naïve higher-behavioral z-score (HBZ), naïve lower-behavioral z-score (LBZ), and stressed animals. Genes encoding subunits of oxidative phosphorylation complexes were significantly down-regulated in both naïve LBZ (Cox7c) and stressed animals (Coa5), while the *Txnip* gene that encoded thioredoxin-interacting protein were up-regulated in stressed animals and negatively correlated with behavioral performance. Our results identify mitochondrial genes associated with distinct adolescent behavioral phenotypes and highlight the negative impact of adolescent stress on vHip mitochondrial respiratory function and redox regulation, in which are partially associated with E/I imbalance and behavioral abnormalities.

RESUMO

SILVA. T.S. **Estresse na adolescência induz alterações comportamentais e desbalanço excitatório/inibitório no hipocampo ventral: envolvimento da desregulação redox e disfunção mitocondrial.** 2023. Tese (Doutorado em Ciências Biológicas, Farmacologia) – Faculdade de Medicina de Ribeirão Preto, Universidade de São Paulo, Ribeirão Preto.

O cérebro adolescente em desenvolvimento é altamente suscetível a experiências sociais e insultos ambientais, influenciando o surgimento de traços de personalidade. Descobrimos anteriormente que o estresse na adolescência leva a mudanças comportamentais duradouras e à desregulação do equilíbrio excitatório/inibitório (E/I) do hipocampo ventral (vHip) associado a distúrbios do neurodesenvolvimento, como esquizofrenia e transtorno bipolar. Os mecanismos neurobiológicos dos transtornos psiquiátricos têm sido associados a danos oxidativos e à capacidade antioxidante reduzida no cérebro. Entretanto, o impacto de estressores graves durante a adolescência, um período crítico de plasticidade, sobre a função mitocondrial, o equilíbrio redox e suas consequências funcionais não são completamente compreendidos. Nossa hipótese é que a função respiratória mitocondrial e a homeostase redox no vHip são afetadas pelo estresse na adolescência, levando a alterações comportamentais e eletrofisiológicas associadas a distúrbios neuropsiquiátricos. Primeiro, realizamos uma caracterização comportamental durante o final da adolescência (dia pós-natal, DPN 47 - 50), incluindo animais ingênuos e animais expostos ao estresse do DPN 31 até o 40 (10 dias de choque nas patas e 3 sessões de contenção), avaliando a sociabilidade (teste de interação social) e a função cognitiva (teste de reconhecimento de novos objetos). Em seguida, descobrimos alterações no equilíbrio E/I analisando a atividade dos neurônios piramidais de glutamato e o número de interneurônios GABAérgicos contendo parvalbumina (PV) e sua possível associação com o estresse oxidativo. Para abordar o impacto dinâmico do estresse na homeostase redox mitocondrial, realizamos respirometria de alta resolução, coloração com DHE, ensaios MitoSox™ e AmplexRed® um (DPN 41) e dez dias (DPN 51) após o protocolo de estresse. Além disso, avaliamos os níveis de glutationa (GSH) e dissulfeto de glutationa (GSSG) no PND 51. Por fim, avaliamos a assinatura transcriptômica de todo o genoma do vHip de animais estressados, realizando um sequenciamento de RNA em massa após os testes comportamentais. Uma semana após o estresse, os animais adolescentes estressados apresentaram: (1) perda de sociabilidade e prejuízo cognitivo; (2) aumento da atividade dos neurônios piramidais do vHip; e (3) redução do número de células positivas para PV e suas redes perineuronais associadas. Essas alterações foram associadas a um aumento do marcador de estresse oxidativo no vHip, que foi colocalizado com interneurônios PV. Ao realizar a análise de respirometria de alta resolução, descobrimos que o estresse afetou a eficiência desacoplada das mitocôndrias (DPN 41) e a capacidade de fosforilação (DPN 51). Além disso, os

animais estressados apresentaram uma desregulação redox de longa duração no vHip, conforme revelado pela análise molecular. Os níveis de GSSG foram aumentados no vHip e no soro de animais estressados e correlacionados negativamente com o desempenho social e cognitivo, indicando que a GSH foi previamente oxidada por ROS em condições de estresse e pode afetar o fenótipo comportamental. Em outra coorte de animais, identificamos três subgrupos de agrupamento por meio da análise de componentes principais da avaliação comportamental: naïve alto z-score comportamental, naïve baixo z-score comportamental e animais estressados. Os genes que codificam subunidades dos complexos de fosforilação oxidativa foram significativamente regulados para baixo tanto nos animais naïve BBZ (Cox7c) quanto nos estressados (Coa5), enquanto o gene Txnip, que codifica a proteína que interage com a tiorredoxina, foi regulado para cima nos animais estressados e correlacionado negativamente com o desempenho comportamental. Nossos resultados identificam genes mitocondriais associados a fenótipos comportamentais distintos de adolescentes e destacam o impacto negativo do estresse na adolescência sobre a função respiratória mitocondrial vHip e a regulação redox, que estão parcialmente associadas ao desequilíbrio E/I e às anormalidades comportamentais.

LIST OF FIGURES

LIST OF TABLES

TABLE OF CONTENTS

1. INTRODUCTION

1.1. Adolescence as a critical period for neurodevelopment: focus on the ventral hippocampus

Adolescence is a temporary period of learning, social adaptation, and dynamic neurobiological maturation, which begins with puberty and ends in adulthood (SPEAR, 2000). In humans, adolescence typically starts by age 10 in girls and by age 12 in boys (DAHL; ALLEN; WILBRECHT, 2018). It can be divided into three stages: early adolescence (10 to 13 years), middle adolescence (14 to 17 years), and late adolescence/young adulthood (18 to 21 years and beyond) (BACKES; BONNIE, 2019). At the beginning of puberty, a cascade of transformational changes is associated with physical growth, metabolic demands, sleep and circadian regulation, and sexual maturation (SISK; FOSTER, 2004). During middle adolescence, a peak of social interactions with peers is observed, promoting risk-taking behaviors and their emancipation from parents (CRONE; DAHL, 2012). The endpoint of adolescence is not well defined, given that adulthood cannot be described only by physical growth but also in terms of cognitive and social processes (COHEN et al., 2016). Therefore, key changes during adolescent development are crucial for adequate sociability and cognitive performance in adulthood.

Social experiences and neurobiological factors interact to shape brain development and permanently change personality traits (LARSEN; LUNA, 2018). Adolescence is a critical period of important experience-dependent social behavior plasticity, such as play behavior and dominance hierarchies (BICKS et al., 2021; BIJLSMA et al., 2022). Beyond the effects on brain development, social experiences impact behavioral outcomes and predict vulnerability and resilience to stress, suggesting individual neurodevelopment trajectories (LARRIEU et al., 2017). Therefore, the individual's experiences can shape neurobiology, especially during sensitive periods of plasticity, when the organism adapts to its surroundings and changes the brain according to the environment's demands. Nevertheless, individual phenotypic differences in late adolescence linked to multiple behavioral domains, such as sociability and cognition, are yet to be fully understood.

The first few years of life represent a sensitive period for growth, early learning, and brain maturation (SHONKOFF et al., 2012). Recent evidence suggests adolescence is a second period of critical plasticity, characterized by rapid growth and learning associated with distinct neuro-maturational processes (DAHL; ALLEN; WILBRECHT, 2018). Studies in humans have shown brain reorganization during adolescence, including patterns of gray matter thinning, white matter integrity, and synapse proliferation (GOLDENBERG et al., 2017). Longitudinal studies have revealed that prefrontal regions increase with age throughout childhood and adolescence, while the amygdala and hippocampus show an increase in size at the onset of puberty, after which stabilize in adolescence and adulthood (MILLS et al., 2016; ØSTBY et al., 2009). In addition, functional connectivity is strengthened during early adolescence between prefrontal regions and limbic circuits, while late adolescence is linked to high-order cognitive processes. The nonlinear maturation processes of subcortical and prefrontal brain areas lead to an imbalance of neural networks in adolescence, which might explain, for example, the typical risk-taking behavior (KONRAD; FIRK; UHLHAAS, 2013). During emotional situations, the relatively early maturation of subcortical brain areas over gains the delayed maturation of prefrontal control, which increases the probability of emotions affecting behavior more strongly than rational decision-making processes in adolescents (DEMIDENKO et al., 2020).

The anterior hippocampus, a region analogous to the ventral hippocampus (vHip) in rodents, is intimately tied to emotion, reward-seeking behaviors, and overall cognitive processes, such as attention, perception, and social cognition (FANSELOW; DONG, 2010). vHip also undergoes major structural and functional remodeling during adolescence (LYNCH et al., 2019). The ventral subiculum (vSub) is the most inferior component of the vHip formation. It lies between the entorhinal cortex and the CA1 subfield of the vHip (GERGUES et al., 2020). At the cellular level, the principal vSub layer comprises a large glutamatergic pyramidal neuron population and subtypes of GABAergic interneurons. The pyramidal neurons in the vSub act as a primary output, conveying hippocampal signals to diverse downstream regions, such as the nucleus accumbens, lateral hypothalamus, entorhinal cortex, and amygdala (CEMBROWSKI et al., 2018). Among the GABAergic interneuron subtypes present in vSub, fast-spiking GABAergic interneurons containing the calcium (Ca^{2+}) binding protein parvalbumin (PV) play key fundamental functions by maintaining a regional excitatory-inhibitory (E/I)

balance (PELKEY et al., 2017). PV interneurons are dynamically regulated to support their sustained fast-spiking activity. For instance, PV protein has been described as a "Ca^{2+} buffer" since it absorbs excess Ca^{2+} levels during sustained activity. In addition, it accelerates the decay of initial Ca^{2+} transients in axon boutons and dendrites during a burst firing (APONTE; BISCHOFBERGER; JONAS, 2008). Complementing their Ca^{2+} buffering capabilities, PV interneurons exhibit hallmark properties that indicate high energy demand to keep their fast-spiking activity. Their soma, dendrites, and presynaptic terminals are enriched with mitochondria much more than pyramidal cells and other interneurons (GULYÁS et al., 2006). These distinct characteristics support their main function, i.e., coordinate pyramidal neuron activity.

During the transition from adolescence to adulthood, PV interneurons undergo upregulation, evidencing the protracted development of the GABAergic neurotransmission (CABALLERO; DIAH; TSENG, 2013). The maturation of PV interneurons and their associated perineuronal nets (PNNs) defines a critical period of neuronal plasticity after postnatal development (HENSCH, 2005). PNNs are specialized lattice-like extracellular matrix structures surrounding the soma, proximal dendrites, and initial axon segments of neurons (GALTREY; FAWCETT, 2007). Through development into adulthood, the proportion of PV interneurons surrounded by PNNs, and the intensity of PNNs increase as the brain reaches maturity. The formation and condensation of PNNs are key components that coincide with the closure of critical periods of postnatal development (REICHELT et al., 2019), since PNNs regulate plasticity by stabilizing and synchronizing synaptic networks to end the adolescent neuroplastic phase (BALMER, 2016). In addition, PNNs protect PV interneurons against oxidative stress and neurotoxins (CABUNGCAL et al., 2013b).

Identifying the neurobiological changes that underpin adolescent development and their associations with behavioral performance is crucial to understand environmental influences during this sensitive period of plasticity. Indeed, structural and functional changes are evident in adolescent brain circuitries related to cognitive, social, and emotional processes, particularly in brain regions that support them, such as the vHip.

1.2. Stress during adolescence and the emergence of neuropsychiatric disorders

During childhood and adolescence, several physiological processes and social dynamics changes occur as the individuals learn to adapt to their environment. Notably, these alterations also make the developing brain highly vulnerable to exposure to environmental factors. Indeed, adolescence has been recognized as a period of increased vulnerability to adverse socio-environmental insults, such as trauma, psychosocial abuses, and maltreatment, contributing to psychiatric disorders (GOMES; RINCÓN-CORTÉS; GRACE, 2016; GOMES; ZHU; GRACE, 2019b). An onset peak for many common mental disorders, including schizophrenia, substance abuse, and mood disorders, has been observed during adolescence (KESSLER et al., 2007). For instance, a large-scale epidemiological meta-analysis revealed that the first mental disorder occurs before age 14 in one-third of individuals, age 18 in almost half (48.4%), and before age 25 in half (62.5%), with a peak/median age at onset of 15/18 years across all mental disorders (SOLMI et al., 2021). Reinforcing the importance of studies investigating the impact of environmental insults on adolescent mental illness, a recent meta-analysis showed an increased prevalence of clinically elevated depression and anxiety symptoms in youth (mean age of 13 years old) during the first year of the COVID-19 pandemic (HAWES et al., 2022).

Although the neurobiological features underline such susceptibility remains unclear, it has been proposed that an elevated stress reactivity and the ongoing maturational processes of the hypothalamic-pituitary-adrenal (HPA) axis during adolescence may contribute to this increased susceptibility. Preclinical studies indicated that adolescent rats show a prolonged glucocorticoid release in response to various stressors compared to adults due to incomplete maturation of negative feedback systems (VÁZQUEZ; AKIL, 1993). Moreover, brain areas that continue to develop during adolescence (e.g., amygdala, hippocampus, and prefrontal cortex) show relatively high levels of glucocorticoid receptors throughout adolescent development (ROMEO, 2013). Thus, interactions between protracted hormonal responses and the continued maturation of stress-sensitive brain areas may explain the increased susceptibility of the adolescent brain to stressful events and the emergence of psychiatric disorders.

The susceptibility to environmental adversities observed in adolescence may arise from their potent glutamatergic inputs from the hippocampal formation (e.g., CA1) and other brain structures (e.g., basal lateral amygdala, thalamus, and hypothalamus) (O'MARA, 2005). During early development, such glutamatergic inputs onto PV interneurons are highly plastic as the organism adapts to the environment, potentially altering the local E/I balance and maturational events (STANIKA et al., 2009). Therefore, the excessive glutamatergic drive can lead to abnormal Ca^{2+} accumulation in the fast-spiking PV interneurons, leading to cell damage and even cell death (STANIKA et al., 2009). As mentioned, PNNs are not yet fully formed in early adolescence, making PV interneurons highly vulnerable to metabolic and oxidative damage (CABUNGCAL et al., 2013b). Therefore, aberrant excitation onto PV interneurons could lead to cell dysfunction and behavioral deficits observed in adulthood.

Accordingly, Gomes and collaborations have shown that the moment of stress exposure seems critical for the behavioral outcomes: while repeated physical stressors during adolescence caused long-term behavioral and electrophysiological changes similar to those observed in rodent models for schizophrenia, stressing adult rats led to short-term changes associated with depressive-like states (GOMES; ZHU; GRACE, 2019a). Specifically, in animals exposed to adolescent stress, there is a persistent decrease in the number of PV interneurons in the vSub. Furthermore, the number of mature PV interneurons enwrapped by PNNs decreased after adolescent stress exposure. In contrast, adult stress does not change these markers. As a possible consequence of adolescent stress-induced loss of PV interneurons, an increase in the firing rate of the pyramidal neurons was also observed in vSub. Indeed, inducing 25% downregulation of cortical PV levels in adolescent rats reduces the interneuron function until adulthood, permanently disrupting E/I balance (CABALLERO et al., 2020). These results suggest that vulnerability to adolescent stress might indeed be a component of the critical period, and stress during this period leads to pathological profiles related to psychiatric disorders (Figure 1).

Figure 1. Adolescent critical period of vulnerability to stress
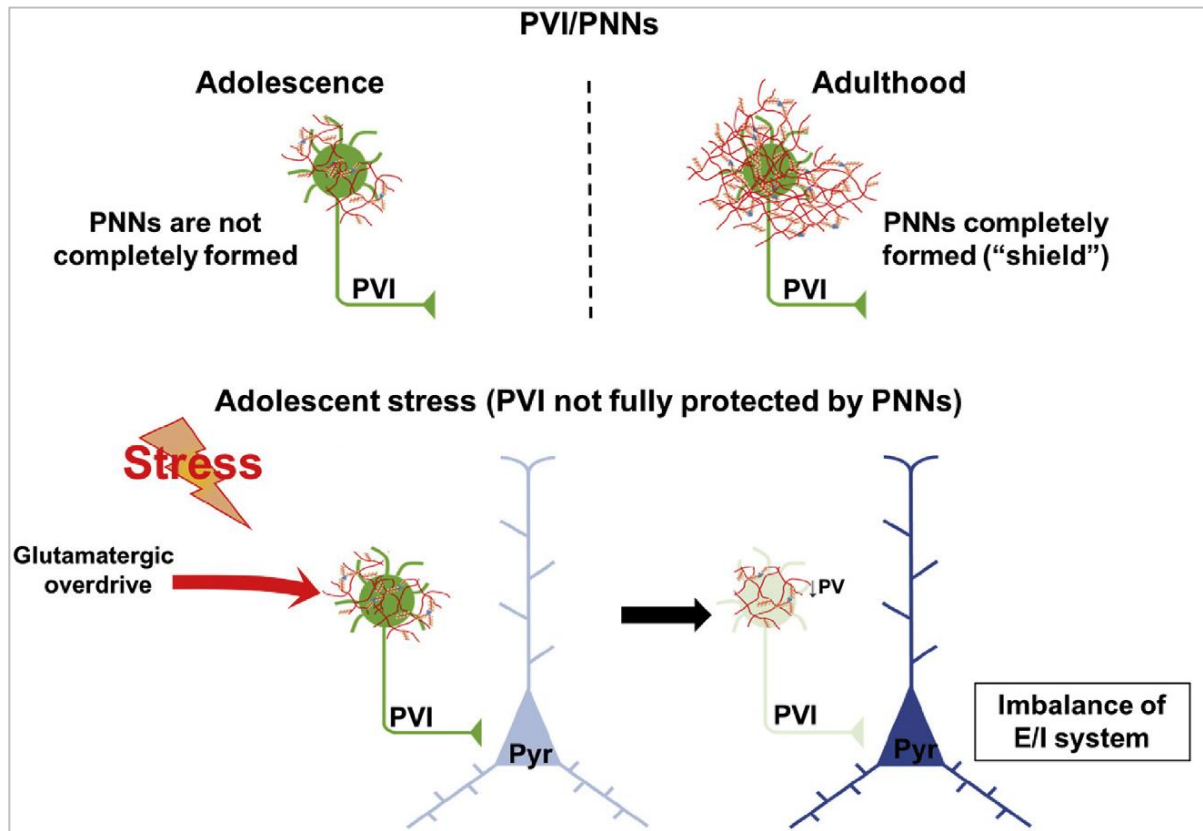
Adapted from (GOMES; ZHU; GRACE, 2019a).

During adolescence, the perineuronal nets (PNNs), a glycosaminoglycan matrix sheath surrounding PVI (Parvalbumin interneurons), are not completely formed. Therefore, exposure to stress during this period can cause abnormal excitation onto PVI in the vHip, leading to PVI dysfunction and, consequently, to an imbalance of the E/I system. In the adult animal, PNNs are completely formed, and PVI are protected from damage.

Hippocampal hyperactivity is proposed to underlie an overactive dopamine system, which has been consistently associated with psychotic symptoms in individuals with schizophrenia (MODINOS et al., 2015). It is because of the dysregulation of a multisynaptic pathway, including the vHip, nucleus accumbens, ventral pallidum, and ventral tegmental area (VTA). The activation of glutamatergic projections from the vHip to the nucleus accumbens, results in the activation of GABAergic projections to the ventral pallidum, which disinhibit the dopamine (DA) neurons in the VTA. Importantly, individuals with psychosis report experiencing more frequent and severe childhood/adolescent trauma than those without psychiatric conditions (MAURITZ et al., 2013). In addition, adolescents at-risk showed cortisol

levels significantly elevated among those who transitioned to psychosis (WALKER et al., 2013). In animals exposed to early adolescent stress, we observed an increased VTA DA neuron population activity and enhanced locomotor response to amphetamine, consistent with clinical observations in patients with schizophrenia (CAVICHIOLI et al., 2023; GOMES; GRACE, 2017a; GOMES; ZHU; GRACE, 2019a, 2019b)

Our previous findings pointed to a harmful impact of stress on the vHip E/I balance and hyperactivity of the VTA DA system, corroborating with evidence that adolescence represents a sensitive period in which highly stressful events may induce detrimental outcomes. Notably, adolescent stress contributes to the emergence of psychiatric disorders, as well as the transition to psychosis (GOMES; GRACE, 2017a; GOMES; RINCÓN-CORTÉS; GRACE, 2016). Considering the importance of adolescent mental health and accomplishment, it is essential to investigate how early exposure to stressors leads to dysfunction in PV interneurons and pyramidal neurons. Also, understanding the relation between changes in the behavioral phenotype, such as social and cognitive performance, and the neurobiological mechanisms induced by stress. Overall, advancing our knowledge of markers and causative mechanisms that change adolescent behavior can contribute to discovering new strategies to prevent the emergence of psychiatric disorders.

1.3. Mitochondria and redox balance: implications for brain function

Mitochondria are essential organelles that regulate several cellular processes, such as adenosine triphosphate (ATP) production, reactive oxygen species (ROS) generation, and intracellular Ca^{2+} signaling (ANNESLEY; FISHER, 2019). Mitochondria comprise double-membrane structures, cristae, and matrix spaces (GREEN; ODA, 1961). The outer mitochondrial membrane is similar to cell membranes, composed of phospholipid bilayers and integral membrane proteins, responsible for the primary transporter of nucleotides, ions, and metabolites between the cytosol and intermembrane mitochondrial space. It is also composed of translocase proteins that permit the entrance of large proteins into the mitochondrion and enzymes

involved in many activities (SCHENKEL; BAKOVIC, 2014). The inner membrane of mitochondria is extensively folded and compartmentalized, forming the mitochondrial cristae to accommodate itself within the outer membrane. There are three types of protein in the inner membrane: (1) those that perform the electron transport chain redox reactions; (2) ATP synthase, which generates ATP in the matrix; and (3) specific transport proteins that regulate metabolite passage into and out of the mitochondrial matrix (PFANNER; WARSCHEID; WIEDEMANN, 2019). The mitochondrial matrix is the space between the membranes, in which 2/3 of the total mitochondrial proteins are localized. It is highly concentrated in mitochondrial ribosomes, mitochondrial DNA genome, and enzymes participating in the oxidation of pyruvate and fatty acids and the citric acid cycle (MANNELLA, 2006).

The most prominent role of mitochondria is oxidative phosphorylation, which produces ATP, the main energy source for cellular biological processes (Figure 2). In oxidative phosphorylation, electrons from nicotinamide adenine dinucleotide (NADH) and flavin adenine dinucleotide ($FADH_2$) donors are transferred to oxygen via oxidation-reduction reactions through a series of four protein complexes (complex I – IV) named the respiratory electron transport chain (ETC). These reactions release energy, generating a proton electrochemical gradient across the mitochondrial membrane. Then, in a phosphorylation reaction, the chemiosmotic potential drives ATP synthases to transform adenosine diphosphate (ADP) into ATP (NOLFI-DONEGAN; BRAGANZA; SHIVA, 2020).

Figure 2. Mitochondrial oxidative phosphorylation
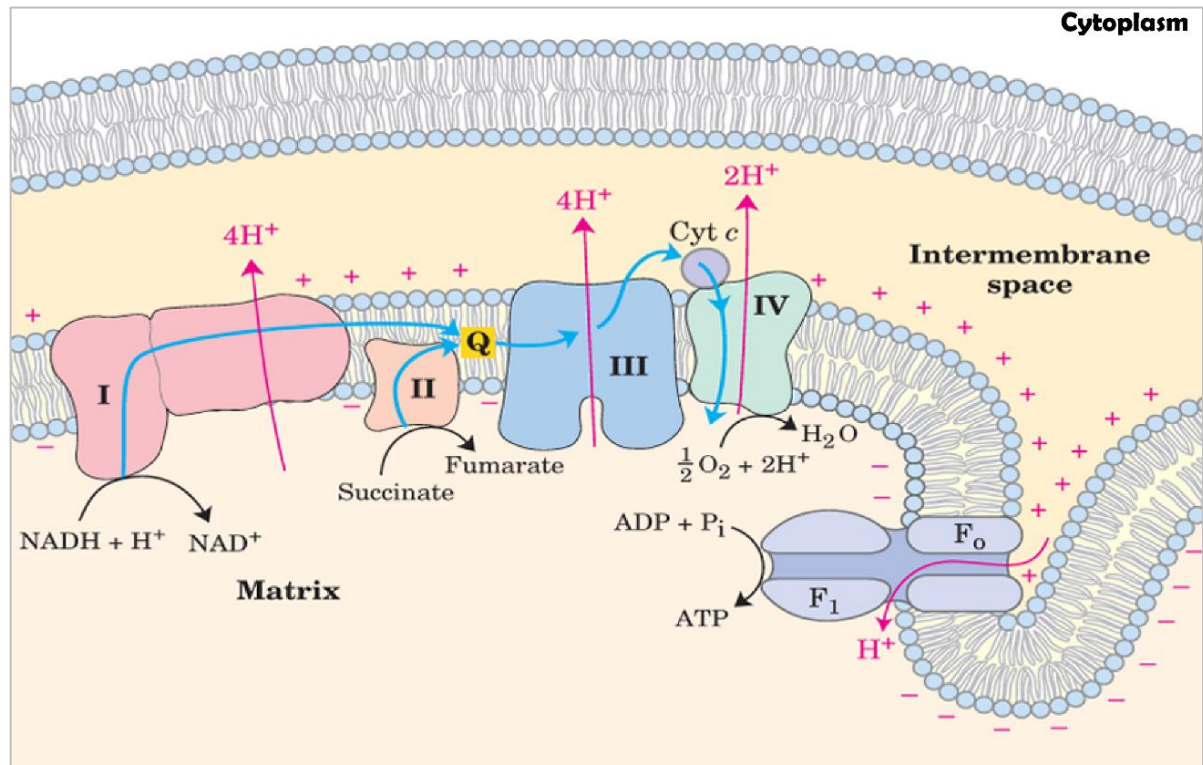
Adapted from: (LEHNINGER, 2008)

The electrons donated by NADH and $FADH_2$ pass through a chain of four protein complexes (Complex I – IV) arranged in the inner membrane. Electron flow is accompanied by proton transfer across the membrane, producing an electrochemical gradient. Protons can reenter the matrix only through proton-specific channels. The proton-motive force that drives protons back into the matrix provides the energy for ATP synthesis to convert ADP into ATP. The electrons are then transferred to the oxygen molecule to form water.

The leakage of electrons from ETC leads to a partial reduction of oxygen to form superoxide (JASTROCH et al., 2010). Immediately, superoxide is dismutated to hydrogen peroxide by the superoxide dismutase (SOD). Hydrogen peroxide is a pleiotropic physiological signaling agent central to the redox regulation of biological activities. For instance, it contributes to orchestrating various processes in cells and organs, including cell proliferation, differentiation, and migration (KAUSAR; WANG; CUI, 2018). Both superoxide and hydrogen peroxide generated in oxidative phosphorylation are considered mitochondrial reactive oxygen species (ROS). Although the mitochondrial ETC is the main source of ROS, they can also be produced by the peroxisomes, endoplasmic reticulum, and phagocytic cells (DE ALMEIDA et al., 2022).

An interactive network of antioxidant enzymes tightly regulates cellular ROS levels (Figure 3). Following the superoxide anion conversion into hydrogen peroxide by SOD, catalases and/or peroxidases reduce hydrogen peroxide to generate water (DE ALMEIDA et al., 2022). Another essential antioxidant system is the reduction of ROS in reactions catalyzed by glutathione-S-transferase. Hydrogen peroxide is reduced by glutathione (GSH) in a reversible reaction catalyzed by glutathione peroxidases, producing glutathione disulfide (GSSG). Due to its high concentration and central role in maintaining the cell's redox state, GSH is one of the most important cellular antioxidants (DRINGEN, 2000). Overall, the balance between oxidative and reductive reactions in the body depends on multiple biochemical processes, such as the ETC that produces ROS during oxidative phosphorylation and the redox sensor system which triggers antioxidant responses.

Figure 3. The antioxidant system regulates the cellular redox states
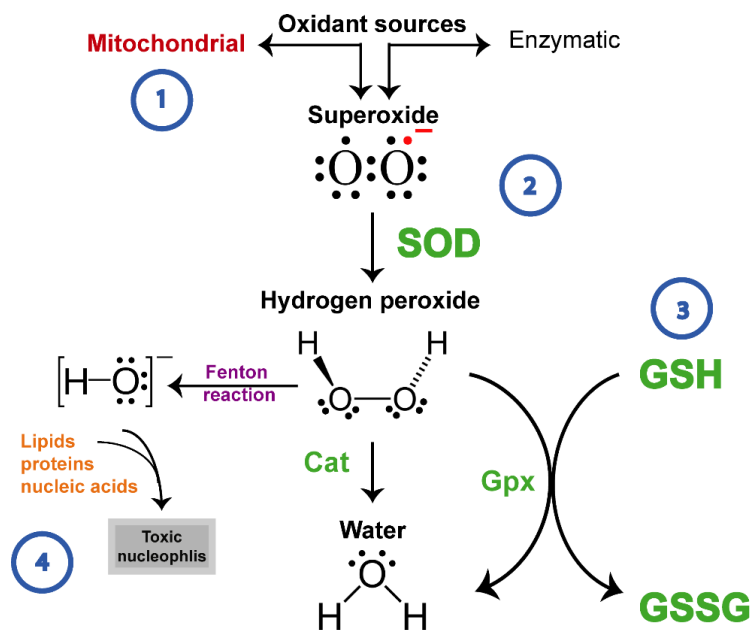
(1) In animals, ROS are produced mainly by mitochondria but to a limited extent enzymatically. The mitochondrial electron transfer respiratory chain generates superoxide during oxidative phosphorylation. **(2)** Superoxide is rapidly converted into hydrogen peroxide by superoxide dismutase (SOD). **(3)** Hydrogen peroxide is reduced by glutathione (GSH) in a reversible reaction catalyzed by glutathione peroxidase (GPx), producing glutathione disulfide (GSSG). It can also be reduced by the catalase (Cat) antioxidant enzyme. **(4)** Hydrogen peroxide may react with metals (the Fenton reaction) to form the highly reactive hydroxide, which irreversibly oxidizes lipids, proteins, and nucleic acids, producing toxic nucleophiles.

In the brain, mitochondria and ROS play essential roles in neurogenesis, neuronal differentiation, migration, and maturation (WILSON; MUÑOZ-PALMA; GONZÁLEZ-BILLAULT, 2018). Synaptic transmission is a highly energy-demanding process, requiring ATP production by mitochondria. Indeed, presynaptic terminals are enriched with multiple mitochondria, while in the dendritic spines of excitatory glutamatergic synapses, mitochondria are typically absent (CHAVAN et al., 2015). This subcellular compartmentalization of energy reflects an adaptation to maximize efficiency in energy utilization. Hence, ATP is generated only when and where it is needed. Neurons have a unique oxidative potential and an adequate supply of oxygen and glucose to survive and maintain normal function. About 60 – 80% of ATP consumption is to maintain neuronal excitability, while neurotransmission processes consume 10 – 20% of it (BÉLANGER; ALLAMAN; MAGISTRETTI, 2011).

Notably, neurons critically depend on mitochondrial function, and the interplay between both is crucial for brain function. An emerging concept proposes mitochondria as an integrator in regulating behaviors, including those of social domain and cognition (PICARD; SHIRIHAI, 2022; ÜLGEN; RUIGROK; SANDI, 2023). For instance, mitochondrial deficits induced by a mutation in the mtDNA gene *Nd6* have been associated with reduced sociability in a social preference task in male mice (YARDENI et al., 2021). Additionally, a strong correlation between age-dependent cognitive decline and an increased prevalence of donut mitochondria (a hallmark of mitochondrial dysfunction) was demonstrated in monkeys (HARA et al., 2014). Although evidence implicated mitochondria in regulating crucial behaviors, few data reveal their involvement in adolescence, normal brain function development, and environmental factors influences.

1.4. Mitochondrial dysfunction: a common feature of psychiatric disorders

Over the past decades, several studies have shown that psychiatric disorders, such as schizophrenia, bipolar disorders, and major depressive disorder, overlap in multiple aspects, varying from etiology to clinical symptoms and treatment (JOU; CHIU; LIU, 2022). One of those commonalities is the key role of mitochondria in psychiatric

conditions, including stress-related psychopathologies (PICARD et al., 2018). Particularly, mitochondrial abnormalities induce neuronal defects, leading to cognitive impairment, learning disabilities, memory disturbances, and affective syndromes (JOU; CHIU; LIU, 2022) (Figure 4). Postmortem studies have observed dysregulated expression of gene-encoded mitochondrial enzymes and regulators in brain regions of individuals with schizophrenia and bipolar disorder (ROBERTS, 2021). Notably, patients with mitochondrial disease reported comorbid brain disorders, such as cognitive deficits, delayed development, and susceptibility to seizures and bipolar affective disorders (COLASANTI et al., 2020; EOM; LEE, 2017).

Figure 4. Mitochondrial abnormalities and the emergence of psychiatric disorders
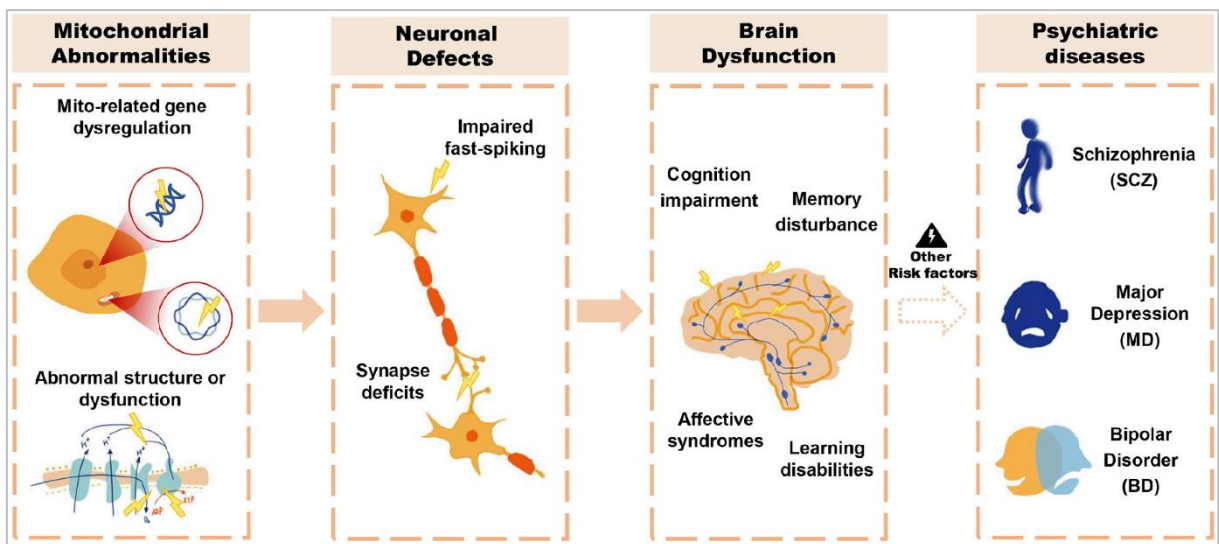
Adapted from: (JOU; CHIU; LIU, 2022)

Mitochondrial abnormalities induce neuronal defects, causing brain dysfunction. Risk factors may interact with mitochondrial dysfunction, leading to the emergence of psychiatric diseases.

Mitochondrial dysfunction can impact multiple brain systems, such as neurotransmitter pathways and neurogenesis. For instance, changes in expression levels of mitochondrial genes and abnormal synapse morphology have been observed in animal models for studying stress-associated psychiatric disorders (WEGER et al., 2020). Emerging evidence proposes that mitochondria play a prominent role in coordinating stress response, making them a possible biological link between environmental insults and psychiatric outcomes (PICARD et al., 2018). It has been

suggested that under stress, mitochondria increase ROS production, which overwhelms the cellular antioxidant capacity, leading to redox dysregulation. The shift in redox balance to pro-oxidant states is named oxidative stress, a failure of compensatory molecular pathways to modulate the cellular redox state. Excessive ROS levels cause oxidative damage to lipids, proteins, and nucleic acids, consequently causing cellular degeneration and even functional decline (DANIELS; OLSEN; TYRKA, 2020). Aligned with that, increased oxidative damage and decreased capacity of antioxidant systems are consistent findings in schizophrenia, autism, and bipolar disorder, as well as in individuals during the prodromal stage who later develop psychosis (PERKINS; JEFFRIES; DO, 2020).

Overall, neurobiological mechanisms of psychiatric disorders have been associated with oxidative damage and reduced antioxidant capacity in the brain (MURRAY et al., 2021; PALANIYAPPAN et al., 2021). Understanding the impact of stress during adolescence on mitochondrial function and redox balance may help conceptualize the risk of the emergence of psychiatric disorders. Moreover, further studies are warranted to develop novel therapeutic strategies targeting mitochondrial function and the antioxidant system, given their crucial importance in regulating and maintaining neuronal integrity.

1.5. Vulnerability of PV interneurons to oxidative stress

PV interneurons require high energy and elevated metabolic activity to maintain their main function, i.e., fast rhythmic neuronal synchrony. A high density of mitochondria supplies the large amounts of ATP needed to sustain it (GULYÁS et al., 2006; KANN et al., 2011). Thus, studies have proposed that PV interneurons produce high amounts of ROS (ZHANG et al., 2016). Consequently, they have a well-regulated antioxidant system for elevated ROS levels, such as the GSH system. Indeed, the availability of cysteine (an amino acid rate-limiting in the GSH synthesis) is linked to PV interneuron activity, supplying their demands to maintain physiological redox status (BAXTER; HARDINGHAM, 2016; CABUNGCAL et al., 2013b). On the other hand, the high metabolic requirements may confer them susceptible to redox dysregulation and oxidative stress. Notably, other interneurons, such as calretinin and calbindin-

containing interneurons, are not particularly sensitive to oxidative stress, reinforcing PV vulnerability due to their fast-spiking activity (STEULLET et al., 2010).

Excessive excitatory drive onto PV interneurons also contributes to their vulnerability to oxidative stress. Under physiological conditions, PV protein buffer the Ca^{2+} that enters through the activation of ionotropic receptors, such as NMDA and AMPA receptors. The remaining physiological levels of Ca^{2+} promote ATP production via mitochondria. However, under conditions that demand elevated PV interneurons activity, there is a toxic accumulation of Ca^{2+} in mitochondria, which disrupts the mitochondrial membrane potential and the electron transport chain (RUDEN; DUGAN; KONRADI, 2020). The developmental trajectory of PV interneurons also renders them vulnerable to many stressors during childhood and adolescence (STEULLET et al., 2017). This increased susceptibility has also been associated with the maturation of the PNNs around these interneurons, which will be complete only at the end of adolescence. Therefore, PV interneurons may be particularly affected by oxidative stress during juvenile postnatal development when their fast-spiking properties are not yet fully developed (CABALLERO; TSENG, 2016), and the formation of the protective PNN enwrapping them is not yet complete (CABUNGCAL et al., 2013b).

The deleterious effects of oxidative stress on PV interneurons impair their E/I balance regulation and maintenance of proper brain function (STEULLET et al., 2017). Indeed, several animal models involving genetic and/or environmental risk factors relevant to the emergence of psychiatric disorders show that PV interneuron deficits are accompanied by oxidative stress in the prefrontal cortex and hippocampus, along with behavioral changes (STEULLET et al., 2017). Notably, many of those findings related to oxidative stress-induced PV interneuron deficits were investigated in animal models based on prenatal/neonatal manipulations, genetic approaches, or insults during adulthood (BRENHOUSE; ANDERSEN, 2011; CARLSON et al., 2011; DO et al., 2009; GOKHALE et al., 2012; INAN et al., 2016; STEVENS et al., 2013; STOJKOVIĆ et al., 2012). It remains unknown if stress during adolescence leads to the disruption of PV interneurons and their PNNs due to oxidative stress, causing behavioral and electrophysiological changes associated with psychiatric disorders.

2. HYPOTHESIS

Adolescence is a critical period for experience-dependent plasticity, in which environmental influences can positively and negatively impact behavioral outcomes later in life (AOKI; ROMEO; SMITH, 2017). Indeed, environmental insults can drastically reduce sociability and cognitive function, which are hallmarks of neurodevelopmental and stress-related disorders, such as schizophrenia (GOMES; ZHU; GRACE, 2019b). Therefore, adolescence is crucial for individuals' well-being and for establishing higher-order cognitive processes. Although adolescent individuals exhibit great variability in behavioral outcomes (CARAS; SANES, 2019), our study focused on the impact of stress given its harmful effects on mental health and the fact that the neurobiological underpinnings of behavioral changes induced by adolescent stress are poorly understood.

During early adolescence, PV interneurons are highly plastic in terms of excitatory drive and neuronal activity, which causes them to be particularly susceptible to damage by stressors (RUDEN; DUGAN; KONRADI, 2020). However, following adolescence, PV interneurons develop PNNs, that attenuate and protect PV interneurons from stress-induced damage (CABUNGCAL et al., 2013b). Accordingly, our previous work has shown a causal role of adolescent stress, a specific reduction in PV interneurons and their associated PNNs, and an increase in vHip pyramidal neuron activity and behavioral changes in adulthood (GOMES; ZHU; GRACE, 2019a). In contrast, no alterations were found in rats when the same stress protocol was applied during adulthood (GOMES; ZHU; GRACE, 2019a). These findings are consistent with evidence that PV interneurons are highly vulnerable to environmental insults during adolescence plasticity. Therefore, it would be paramount to progress in understanding the mechanisms that stress lead to deficits in PV interneurons and associated behavioral changes during late adolescence.

Several studies have pointed to redox dysregulation as one "hub" of neurodevelopmental disorders and the emergence of psychosis in early adulthood (PERKINS; JEFFRIES; DO, 2020). In a dysregulated stress response system, mitochondria produce increased ROS, which overwhelms the antioxidant capacity and can damage cells. Aligned with that, PV interneurons have elevated metabolic activity

and oxidative phosphorylation to support their high-frequency activity, making them particularly vulnerable to oxidative stress and increased metabolic demand (STEULLET et al., 2017). Therefore, we hypothesized that exposure to adolescent stress would increase the oxidative stress on PV interneurons in the vHip, and consequently, it results in deficits in the E/I balance, leading to behavioral and molecular changes related to neurodevelopmental disorders. To address the gap between oxidative stress in the vHip and behavioral changes, we postulated a deleterious impact of stress on mitochondrial function and redox balance. Lastly, we also hypothesized that adolescent stress exposure changes the expression of mitochondria-associated genes in the vHip, and their expression levels will correlate with distinct adolescent behavioral phenotypes.

3. AIMS

3.1.   Main aim

We aimed to investigate the impact of adolescent stress on behavioral outcomes and their underlying pathological mechanism, focusing on the dysregulation of inhibitory and excitatory circuits and molecular changes in mitochondrial respiratory function and redox homeostasis of the vHip.

3.2.   Specific aims

- o To evaluate the impact of stress on sociability and cognitive function in adolescent animals;
- o To assess the impact of stress on PV interneurons and their associated PNNs, as well as on pyramidal neuron activity in the vHip;
- o To investigate possible oxidative damage induced by stress in the vHip and its co-localization with PV interneurons;
- o To dynamically characterize the impact of stress, i.e., one and ten days after stress, on mitochondrial respiratory function and redox balance (ROS levels and antioxidant enzyme activity) in the vHip;
- o To determine the impact of stress on GSH levels in the vHip and serum and its correlation with behavioral performance on sociability and cognitive tasks;
- o To reveal the transcriptomic profile of the vHip of distinct adolescent behavioral phenotypes and stressed animals;
- o To relate mitochondria-associated genes with distinct adolescent behavioral phenotypes and stress response.

4. METHODS

4.1. Animals

Male and female Sprague-Dawley rats (postnatal day, PND 70) were obtained from the University of São Paulo Central Animal Facility, Ribeirão Preto. Rats were allowed to acclimatize for one week in the animal facility before breeding. Mating was confirmed by the presence of spermatozoa in the vaginal smear and birthday defined PND 0. At PND 21, pups were weaned. We opted to use only the male offspring, as we previously found that female adolescent rats did not show behavioral and electrophysiological changes induced by the stress protocol used here (Klinger et al., 2019). Animals were randomly assigned to all experimental groups, each cage devoted to a specific experimental procedure. Rats were housed (2 – 3 animals per cage) in a temperature (22 °C) and humidity (47%) controlled environment (12 h light/dark cycle; lights on at 6 AM) with water and food *ad libitum*. All procedures were approved by the Ribeirão Preto Medical School Ethics Committee (CEUA-FMRP 155/2018 e 248/2019), which follows Brazilian and International regulations.

4.2. Stress procedure

Animals were exposed to inescapable footshock (FS; from PND 31 – 40) daily and three restraint stress (RS) sessions (PD31, 32, and 40). Using this protocol, we previously found marked behavioral and electrophysiological changes that persist until adulthood (CAVICHIOLI et al., 2023; GOMES; GRACE, 2017b; GOMES; ZHU; GRACE, 2019a). Briefly, rats were exposed to one session of FS per day for 10 consecutive days. In each session, animals were placed in a Plexiglas chamber with a grid floor of 0.48 cm stainless steel rods spaced 1.6 cm apart (EP107R, Insight, Brazil). Twenty-five FS (1.0 mA, 2 s) were delivered pseudo-randomly (5 cycles of 30, 60, 40, 60, and 90 s). Immediately after receiving FS, rats were submitted to RS for 1 h in Plexiglas cylindrical size-adjusted restraint tubes on the first, second, and last day of

FS exposure. Cylinders measured 14.0 × 3.9 cm (length × diameter) for rats at PND 31 – 32 and 20.3 × 5.1 cm for rats at PND 40, ventilated by holes (1 cm diameter). Naïve animals were left undisturbed in their home cages.

4.3. Behavioral tests

4.3.1. Elevated Plus-Maze test (EPM)

The EPM is a test widely used for studying anxiety-related behaviors (WALF; FRYE, 2007). It consisted of 2 opposite open arms (50 × 10 cm), crossed at a right angle by 2 arms of the same dimensions enclosed by 40 cm high walls with no roof. The maze was located 50 cm above the floor, and a 1 cm high edge made of Plexiglas surrounded the open arms to prevent falls. Rat behaviors were filmed for 5 min and analyzed using the Any-Maze software (Stoelting, USA). The parameters analyzed were the percentage of entries and time in the open arms and the number of entries into the enclosed arms. The percentage of time in the open arms was calculated with time in open and closed arms, excluding the time in the center of the EPM.

4.3.2. Light Dark Box (LDB)

Anxiety-like behaviors were also evaluated in the LDB apparatus. LDB has two compartments that are connected by a door. The light and dark compartments (240 x 210 cm) have a grid floor. Animals were placed in the dark chamber and allowed to explore the apparatus freely for 5 min after the first entry into the light zone. The time spent in the light zone was analyzed by the ANY-maze software (Stoelting, USA).

4.3.3. Social Interaction Test (SIT)

Animals were placed in the center of a circular arena (60 cm height × 65 cm diameter) and allowed to explore it for 5 min. Then, an unfamiliar male Sprague-Dawley rat (PND 50 – 54) was introduced into the arena as a social target for 10 min. The social interaction time was measured when the tested animal was sniffing the unfamiliar rat's anogenital region, head, or body and when they were following, crawling over and under each other. A blind experimenter quantified the social interaction time.

4.3.4. Novel Object Recognition (NOR)

Two hours after the SIT, each animal was habituated in a circular arena (60 cm height × 65 cm diameter) for 10 min. NOR test was conducted in the same circular arena 24 h later. Animals were submitted to two trials separated by 1 h. During the first trial (acquisition trial, T1), rats were placed in the arena containing two identical objects for 5 min. For the second trial (retention trial, T2), one of the objects presented in T1 was replaced by an unknown (novel) object. Animals were then placed back in the arena for 5 min. Object exploration was defined as when the animal faced the object at 2 cm of distance or less while watching, licking, sniffing, or touching it with the forepaws while sniffing. A blind experimenter quantified object exploration. Recognition memory was assessed using the discrimination index:

$$\frac{(\text{Time novel object} - \text{Time familiar object})}{(\text{Time novel object} + \text{Time familiar object})}$$

4.3.5. Behavioral z-score index

The integrated behavioral z-score method allows the normalization of individual data observed in different behavioral parameters to decrease the intrinsic variability of

single tests and enhance the sensitivity and reliability of the individual phenotyping (Guilloux et al., 2011). First, we obtained the normalized social interaction time (SIT) and discrimination index (NOR) data. EPM normalized data was calculated by averaging the z-normalized data of the following parameters: the percentage of entries and time spent in the open arms and the number of enclosed arms entries. The following equation was used to calculate z-normalized data:

$$\frac{(x - \textit{mean of naïve group})}{\textit{standard deviation of naïve group}}$$

Then, the integrated behavioral z-score was calculated by averaging the z-normalized data obtained per rat in the EPM, SIT, and NOR.

4.4.   *In vivo* recordings of vHip pyramidal neurons

Rats were anesthetized with chloral hydrate (400 mg/kg, i.p.) and mounted on a stereotaxic frame. The coordinates for the vHip were 5.3 mm posterior from bregma, 4.4 mm lateral to the midline, and 5.5 – 8.0 mm ventral from the brain surface. Electrodes were lowered through 6 tracks inside the vHip. Pyramidal neurons were identified by typical electrophysiological characteristics such as firing rate (average up to 2 Hz) and action potential shape (half–width > 0.4 ms) (CAVICHIOLI et al., 2023). The firing rate of these neurons was measured. Each identified pyramidal neuron was recorded for 1–3 min (Figure 5). After the electrophysiological recordings, the electrode sites were marked via iontophoretic ejection of Chicago Sky Blue dye from the electrode (20 µA constant negative current, 20 min). Then, rats were euthanized by an overdose of chloral hydrate; the brains were removed, fixed for at least 24 h in 8% paraformaldehyde (PFA), cryoprotected in 30% sucrose, and sectioned for histological confirmation of the electrode sites.

Figure 5. *In vivo* **electrophysiology of vHip pyramidal neurons**
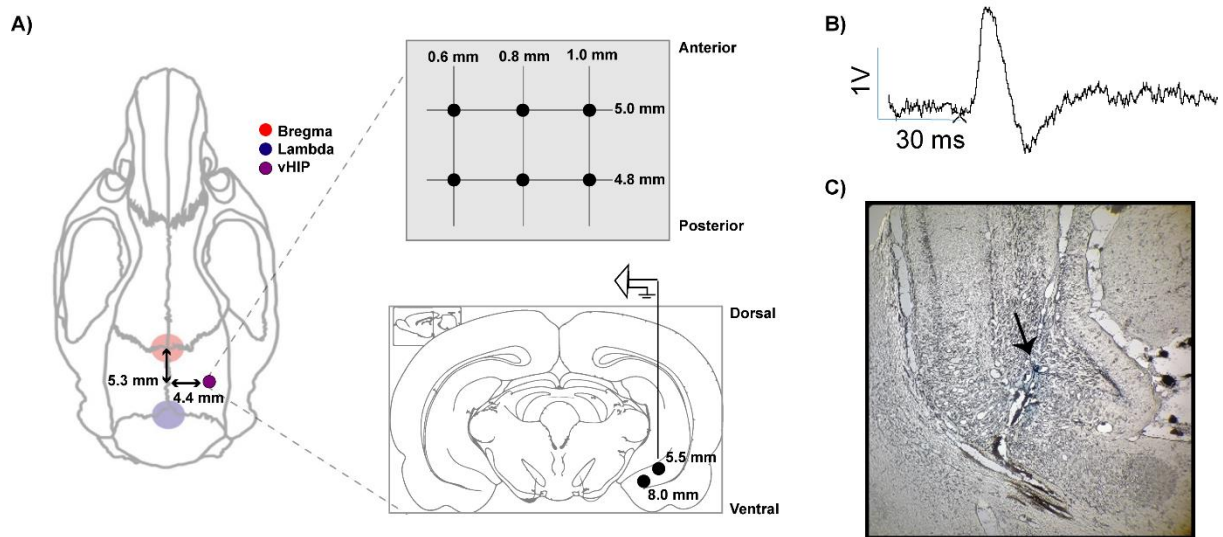
(A) Dorsal view of the skull of Sprague Dawley rats. Colorful represents the position of bregma (red), lambda (blue), and vHip (purple). The coordinates sites for vHIP of rats at PND 51 were defined as 5.3 posterior from bregma, 4.4 mm lateral to the midline, and 5.5 – 8.0 mm ventral from the brain surface. Electrodes were lowered through 6 tracks inside the vHip. **(B)** Typical electrophysiological characteristics of pyramidal neurons. **(C)** Black arrow indicates histological confirmation of the electrode sites

4.5.   Biomolecular analyses

4.5.1. High-resolution respirometry

High-resolution respirometry is an approach to assess cellular oxygen consumption by evaluating mitochondrial respiratory states and maximal mitochondrial electron transport system capacity in fresh-permeabilized tissues (DJAFARZADEH; JAKOB, 2017). Naïve and stressed rats (n = 6/group) were anesthetized (urethane 25%, 1 mL/100 g/rat), and 2 mg of fresh vHip samples from both hemispheres, respectively finely cut into pieces, were used in these experiments. The samples were permeabilized in BIOPS solution (2.7 mM EGTA, 20 mM imidazole, 20 mM taurine, 50 mM acid 2-(N-morfolino) ethanesulfonic potassium, 0.5 mM dithiothreitol, 6.5 mM MgCl$_2$, 15 mM phosphocreatine, 0.57 mM ATP, pH 7.1) containing 0.01% saponin for 5 min at 4 ^{o}C, then carefully transferred to the chambers of a Oxygraph-2k respirometer

(Oroboros, Austria), containing 2.1 mL of air saturated respiration medium MIR05 (0.5 mM EGTA, 3 mM $MgCl_2$, 60 mM K-lactobionate, 20 mM taurine, 10 mM KH_2PO_4, 20 mM HEPES, 110 mM sucrose, 1 g/L albumin, pH 7.1). Basal respiratory rates were determined after adding 9 mM glutamate and 5 mM malate. OXPHOS rates were determined after 1 mM ADP addition to the chambers. LEAK respiration (non-phosphorylating resting state) rates were attained with 1 µg/mL oligomycin. Maximal capacity rates of the Electron Transfer System (ETS) were defined after 2 pulses of the mitochondrial uncoupler carbonyl cyanide m-chlorophenylhydrazone (CCCP, 1 µM). Finally, residual oxygen consumption (Rox) rates were determined by adding 1 mM NaCN. Rox rates were subtracted from all other measurements. The experiments were made in triplicate and illustrative performed protocol is described in Figure 6.

Figure 6. Illustrative Oroboros Oxygraph-2k runs for performed protocol
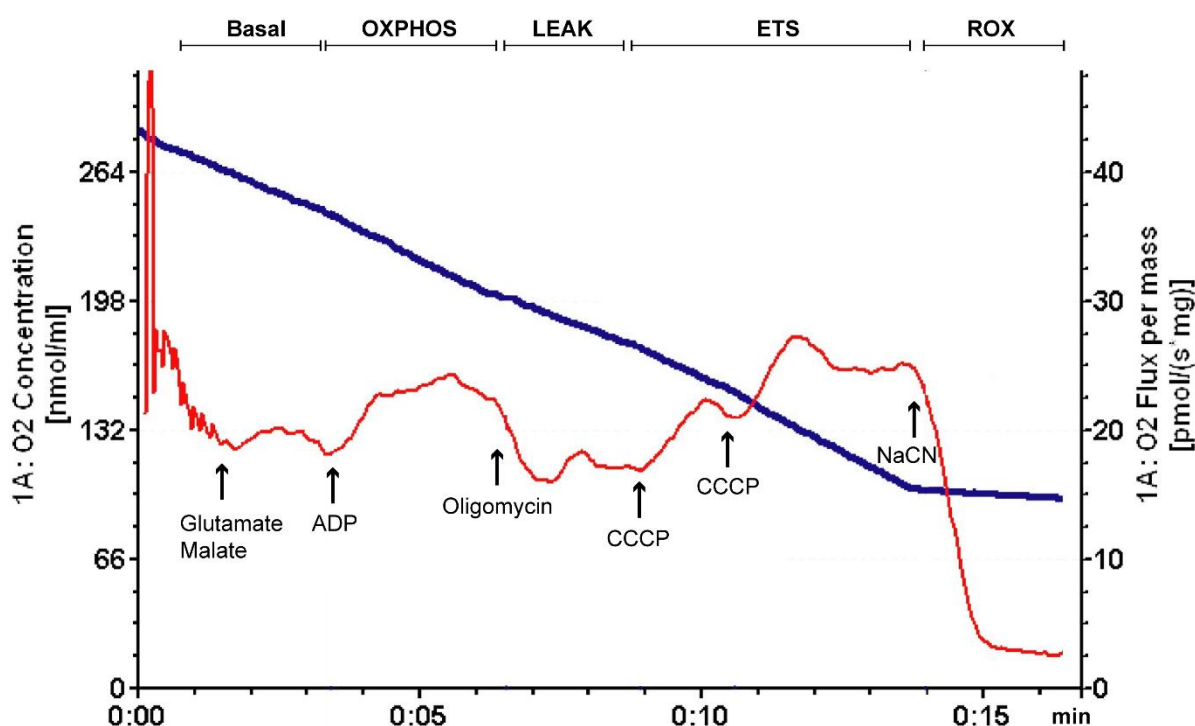
Representative high-resolution respirometry run for the performed protocol in vHIP of Sprague-Dawley rats using an Oxygraph-2k respirometer. The blue line represents O_2 concentration [nmol/ml], and the red line indicates O_2 flux per mass [pmol/(s^{-1}.mg)] in one chamber. OXPHOS = Oxidative Phosphorylation; ETS = Electron Transfer System; ROX = Residual Oxygen

4.5.2. *In situ* reactive oxygen species (ROS) measurement

Dihydroethidium (DHE, Sigma) staining allows the precise localization of ROS (superoxide and other free radicals) in specific brain regions. DHE is oxidized by superoxide or other ROS to form red fluorescent compounds. In another cohort of animals, naïve and stressed rats (n = 5–6/group) were anesthetized (urethane 25%, 1 mL/100 g/rat) and were perfused with 200 mL of 0.01 M phosphate sodium buffer (PBS, pH 7.4). After perfusion, each brain was embedded in Tissue-tek® (Sakura, FB4583), frozen in isopentane (−40 °C, Sigma, USA), and stored at −80 °C until histological processing. Coronal sections (5 μm) of the vHip (within −4.8 mm to −6.3 mm from bregma) were cut using a freezing cryostat (Leica, model CM1850) and incubated with DHE (10 μmol/L) in dark wet chambers, at room temperature, for 45 min. Then, sections were fixed in 4% PFA in 0.01 M PBS for 10 min. Image acquisition was performed by confocal fluorescence microscopy (Confocal Leica SP5) in 20x. Bright red fluorescence represented ROS levels (relative fluorescence units, RFU) and was evaluated using Fiji software (National Institutes of Health, USA). For negative control, sections were incubated as described above but without DHE.

4.5.3. MitoSOX™ and AmplexRed® assays

An independent experimental group was used to measure the release of hydrogen peroxide (H_2O_2) from vHip samples and the production by mitochondria. For these purposes, we used Amplex® Red Hydrogen Peroxide/Peroxidase Assay Kit (ThermoFisher, A22188) and MitoSOX™ mitochondrial superoxide indicator (ThermoFisher, M36008) assay. Naïve and adolescent stressed animals (n = 7 – 8/group) were anesthetized with 25% urethane (1 mL/100 g/rat), perfused with ice-cold 0.01 M PBS, and decapitated. vHip tissues were immediately collected, cut into approximately 1 mm^3 cubes, and added into HAM – F12 culture medium containing B27 supplement without antioxidants and collagenase type IV (0.05%). The tissues were incubated under gentle agitation for 30 min at 37 °C for cell dissociation. Next, a cell suspension was obtained by pipetting up and down the tissue, followed by

centrifugation at 1200 g for 10 min. The collagenase-containing medium was discarded, and the pellet was resuspended in HBSS to a dilution of 200 µg/µL.

For the measurement of the quantity of superoxide anion in the vHip, the MitoSOX™ assay was used. It corresponds to a DHE derivative, conjugated with a long aliphatic chain containing a phosphonium group, which targets the probe to the mitochondrial matrix. The MitoSOX™ reacts with the superoxide anion, forming an intensely fluorescent compound. The fluorescence intensities of the samples were determined spectrophotometrically in the FlexStation apparatus (Molecular Devices, USA) according to the manufacturer's guidelines. The values were expressed for t = 0 as RFU.

The amount of hydrogen peroxide was measured using the Amplex® Red Assay Kit according to the manufacturer's instructions. Amplex® Red (AR) reagent is a highly sensitive and stable probe for detecting hydrogen peroxide in living samples, especially for cell-based assays. It is based on the following reaction, conducted in the presence of horseradish peroxidase (HRP):

$$AR \ + \ H_2O_2 \ \overset{\text{HRP}}{\longrightarrow} \ Resorufin \ + \ O_2$$
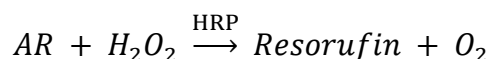
Resorufin (7-Hydroxy-3H-phenoxazin-3-one) is a highly fluorescent product with an excitation maximum at 530 – 570 nm and an emission maximum at 580 – 590 nm, allowing to monitor H_2O_2 extracellular flux fluorometrically, as a measure of ROS production by living cells. Fluorescence intensity was evaluated every 5 min for 20 min in the FlexStation apparatus (Molecular Devices, USA). Values were expressed as $H_2O_2/\mu mol.min^{-1}.mg^{-1}$. For time = 0, the initial fluorescence values were transformed, through the standard curve, into the initial amount of hydrogen peroxide, and for time > 0, these conversions indicate consumption of hydrogen peroxide.

Next, we performed the tissue peroxidase activity assay. The HRP enzyme, which catalyzes the reaction of hydrogen peroxide with the AmplexRed® assay, was removed from the reaction buffer. Then, an excess of H_2O_2 was added to each sample, allowing the evaluation of the endogenous peroxidase activity of the cell suspensions. The values were evaluated for t = 0 and expressed as enzyme activity per reaction volume ($\mu U.mL^{-1}.mg^{-1}$).

4.5.4. Glutathione/Glutathione disulfide (GSH/GSSG) assay

vHip GSH and GSSG levels were measured by a green fluorescence assay kit (ab205811, Abcam, UK). For that end, at PND 51, animals were anesthetized (urethane 25%, 1 mL/100 g/rat) and perfused with cold 0.01 M PBS. vHip from both hemispheres was collected and snapped frozen in liquid nitrogen until use for GSH total extraction (n = 6/group). 20 mg of tissue were resuspended in 400 µL of ice-cold Mammalian Lysis Buffer and homogenized with 10-15 passes. Then, samples were centrifuged at 12,000 x g for 10 min at 4 °C. Supernatants were collected and deproteinized by adding 1 volume of trichloroacetic acid (TCA, 100% w/a) into 5 volumes of samples. After 10 min of incubation, samples were centrifuged at 12,000 x g for 5 min at 4 °C. Samples were neutralized by adding sodium bicarbonate ($NaHCO_3$) to supernatant and vortex. After confirming the pH was equal to 5 – 6, samples were centrifuged (13,000 x g for 15 min at 4 °C), and the supernatant was used to measure reduced GSH and total GSH. The fluorescence intensities of the samples were determined spectrophotometrically in the FlexStation apparatus (Molecular Devices, USA) according to the manufacturer's guidelines.

The following linear regression obtained changes in fluorescence intensity with GSH concentration:

$$Log(_y) = (A + B) * Log(x)$$

Then, the dilution factor corrected the final concentration (µM) of GSH and/or Total GSH + GSSG. The concentration of GSSG (µM) in the test samples was calculated as the following equation:

$$GSSG = {total\ GSH - GSH}/_2$$

4.5.5. Immunofluorescence

All immunohistochemical procedures followed previously reported protocol with minor modifications (GOMES; ZHU; GRACE, 2019a). In brief, rats were deeply anesthetized with urethane 25% (1 mL/100 g/rat) and transcardially perfused with 0.01 M PBS, followed by 4% PFA in 0.01 M PBS (pH = 7.6). Then, brains were removed, post-fixed in 4% PFA for 2 h, and stored in 30% sucrose. Serial 30 µm-thick coronal sections of the vHip were collected using a cryostat (CM-1900, Leica). For each animal, five to six sections 300 µm apart spanning the rostrocaudal axis of the vHip (within −4.8 mm to −6.3 mm from bregma) were collected and stained. Specifically, sections were incubated in a combination of 1% normal goat serum, 0.1% Triton X-100, rabbit anti-PV antibody (1:2000, Swant, PV 25), biotinylated Wisteria floribunda agglutinin (WFA; 1:1000 dilution, Vector Labs, #B1355) and mouse Anti-8-OxodG antibody (1:500, Abcam, ab62623) for 24 h at 4 °C. The sections were then incubated with a mixture of 1% normal goat serum, goat anti-rabbit Alexa Fluor 488 (1:1000, Abcam, ab150077), Alexa Fluor 594 conjugated to streptavidin (1:1000, Abcam, ab272189), and goat anti-mouse Alexa Fluor 647 (1:1000, Abcam, ab150115). The sections were mounted with Fluoroshield Mounting Medium with DAPI (Abcam, ab104139) to visualize the border of the vSub.

4.5.5.1. Image acquisition and analysis

For image acquisition, the focus was set on PV positive cells for imaging, and digital images were obtained using Leica Application Suite X (Leica Microsystems). Under 20x magnification, the vSub regions of each rostrocaudal section were imaged by z-stacks (512 × 512 µm-images along the medial-temporal axis) using a confocal microscope (SP5, Leica). An abrupt widening of the pyramidal layer defined the border between CA1 and vSub. The boundary between the subiculum and presubiculum was characterized by a sharp reduction in PV intensity and a decrease in cell size visualized by DAPI. For cell count, only the pyramidal cell layers, where most PV interneurons were located, were counted. The exposure time for PV was calibrated such that most

of the PV-positive cells in the naïve group were visible and within the dynamic range, and all subsequent images of the remaining age groups were taken at an identical exposure. Similar techniques were applied to PNN, 8-OxodG, and DAPI to identify optimal exposure time. PNNs were identified by staining for WFA, a lectin that selectively labels residues of glycoproteins within the PNNs. While this does not show the PNN structure explicitly, nor are PNNs located exclusively around PV neurons (LENSJØ et al., 2017), counterstaining for PV enables us to tell if the structure is indeed a perisomatic PNN encompassing PV interneurons.

For analysis, acquired images were first converted to maximum projection (z-stacks). The PV positive cell count was then performed using Fiji software, cell counts plugin. Also, the fluorescence intensity of PNN and 8-OxodG labeling were analyzed in Fiji software. Data were reported as integrated density (arbitrary units, AU). For co-localization analysis, the intensity of a pixel in one channel was evaluated against the corresponding pixel in the second channel of a dual-color image. The Manders' overlap coefficients were obtained using the co-localization threshold plugin in the Fiji software to measure the amount of PV/PNN and PV/8-OxodG co-localization.

4.6. Gene expression profiling from rat vHip

4.6.1. RNA isolation

Following the behavioral tests on PND 51, animals were anesthetized (urethane 25%, 1 mL/100g/rat) and perfused with cold 0.01 M PBS (pH = 7.4). vHip from both hemispheres was collected and snapped frozen in liquid nitrogen until use for RNA extraction (n=8/group). To this end, we used RNAqueous-Micro Total RNA Isolation Kit (ThermoFisher Scientific; #AM1931), according to the manufacturer's instructions.

4.6.2. Bulk-RNA sequencing

The extracted RNA was used for performing the transcriptomic analysis from the vHip of naïve and adolescent-stressed rats (n = 8/group) using bulk RNA barcoding and sequencing, as previously described (ALPERN et al., 2019). Briefly, the RNA samples were reverse transcribed with individual barcoded oligo-dT primers. Then, all samples were pooled together, and the second strand synthesis generated the double-stranded cDNA via the nick translation method. Illumina-compatible libraries were prepared by tag-mentation of 5 ng of full-length double-stranded cDNA. Then, the library was amplified, profiled, and sequenced using the Illumina NextSeq 500 platform.

4.6.3. Transcriptomic analysis

Following a quality assessment with FastQC, gene reads were mapped with HISAT2 onto Rnor_6.0/rn6 genome assembly for *Rattus norvegicus*. Mapped reads were counted for each gene locus using the feature. Counts function of the subread (2.0.2) package. We normalized count data by size factor and applied a variance stabilizing transformation for visualization purposes. Low-abundance genes were removed before data normalization, keeping only genes with at least ten reads in all samples. Subsequently, we performed a generalized linear model to assess differentially expressed genes (DEGs) using the DESeq2 package (LOVE; HUBER; ANDERS, 2014). *p-values* were corrected for multiple testing using the Benjamini–Hochberg method (BENJAMINI; HOCHBERG, 1995). Transcriptomic analysis was performed in R (R Core Team, 2014).

4.6.4. Gene annotation analysis

Only DEGs with p-adj < 0.1 were considered for gene set enrichment analyses. Gene set enrichment analyses were derived from Database for Annotation, Visualization and Integrated Discovery (DAVID) for functional annotation of gene lists (SHERMAN et al., 2022).

4.7. Statistical analyses

All data were subjected to tests to verify the homogeneity of variances (Bartlett's test) and if they followed a normal distribution (Shapiro–Wilk test). Those that met these parameters were subjected to parametric analysis (Student's t-test, one-way or two-way ANOVA followed by post-hoc Turkey's test) and data were expressed as mean ± SEM. Otherwise, they were subjected to nonparametric analysis (Mann-Whitney test) and data were represented as box and whiskers (minimum and maximum value). Significant differences were indicated by $p < 0.05$. In RNA-seq analysis, p-values were corrected using the Benjamini–Hochberg method for multiple testing. Statistical analyses were performed with Prism 8.0 (Graphpad Software Inc.) and R (R Core Team, 2014).

4.7.1. Principal component analysis for behavioral characterization

Behavioral data analysis was performed in R (R Core Team, 2014). Each animal's behavioral z-scores (LBD, SIT, and NOR) were calculated, and their dimensionality was reduced by Principal Component Analysis (PCA). We performed an unsupervised clustering method (k-means) that separated the animals into three clusters for PC1 and PC2.

5. EXPERIMENTAL DESIGN

5.1. Evaluating the impact of adolescent stress on behavior and inhibitory and excitatory neurons

Rats were exposed to adolescent stress protocol from PND 31 until 40 (n = 12). Naïve animals were left undisturbed in their home cages (n = 11). All animals were subjected to behavioral tests (SIT and NOR) one week after the end of stress, from PND 47 to 49. At PND 51, vHip samples were collected for immunohistochemistry (n = 5-6/group). From PND 52 until 63, *in vivo* recordings of pyramidal neurons were performed in the vHip in another group of animals (n = 6/group) (Figure 7).

Figure 7. Experimental design to evaluate the impact of adolescent stress on behavior and inhibitory and excitatory neurons in the vHip
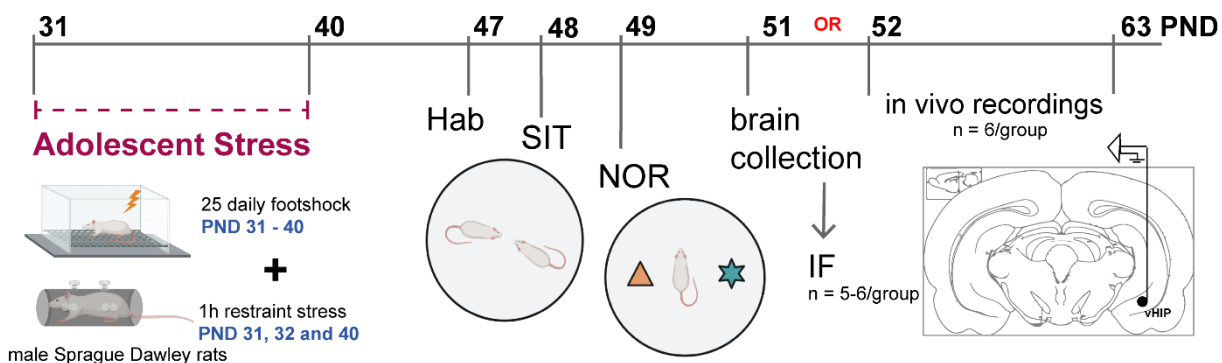
Hab = habituation; SIT = social interaction test; NOR = novel object recognition task; IF = immunofluorescence; PND = postnatal day.

5.2.   Uncovering the impact of stress on mitochondrial function and redox homeostasis in the vHip

One day (PND 41) and ten days (PND 51) after stress protocol, vHip samples were collected to evaluate mitochondrial oxygen consumption (high-resolution respirometry), ROS levels (DHE staining, MitoSOX™, and AmplexRed® assays) and antioxidant enzymes activities (AmplexRed® assay) in naïve and stressed animals (n = 5 – 8/group) (Figure 8).

Figure 8. Experimental design to uncover the impact of stress on mitochondrial function and cellular redox homeostasis in the vHip
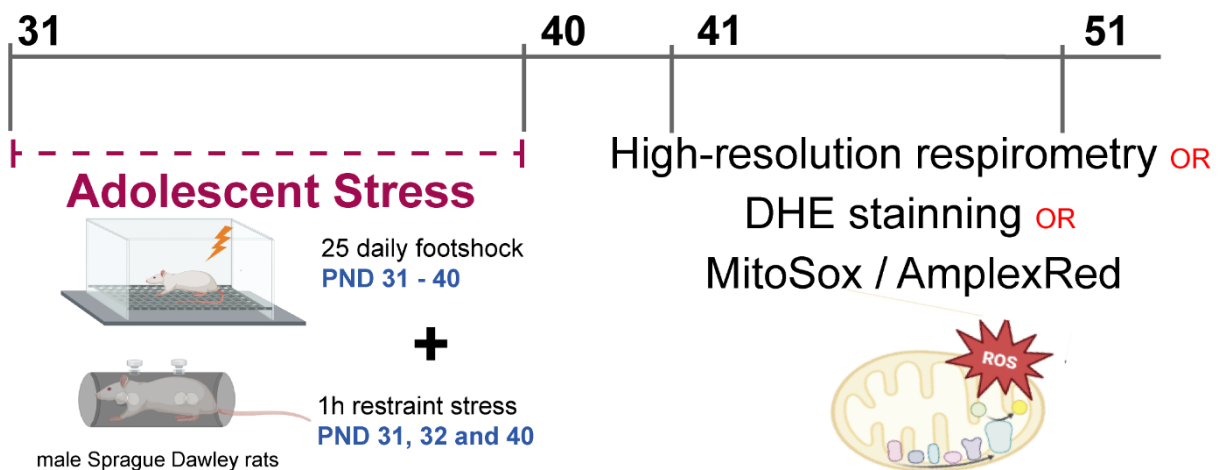
PND = postnatal day.

5.3.　　Investigating GSH/GSSG in serum and vHip of stressed animals

Rats were exposed to adolescent stress from PND 31 until 40 (n = 6). Naïve animals were left undisturbed in their home cages (n = 6). All animals were subjected to behavioral tests (SIT and NOR) one week after stress, from PND 47 to 49. At PND 51, serum and vHip samples were collected (n = 6/group) for GSH/GSSG assay (Figure 9).

Figure 9. Experimental design to investigate GSH/GSSG in serum and vHip of stressed animals
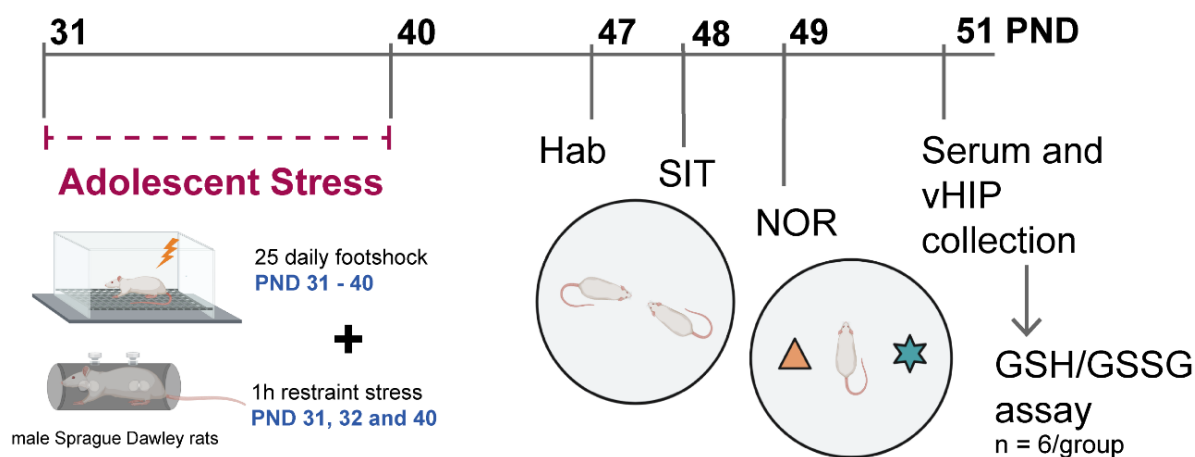
Hab = habituation; SIT = social interaction test; NOR = novel object recognition task; PND = postnatal day.

5.4. Revealing the vHip transcriptomic profile and its correlation with distinct behavioral phenotypes and stress response

Rats were exposed to adolescent stress protocol from PND 31 until 40 (n = 8). Naïve animals were left undisturbed in their home cages (n = 8). One week after stress, all animals were subjected to behavioral tests (EPM, LDB, SIT, and NOR) from PND 47 until 50. At PND 51, vHip samples were collected (n = 5-6/group) for RNA extraction. Then, samples were shipped to the laboratory of Dr. Carmen Sandi, at the Écolé Polytechnique Fédérale de Lausanne, Switzerland, where bulk-RNA sequencing and downstream bioinformatic analyses were performed (n = 8/group) (Figure 10).

Figure 10. Experimental design to describe the transcriptomic profiles of vHip and their correlation with distinct behavioral phenotypes and stress response
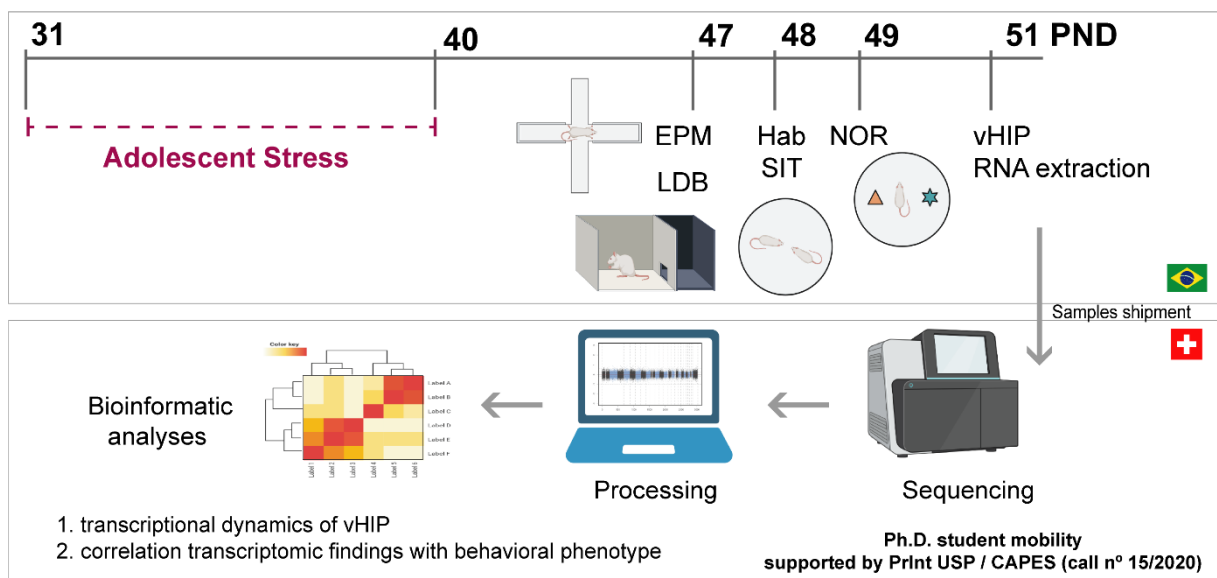
EPM = elevated plus maze; LDB = light – dark box test; Hab = habituation; SIT = social interaction test; NOR = novel object recognition task; PND = postnatal day.

6. RESULTS

6.1. Adolescent stress exposure causes behavioral deficits

We previously showed that the exposure of adolescent rats to combined stressors leads to long-lasting behavioral changes, along with molecular changes that appeared at late adolescence (PND 51) and lasted until adulthood (PND 75)(GOMES; ZHU; GRACE, 2019a). These findings underscore the importance of adolescence as a critical period of vulnerability to long-lasting induced changes. However, it was unknown if behavioral changes were already present in early periods, i.e., during late adolescence. Here, we evaluated the effect of adolescent stress on body weight gain from PND 31 until 47, and sociability and cognitive function during late adolescence (PND 47 – 50).

The combined stressors did not change the percentage of body weight gain (Figure 11.A). However, stressed animals showed reduced social interaction time with an unfamiliar rat (Figure 11.B). In the NOR acquisition trial, there was no difference between the exploration of identical objects placed on the arena's right or left side (Figure 11.C), indicating a lack of spatial preference. Two-way ANOVA revealed an effect of condition (naïve vs. stress), suggesting a possible difference in time of object exploration between groups. However, no significant changes were observed between the exploration of the two objects considering the same condition, i.e. naïve and stress groups (Figure 11.C). In the retention trial, a greater exploration of the novel object was observed in both groups. However, stressed animals showed less exploration of the novel object (Figure 11.D). These findings were reflected in the discrimination index, which was reduced in the stress group (Figure 11.E). Our results reinforce the deleterious impact of adolescent stress on social and cognitive performance.

Figure 11. Effects of stress on body weight gain and behavior
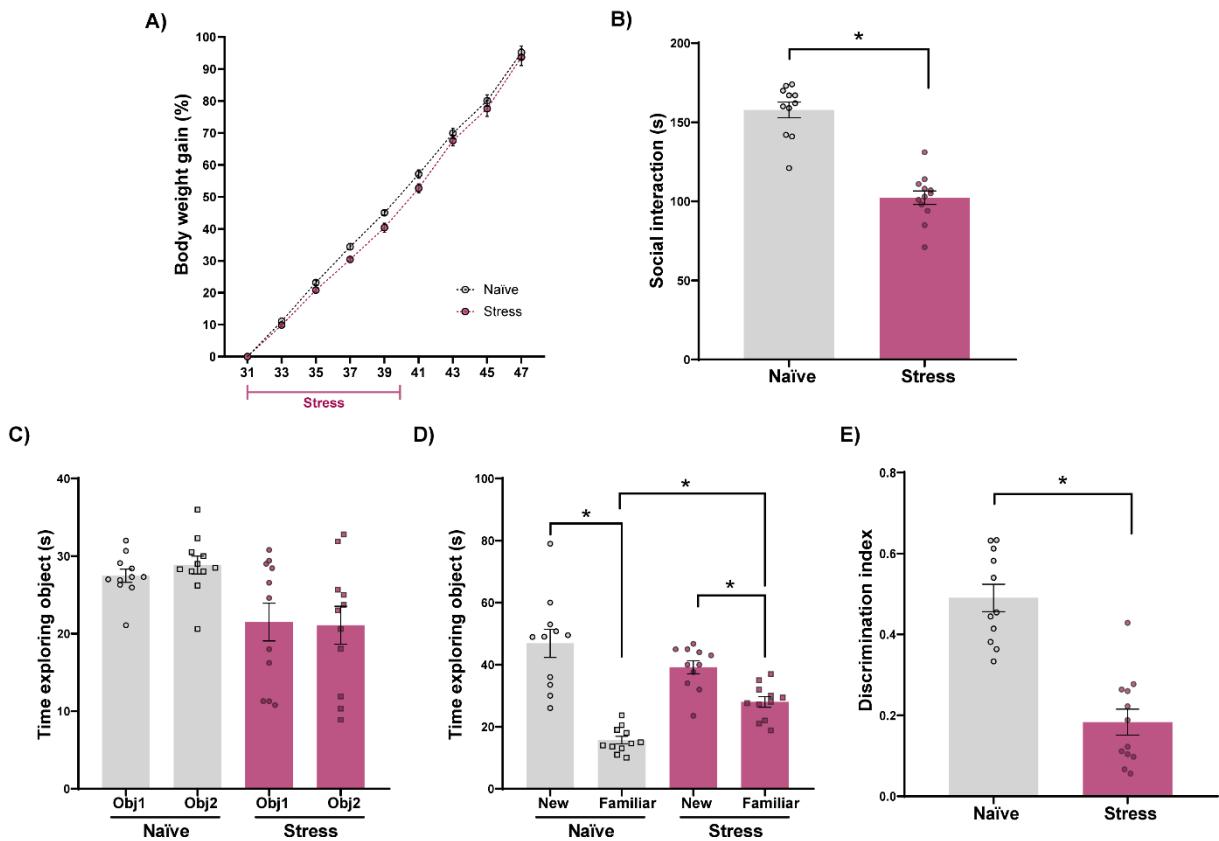
(A) Adolescent stress did not change body weight from PND 31 to PND 47. **(B)** Adolescent stress decreased social interaction time ($t_{21} = 8.46$, $p < 0.0001$). **(C)** All groups explored equally the identical objects placed on the left and right sides of the arena in the acquisition trial (Interaction: $F_{(1,40)} = 0.24$, $p = 0.63$; Object: $F_{(1,40)} = 0.06$, $p = 0.79$; Condition: $F_{(1,40)} = 13.55$, $p = 0.0007$). **(D)** In the retention trial, all groups explored more the novel object (Interaction: $F_{(1,40)} = 13.49$, $p = 0.0007$; Object: $F_{(1,40)} = 60.27$, $p < 0.001$; Condition: $F_{(1,40)} = 0.71$, $p = 0.40$). Stressed animals explored the familiar object more than the naïve group ($p = 0.01$). **(E)** Adolescent stress impacted the discrimination index in the NOR test ($t_{21} = 6.57$, $p < 0.0001$). n = 11-12/group. Data are shown as mean ± SEM. * $p < 0.05$; unpaired t-test or Two-way ANOVA, followed by Tukey's multiple comparison test.

6.2. Effects of adolescent stress on inhibitory and excitatory neurons

During adolescence, PV interneurons are highly vulnerable to stress (GOMES; ZHU; GRACE, 2019a). In addition, the formation of their associated PNNs is not complete until early adulthood (FAWCETT; OOHASHI; PIZZORUSSO, 2019). Here, we evaluated the expression of PV and PNNs in the vHip at PND 51 (following behavioral tests), which corresponds between 1 and 2 weeks after stress exposition. Stress during adolescence decreased the number of PV-positive cells at PND 51 (Figure 12.A) and the fluorescence intensity of PNNs (Figure 12.B). It also impacted the Mander's overlap coefficient of PV-positive cells and PNNs fluorescence, indicating a decreased PV and PNN co-localization (Figure 12.C).

Figure 12. Impact of adolescent stress on vHipp PV interneurons and their associated PNNs
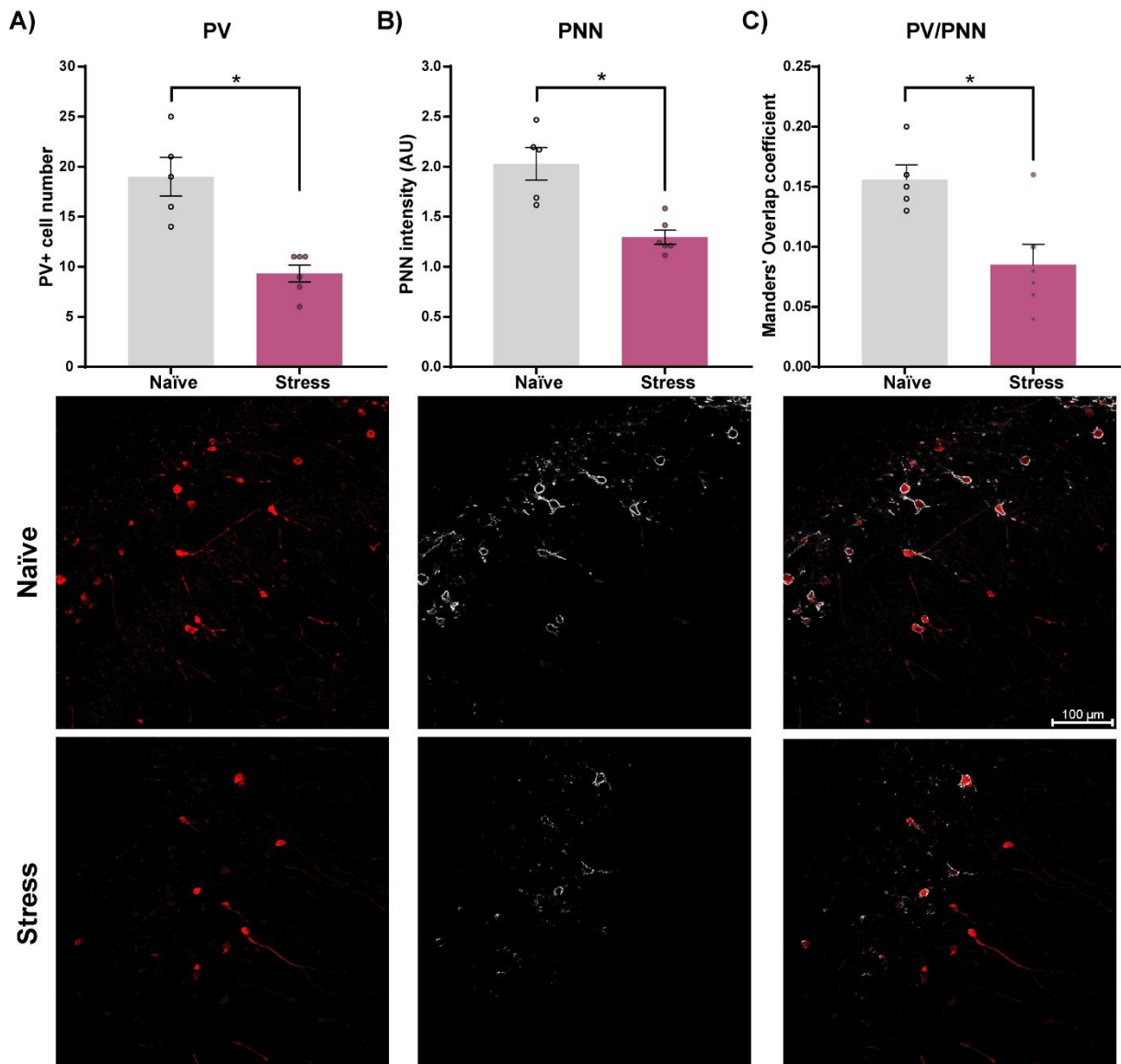
(A) Adolescent stress decreased the number of PV positive cells ($t_9 = 4.90$, p = 0.008), **(B)** PNN fluorescence intensity ($t_9 = 4.43$, p = 0.002), and **(C)** PV/PNN co-localization ($t_9 = 2.67$, p = 0.01). Representative images of the vHip of naïve and stressed animals. n = 5-6/group. Data are shown as mean ± SEM. * p < 0.05; unpaired t-test.

Given that early adolescent stress decreased the number of PV-positive cells, which could change the E/I balance, we recorded the activity of pyramidal neurons in the vHip (PND 52 – 63). An increase in the firing rate of vHip pyramidal neurons observed in stressed animals (Figure 13). These findings indicate that adolescent stress potentially led to E/I dysregulation in the vHip.

Figure 13. Impact of adolescent stress on vHip pyramidal neuron activity
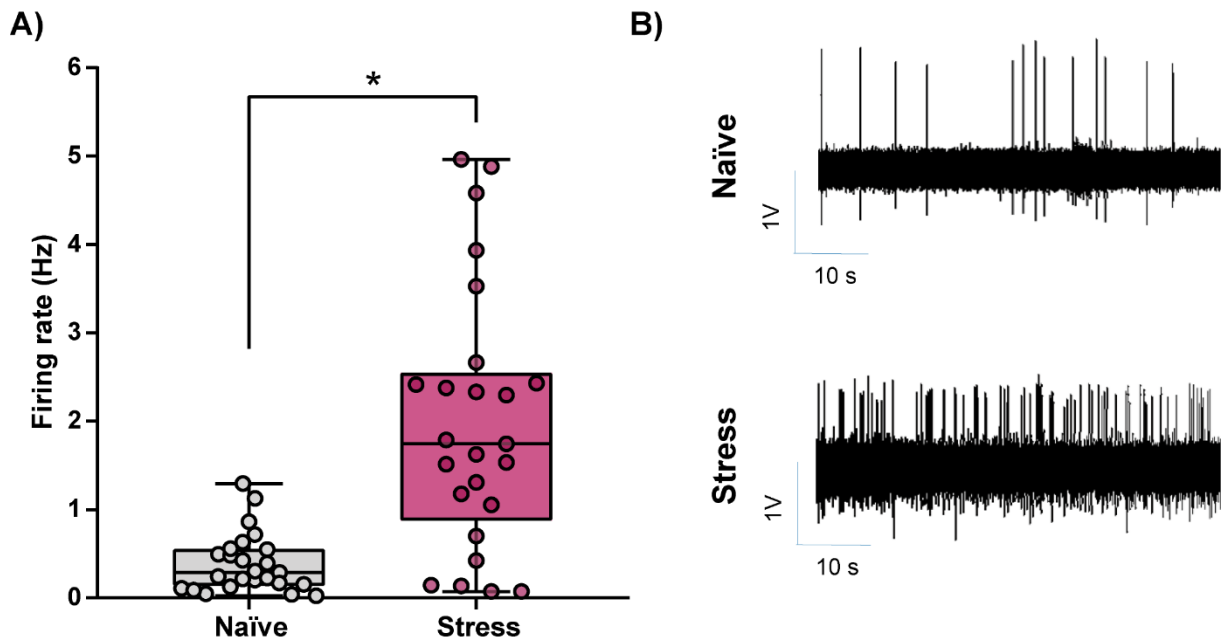
(A) Adolescent stress increased the firing rate of pyramidal neurons in the vHip 1 – 2 weeks after stress (naive group: n = 25 neurons from 6 rats, 0.39 ± 0.06 firing rate; stress group: n = 25 neurons from 6 rats, 1.97 ± 0.30 firing rate). Data are represented as box and whiskers (minimum and maximum value). U = 99; * p < 0.0001; Mann-Whitney test. **(B)** Representative traces of spike activity from vHip pyramidal neurons from naïve and stressed animals.

6.3. Oxidative damage and its co-localization with PV interneurons in the vHip

Converging evidence points to oxidative stress as a pivot in stress-induced behavioral changes (SCHIAVONE et al., 2013). Deleterious cell damage may result from dysregulation in oxidative balance (SALIM, 2017). We performed immunohistochemistry for 8-OxodG, the most common DNA lesions resulting from ROS (HAHM et al., 2022), 10 days after adolescent stress to assess potential cell DNA damage. As expected, stressed animals showed more 8-OxodG fluorescence intensity in the vHip (Figure 14.A), indicating oxidative damage.

PV interneurons are energy-demanding to support high-frequency neuronal synchronization (KANN; PAPAGEORGIOU; DRAGUHN, 2014). Thus, they are vulnerable to redox dysregulation and more prone to oxidative damage after insults (STEULLET et al., 2017). Given that adolescent stress decreased the number of PV-positive cells, we considered PV intensity fluorescence of the region of interest and characterized the degree of overlap with 8-OxodG fluorescence intensity. Manders' overlap coefficient indicated that PV and 8-OxodG co-localization increased after adolescent stress (Figure 14.B), indicating that PV interneurons deficits caused by adolescent stress were accompanied by oxidative stress.

Figure 14. Measurement of oxidative damage in vHip PV interneurons after adolescent stress
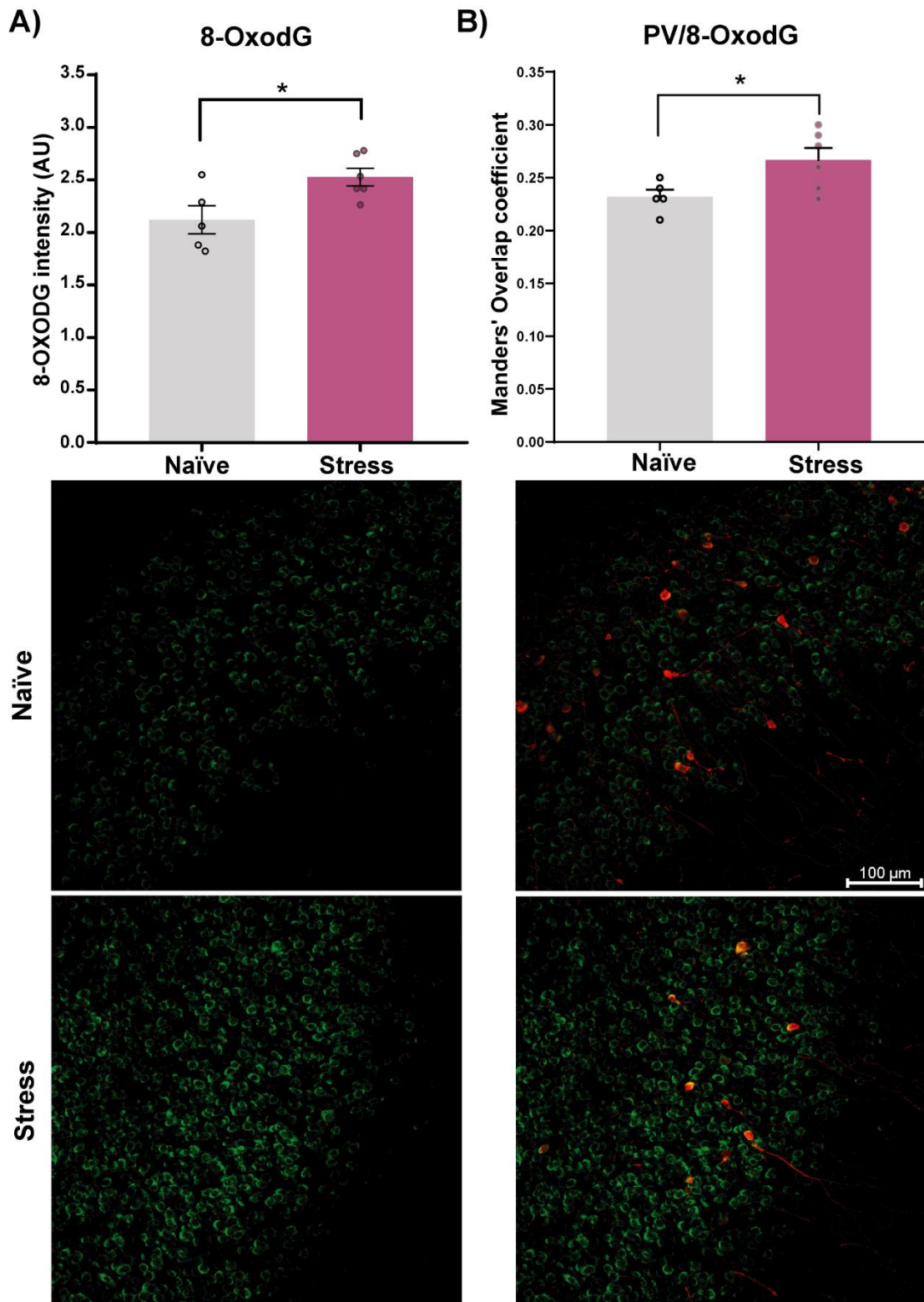
(A) Stress increased the fluorescence intensity of the cell DNA damage marker 8-OxodG ($t_9 = 2.67$, p = 0.02) and (**B**) its co-localization in PV-positive cells ($t_9 = 2.47$, p = 0.03) at PND 51. n = 5–6/group. AU = arbitrary units. Data are shown as mean ± SEM. * p < 0.05; unpaired t-test.

6.4. Behavioral changes caused by adolescent stress correlated with E/I circuit dysregulation and oxidative stress in the vHip

Extensive studies have shown that PV interneurons are essential to support complex behaviors in social and cognitive tasks (FUCHS et al., 2007). To better comprehend the association between behavioral changes, oxidative stress, and E/I balance dysregulation in the vHip, we performed Pearson's correlation analyses of social interaction time (SIT), discrimination index (NOR), and pyramidal neuron activity, PV-positive cell number, PNN and 8-OxodG intensity in the vHip (Figure 15).

Deficits in sociability and cognitive function were associated with decreases in vHip PV-positive cells. In contrast, only social interaction time was correlated with PNN intensity. Better behavioral performance in SIT was negatively correlated with increased 8-OxodG intensity marker and higher pyramidal firing rate. Such correlations were not observed for NOR. In addition, high levels of 8-OxodG were associated with reduced PV-positive cell number and PNN intensity. We also observed a positive correlation between SIT and NOR.

Figure 15. Correlation matrix of behavioral tests and PV-positive cell number, PNN and 8-OxodG intensity and pyramidal neurons firing rate in the vHip
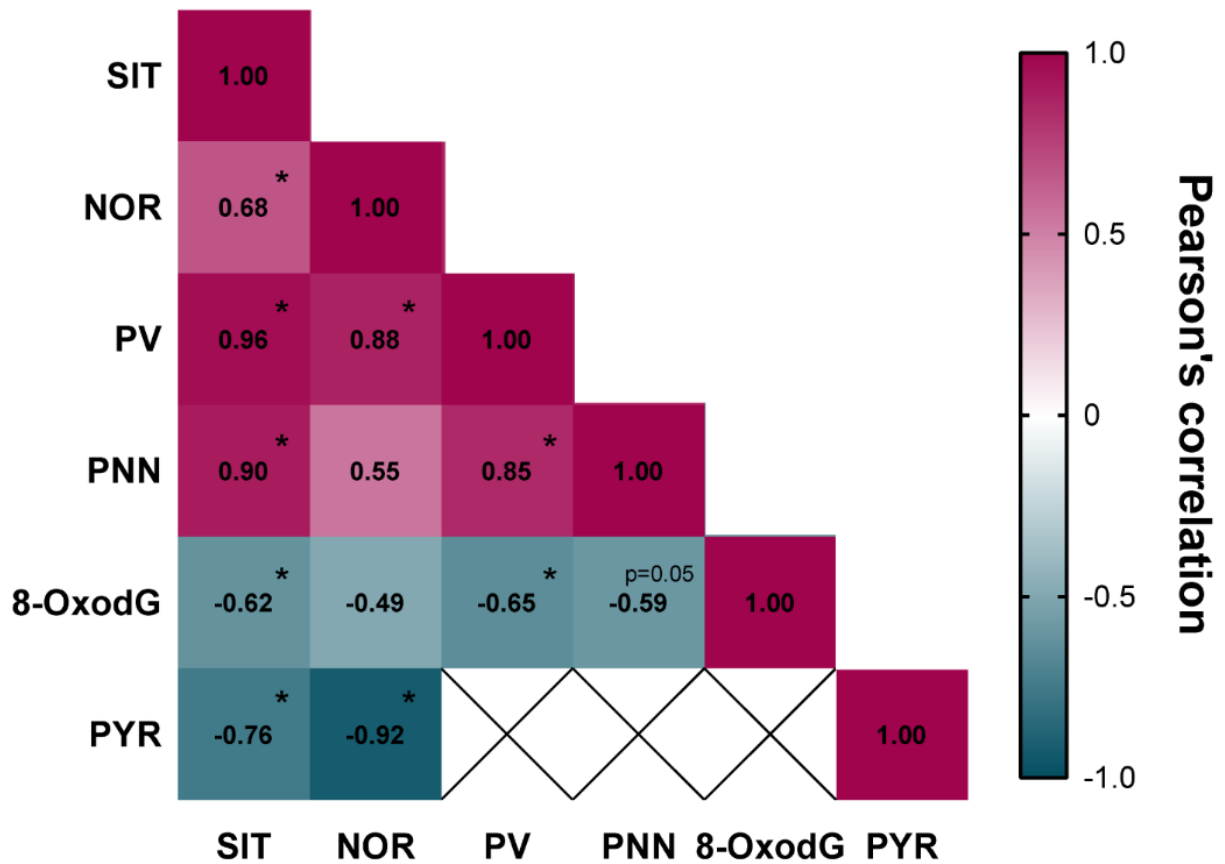
A positive correlation was observed between SIT and NOR; SIT and PV; NOR and PV; SIT and PNN. PYR, and was negatively associated with SIT and NOR, and 8-OxodG. While PV interneurons were negatively associated with 8-OxodG. r values are described in the correlation matrix after Pearson's correlation analysis. * $p < 0.05$. SIT = social interaction test; NOR = novel object recognition; PYR = pyramidal neurons firing rate.

6.5. Adolescent stress leads to mitochondrial respiratory dysfunction

To dynamically characterize the impact of stress on mitochondrial function, we performed high-resolution respirometry of vHip samples one (PND41) and 10 days after the stress (PND51). Stressed animals at PND41 showed increased LEAK respiration (L) and electron transfer capacity (E) (Figure 16.A), indicating increased mitochondrial uncoupling. While at PND51, stressed animals showed decreased oxygen consumption at OXPHOS state (P) (Figure 16.B), indicating reduced mitochondrial OXPHOS capacity in the vHip.

Figure 16. Effects of adolescent Stress on vHip mitochondrial respiration
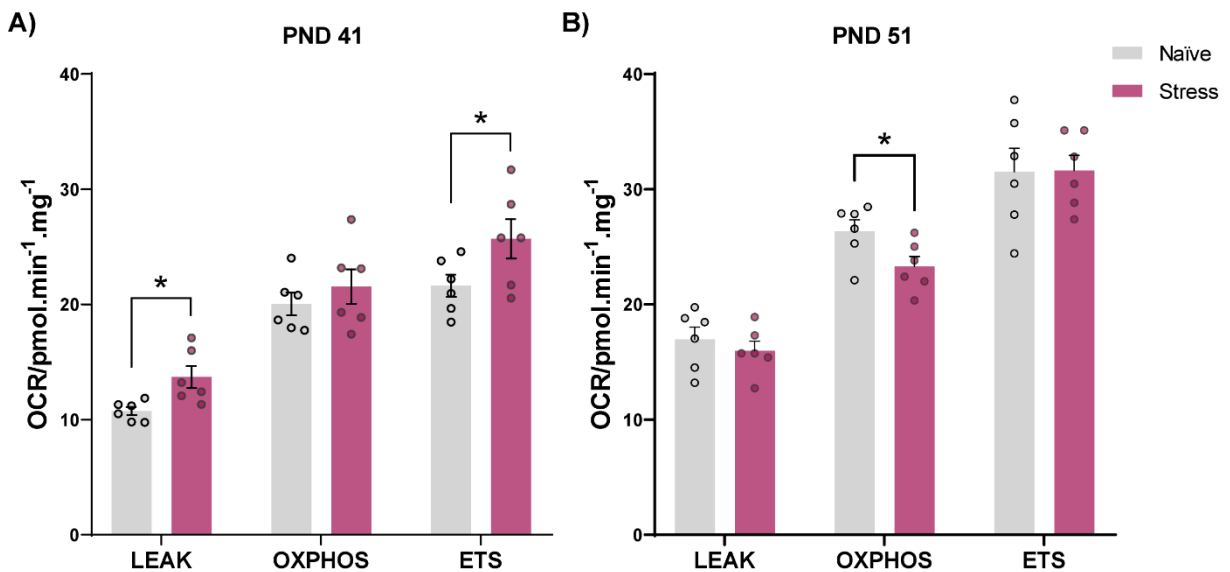
(A) Mitochondrial respiration in the vHip of naïve and stressed animals was evaluated on PND 41 (n = 5–6/group) and PND 51 (n = 6/group). Adolescent stress increased Leak ($t_{10} = 2.91$, $p = 0.01$), without changes in OXPHOS capacity ($t_{10} = 0.83$, $p = 0.42$) and electron transport system capacity (ETS) ($t_{10} = 2.08$, $p = 0.07$). **(B)** At PND 51, stress decreased OXPHOS capacity ($t_{10} = 2.34$, $p = 0.04$) and did not impact Leak ($t_{10} = 0.59$, $p = 0.56$) nor ETS ($t_{10} = 0.12$, $p = 0.91$). Data are shown as mean ± SEM. * $p < 0.05$; unpaired t-test.

6.6.   Adolescent stress induces dysregulation in ROS levels in the vHip

Mitochondrial electron transport is the primary source of ROS, and its dysregulation can lead to changes in ROS levels (LAMBERT; BRAND, 2009). To measure the quantity of superoxide in the vHip, we performed DHE staining in fresh tissue for superoxide from all available sources and MitoSox™ assay for mitochondria-specific superoxide production. We found an increased fluorescence intensity of DHE in the vHip of stressed animals at PND41, and a tendency to decrease at PND 51 (Figure 17.A), indicating higher levels of ROS immediately after the stress protocol. Representative images of DHE staining in the vHip are shown in Figure 17.B. Using the MitoSOX™ probe, we also observed decreased levels of mitochondria-specific superoxide at PND 51, without changes at PND 41 (Figure 17.C).

Figure 17. Impact of adolescent stress on vHip superoxide levels
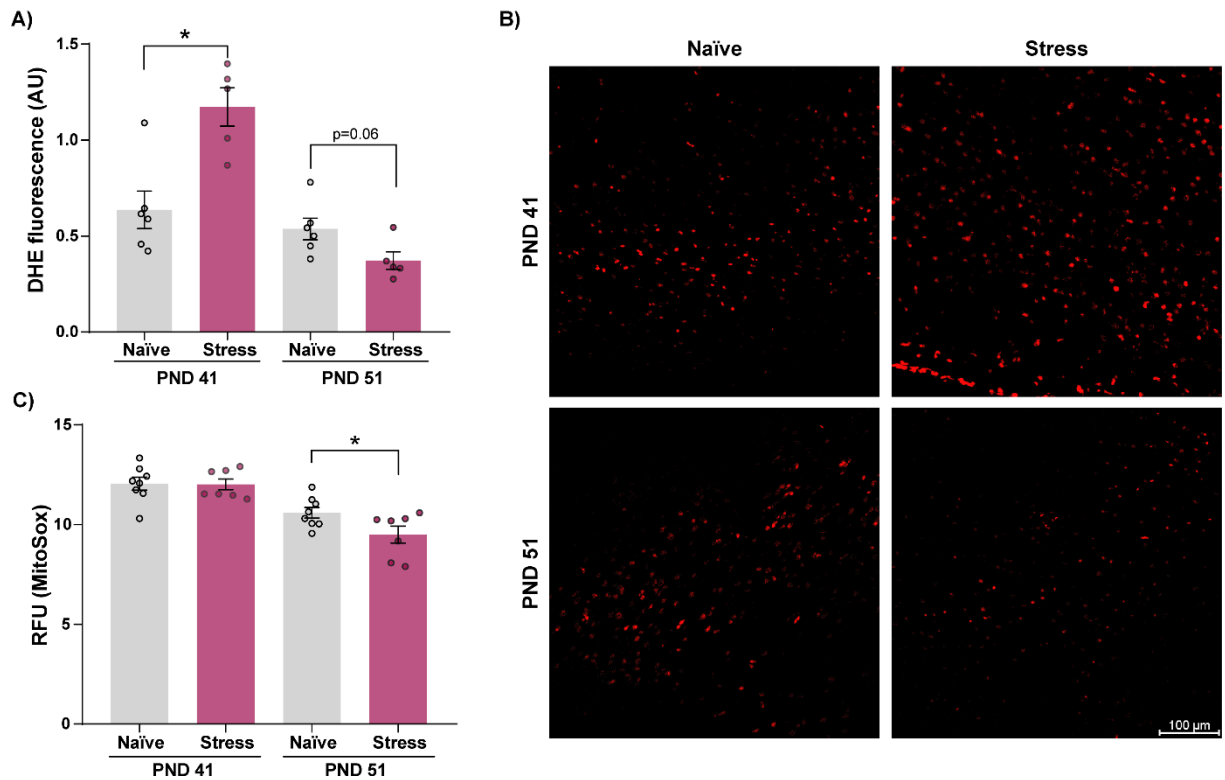
(A) Stress increased *in situ* ROS levels at PND 41 (t_{10} = 3.58, p = 0.006), with a tendency to decrease at PND 51 (t_9 = 5.25, p = 0.0005); n = 5-6/group. **(B)** Representative images of DHE staining (red) in the vHip. AU = arbitrary units. **(C)** Stress did not change mitochondrial $O_2^{\bullet-}$ levels at PND 41 (t_{13} = 0.09, p = 0.92) but decreased at PND 51 (t_{13} = 2.24, p = 0.04). n = 7-8/group. RFU = Relative fluorescent units. Data are shown as mean ± SEM. * p < 0.05; unpaired t-test.

AmplexRed assay has been used to detect hydrogen peroxide released from biological samples (VOTYAKOVA; REYNOLDS, 2001). Here, we did not observe changes in the regression lines' angular coefficient of hydrogen peroxide consumption rate between groups at PND 41 and PND 51 (Figure 18.A). These results indicate that our stress protocol did not impact the release of hydrogen peroxide from vHip cells. On the other hand, adolescent stress increased hydrogen peroxide levels in the initial time point of measurement at PND 41 (Figure 18.B), with no changes at PND 51 (Figure 18.C). Given that mitochondrion generate approximately 90% of cellular ROS (BALABAN; NEMOTO; FINKEL, 2005), these results reinforce the potential impact of adolescent stress on vHip mitochondrial function.

Figure 18. Effects of adolescent Stress on vHip hydrogen peroxyde production and levels
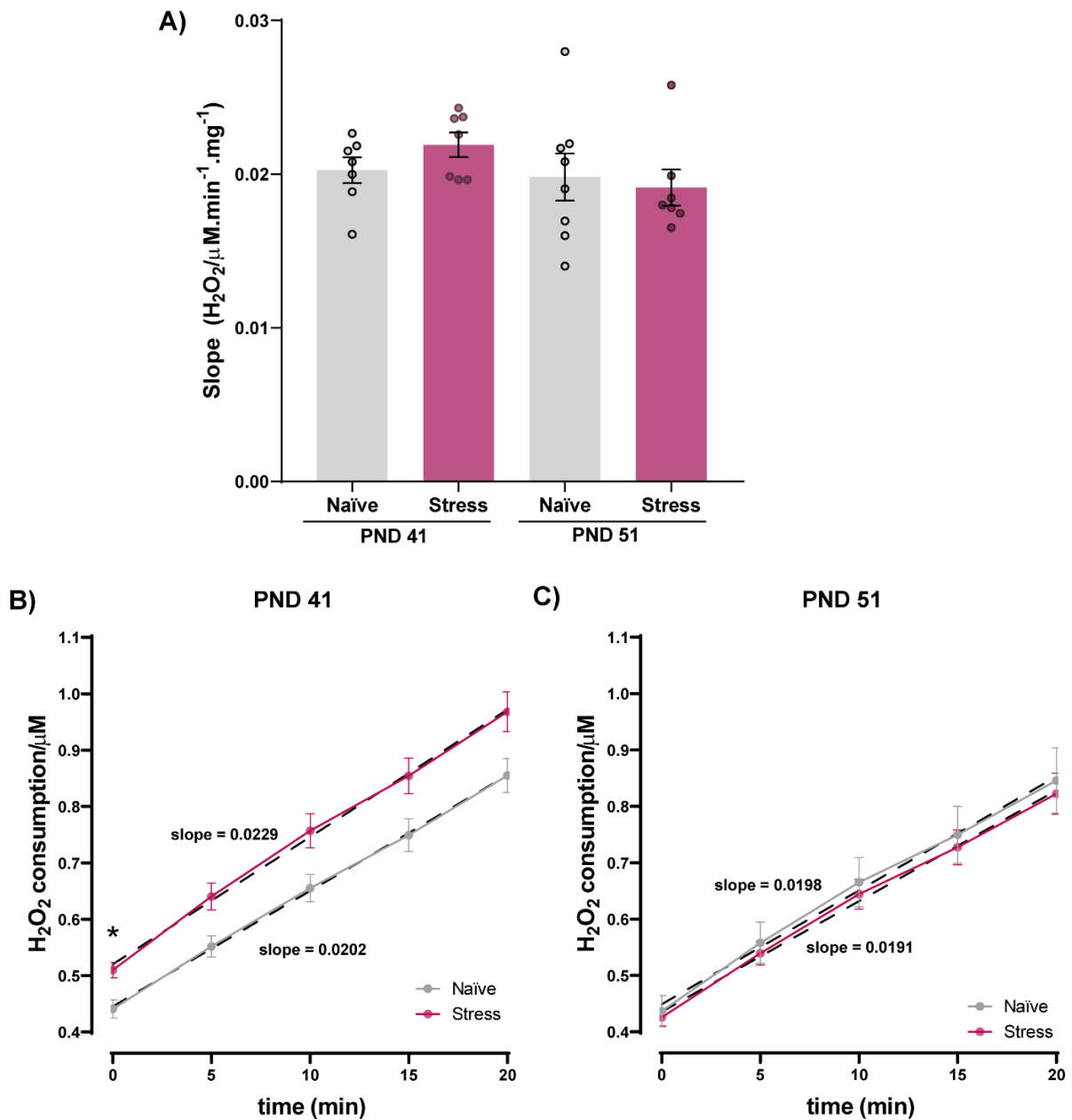
(A) Adolescent stress did not induce changes in the H_2O_2 released rate (slope) from vHip cells at PND 41 ($t_{13} = 1.43$, $p = 0.18$) and PND 51 ($t_{13} = 0.34$, $p = 0.73$). Unpaired t-test. **(B)** At PND 41, H_2O_2 levels were increased in the initial of incubation, time = 0 min. (Interaction: $F_{(4,52)} = 1.857$, $p = 0.13$; Condition: $F_{(1,13)} = 6.89$, $p = 0.02$; Time = $F_{(1.230, 15.99)} = 727.0$, $p < 0.001$), **(C)** with no changes at PND 51 . (Interaction: $F_{(4,52)} = 0.09$, $p = 0.98$; Condition: $F_{(1,13)} = 0.13$, $p = 0.72$; Time = $F_{(1.052, 13.67)} = 389.1$, $p < 0.001$). Two-way ANOVA of repeated measures, followed by Turkey's multiple comparisons. n = 7–8/group. Data are shown as mean ± SEM. * p < 0.05.

6.7. Adolescent stress leads to changes in the antioxidant enzymes

Antioxidant enzymes are important in maintaining physiological redox states since they can stabilize ROS (YANG; LEE, 2015). Stressed animals at PND41 showed increased peroxidase activity, without changes at PND 51 (Figure 19). These results indicate a redox imbalance caused by changes in free radical levels and enzymes that catalyze ROS.

Figure 19. Impact of adolescent stress on antioxidant peroxidase enzymes in the vhip
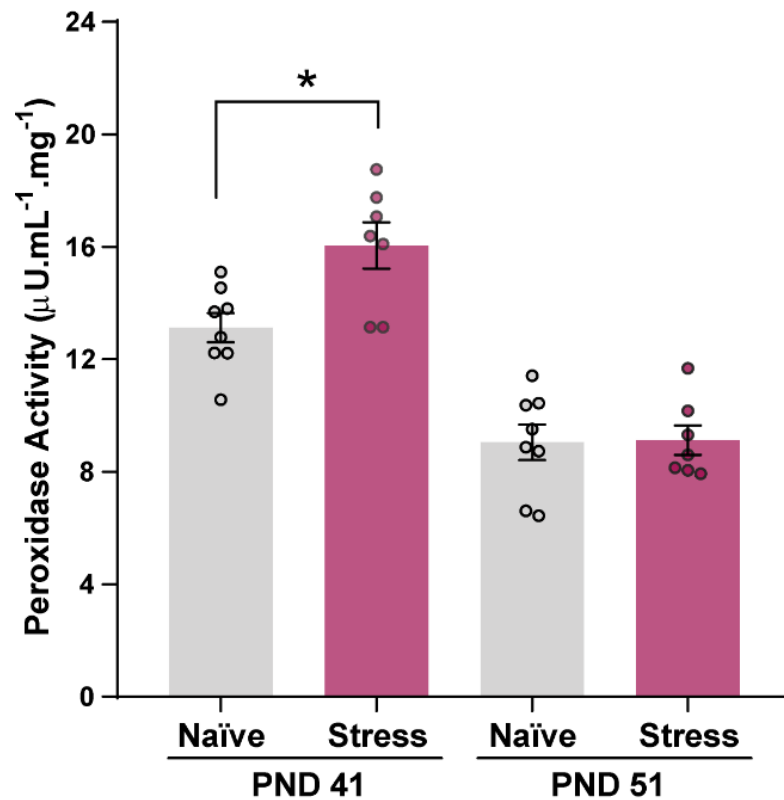
Stress during adolescence increased peroxidase activities at PND 41 (t_{13} = 3.104, p = 0.008), without changing it at PND 51 (t_{13} = 0.01, p = 0.92). n = 7–8/group. Data are shown as mean ± SEM. * p < 0.05; unpaired t-test.

6.8. Effects of adolescent stress on GSH and GSSG in the vHip and serum

GSH is the principal endogenous antioxidant that maintains the body's redox balanceincluding the brain (AOYAMA, 2021; PERKINS; JEFFRIES; DO, 2020). The GSH system is a key regulator of the redox state of PV interneurons (PERKINS; JEFFRIES; DO, 2020). In the presence of H_2O_2, GSH reduces the hydroxyl radical present in the molecule through glutathione peroxidase action and consequently is oxidized (GSSG)(DRINGEN; HIRRLINGER, 2003). Here, we evaluated total, reduced GSH and GSSG in the vHip and serum of naïve and stressed animals at PND 51 following behavioral tests.

As previously reported in this study, stress-induced loss of sociability and cognitive impairment (Figure 20.A – B). In the vHip, stress tended to increase total GSH (Figure 20.C), without changes in reduced GSH (Figure 20.D) and GSSG (Figure 20.E). In contrast, stressed animals showed high levels of total and reduced GSH (Figure 20.F – G), and GSSG (Figure 20.H) in serum at PND 51. These results highlight that stress also impacted the antioxidant defenses in adolescent animals' brain and peripheral system.

Figure 20. Impact of adolescent stress on GSH and GSSG in the vHip and serum
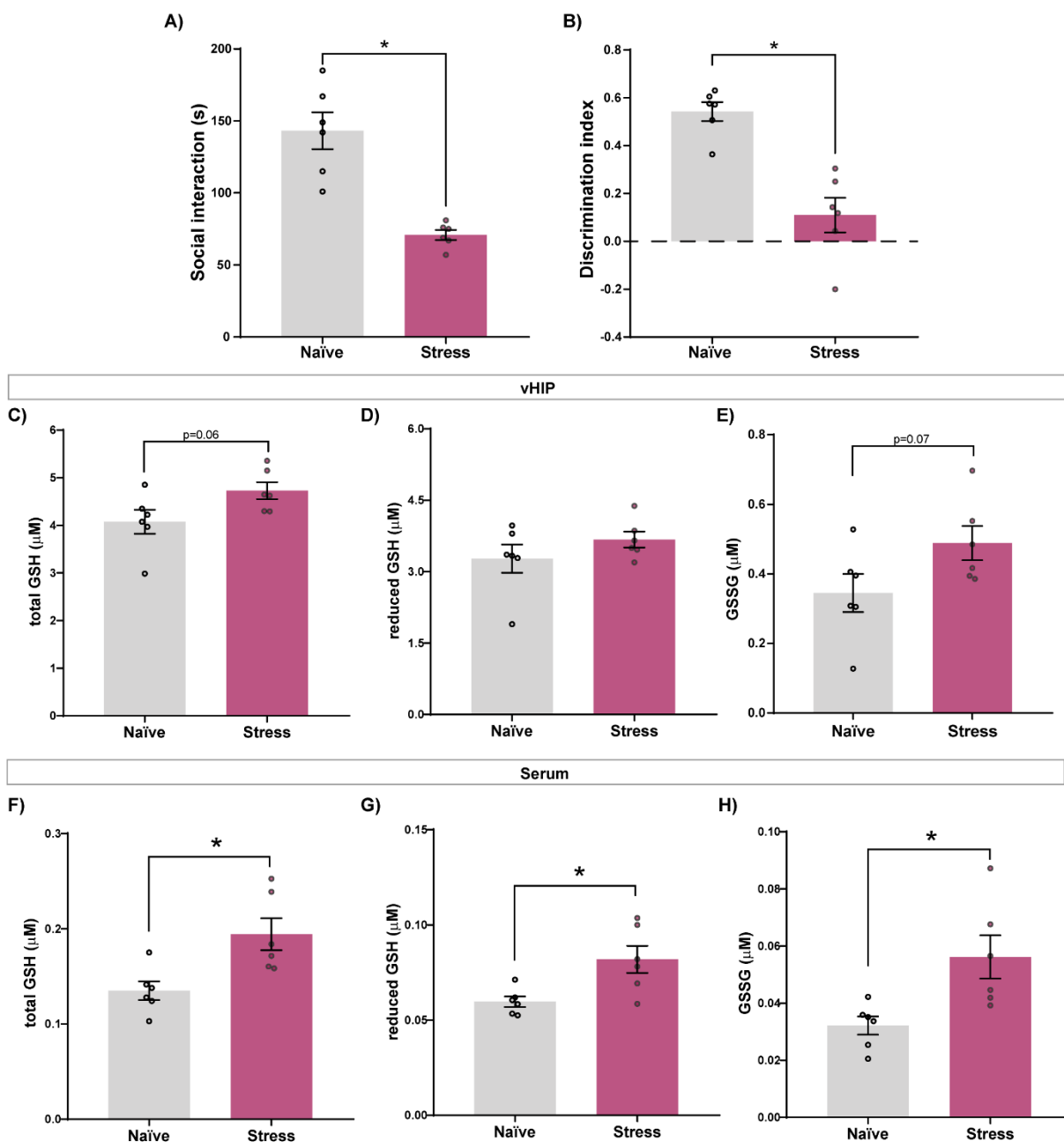
(A) Stress reduced social interaction time ($t_{10} = 5.45$, $p = 0.003$) and (B) discrimination index in the NOR test ($t_{10} = 5.27$, $p < 0.001$). (C) Stress tends to increase total GSH levels in the vHip ($t_{10} = 2.11$, $p = 0.06$), (D) without changes in reduced GSH ($t_{10} = 1.17$, $p = 0.26$) and (E) GSSG ($t_{10} = 1.95$, $p = 0.07$). While in the serum, stressed animals showed increased levels of (F) total GSH ($t_{10} = 3.06$, $p = 0.01$), (G) reduced GSH ($t_{10} = 2.91$, $p = 0.01$) and (F) GSSG ($t_{10} = 2.92$, $p = 0.01$). n = 6/group. Data are shown as mean ± SEM. * $p < 0.05$; unpaired t-test.

64

We performed a Pearson correlation analysis to comprehend better the association between behavioral changes and GSH and GSSG levels in the vHip and serum (Figure 21). A negative correlation was observed between: SIT and tGSH (vHip and serum); SIT and rGSH (serum); SIT and and GSSG (serum), suggesting that animals with better sociability showed lower levels of GSH and GSSG. Similar results were found for NOR. While a positive correlation was observed between: tGSH (vHip) and rGSH (vHip); tGSH (vHip) and tGSH (serum); tGSH (vHip) and GSSG (serum); tGSH (serum) and GSSG (serum); GSSG (vHip) and GSSG (serum).

Figure 21. Correlation matrix of behavioral tests and GSH and GSSG levels in the vHip
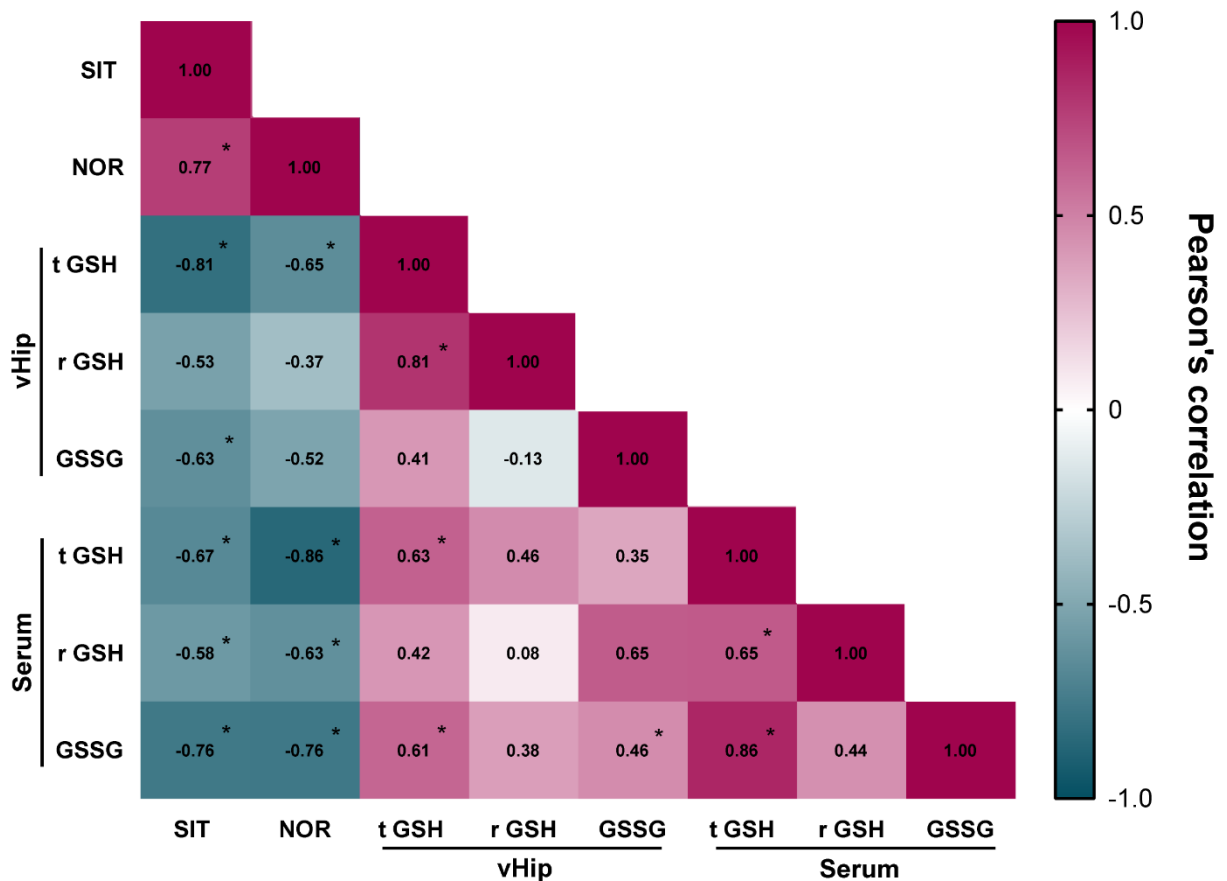
A negative correlation was observed between: SIT and tGSH (vHip and serum); SIT and rGSH (serum); SIT and GSSG (serum). Similar results were found for the discrimination index in the NOR test. While a positive correlation was observed between: tGSH (vHip) and rGSH (vHip); tGSH (vHip) and tGSH (serum); tGSH (vHip) and GSSG (serum); tGSH (serum) and GSSG (serum); GSSG (vHip) and GSSG (serum). r values are described in the correlation matrix. * p < 0.05. Pearson's correlation analysis. SIT = social interaction test; NOR = novel object recognition; tGSH = total GSH; rGSG = reduced GSH.

6.9. Revealing individual behavioral variability during adolescence

Previous studies indicate that adolescent animals exhibit significant variability in neuronal dynamics, affecting behavioral phenotypes related to decision-making strategies and skill learning (CARAS; SANES, 2019; DEMIDENKO et al., 2020; GOLDENBERG et al., 2017). However, individual phenotypic differences linked to behavioral performance in adolescent animals are still understudied. Here, we investigated individual differences in late adolescence considering three behavioral domains (anxiety, sociability and cognitive function) and their modulation by a previous stress exposure in early adolescence.

First, we performed a behavioral characterization comparing naïve and stress animals. Although no change was observed in the EPM (Figure 22.A – C), stressed animals spent less time in the light zone of the LDB, indicating an anxiogenic-like response (Figure 22.D). Moreover, stressed animals showed loss of sociability (Figure 22.E) and a lower discrimination index in the NOR test than naïve animals (Figure 22.F). After applying a z-normalization for all behavioral parameters to integrate data from all tests in a single index, the integrated behavioral z-scores (Figure 22.G) and a heatmap of z-normalized behavioral data (Fig. 22.I) revealed a high intra-group variability for naïve animals. In contrast, stressed animals are narrowly distributed, alluding to stress's detrimental and more homogenous impacts.

Figure 22. Effects of stress on adolescent behavior
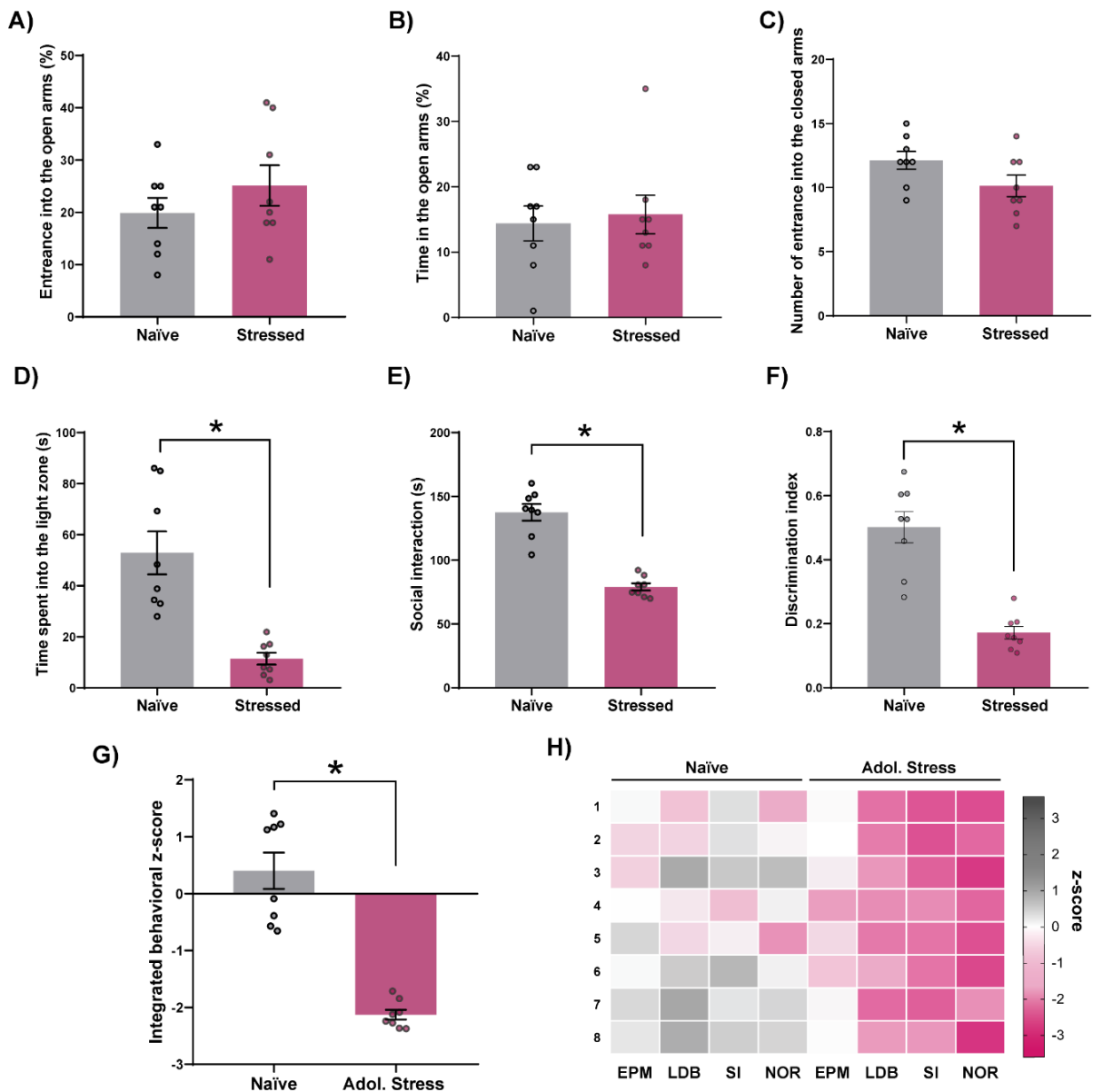
(A) Adolescent stress did not change the % of entries ($t_{14} = 1.08$, $p = 0.30$) and (B) time spent in the open arms ($t_{14} = 0.35$, $p = 0.73$), and (C) number of entries into the closed arms of the EPM ($t_{14} = 1.85$, $p = 0.09$). (D) Adolescent stress decreased time spent in the light zone of the LDB ($t_{14} = 4.74$, $p = 0.0003$), (E), social interaction time ($t_{14} = 8.33$, $p < 0.0001$), and (F) the discrimination index in the NOR test ($t_{14} = 6.30$, $p < 0.0001$). (G) Integrated z-score computed from the scores of the EPM, LDB, SIT, and NOR, and (H) a heatmap of each behavioral z-score indicates the impact of adolescent stress on behavior. n = 8/group. Data are shown as mean ± SEM. * $p < 0.05$; unpaired t-test.

To better understand behavioral variability in naïve and stressed animals, we performed a principal component analysis (PCA) on the z-normalized behavioral scores. Clustering analysis for the first and second principal components (PC) separated animals into three groups (Figure 23.A). PC1 (80.7% explained variance) composition was mainly determined by the time spent in the light zone of the LDB (38.5%) and social interaction time (35.4%). In contrast, for PC2 (14.4% explained variance) discrimination index in the NOR test overweighed (60.9%) (Figure 23.B). Remarkably, clusters 1 and 2 are composed of naïve animals, separated by the contribution of PC2. Stressed animals comprise cluster 3, a distinct group related to PC1 values. We refer to these three groups as naïve higher-behavioral z-score (HBZ), naïve lower-behavioral z-score (LBZ), and stressed animals, according to their respective behavioral phenotypes (Figure 23.C).

Compared to naïve HBZ, naïve LBZ showed unaltered exploration of open and enclosed arms of the EPM (Figure 23.D – F) but decreased time spent in the light zone of the LDB (Figure 23.G), reduced social interaction time (Figure 23.H), and deficits in the NOR test (Figure 23.I). Except for the EPM, stressed animals showed marked impairments in all behavioral tests, which differed from both naïve groups (Figure 23.G – I). Therefore, these data further indicate that adolescent naïve animals cluster into two distinct behavioral phenotypes, and stress affects all exposed animals constituting a third separate cluster.

Figure 23. Animals cluster into three groups based on behavioral phenotypes
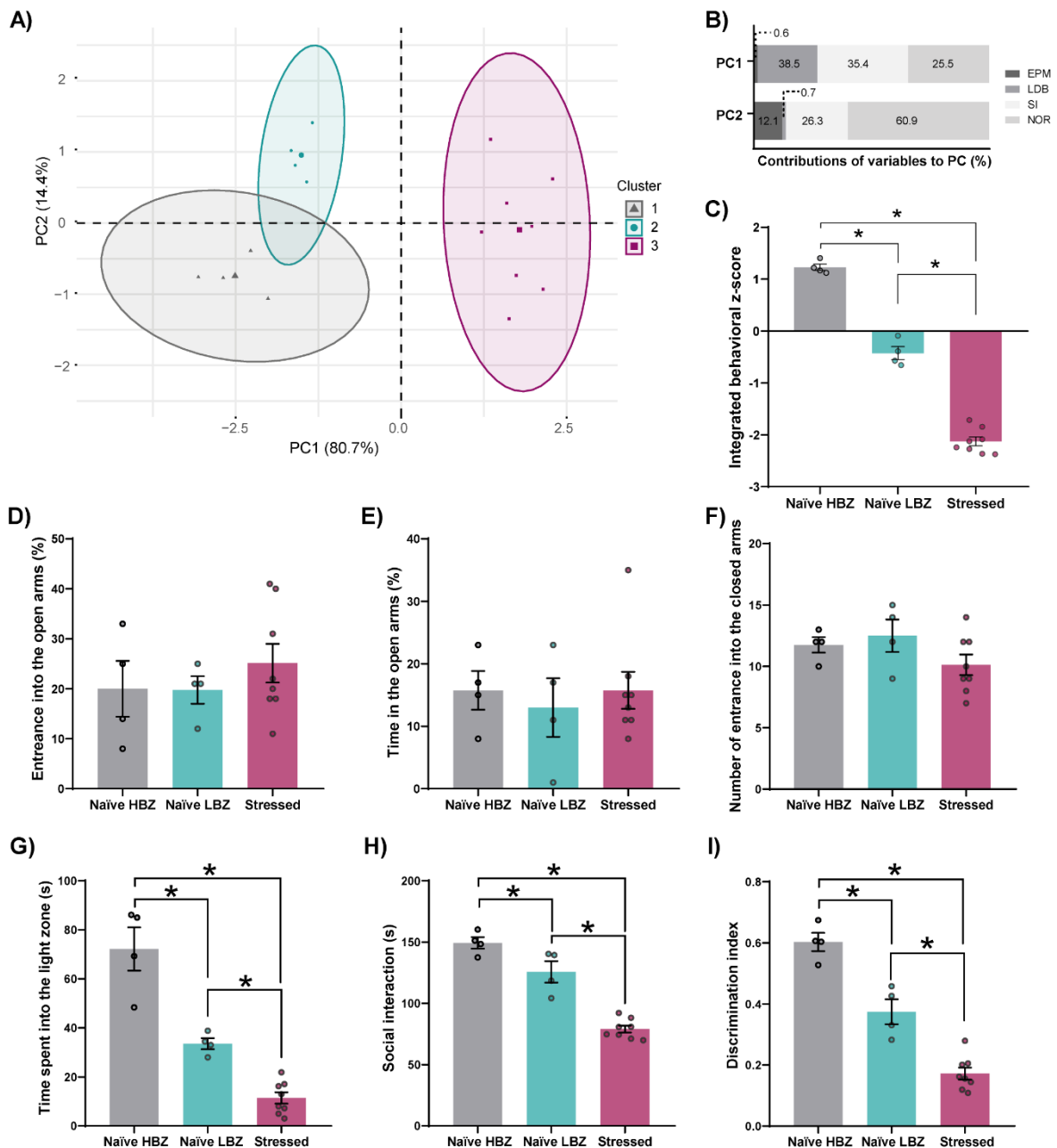
(A) Expression of significant PCs after behavioral analyses. Dots represent integrated z-scores from the four behavioral paradigms for each rat. Three groups of individuals (gray, blue, and purple dots) were separated by unsupervised k-meaning clustering (n = 4 naïve HBZ, n = 4 naïve LBZ, n = 8 stressed). **(B)** Representative contributions of each behavioral paradigm to the two PCA components. **(C)** Intergroup comparisons of the integrated behavioral z-score: naïve HBZ, naïve LBZ and stressed animals ($F_{2,13} = 422.5$, $p < 0.0001$). **(D)** No differences were observed among groups in the % of entries ($F_{2,13} = 0.55$, $p = 0.59$) and **(E)** time spent into the open arms ($F_{2,13} = 0.17$, $p = 0.85$), and **(F)** number of entries into the closed arms of the EPM ($F_{2,13} = 1.72$, $p = 0.22$). Naïve LBZ and stressed animals **(G)** spent less time in the light zone of the LDB test ($F_{2,13} = 49.26$, $p < 0.0001$), and **(H)** presented reduced sociability ($F_{2,13} = 58.92$, $p < 0.0001$). Also, **(I)** both groups displayed a decreased discrimination index in the NOR test ($F_{2,13} = 62.91$, $p < 0.0001$). Data are shown as mean ± SEM. * $p < 0.05$; one-way ANOVA, followed by Tukey's multiple comparison test.

6.10. Transcriptomic analysis reveals changes in mitochondrial-associated genes in the vHip

Given that cluster analysis uncovered variable behavioral phenotypes among naïve animals, we hypothesized that this variability and impinged by stress would reflect changes in the vHip gene expression profiles. Applying a hypothesis-free transcriptomic analysis of the vHip, we performed a series of analyses contrasting two groups at a time (naïve LBZ vs. naïve HBZ; stressed vs. naïve HBZ; stressed vs. naïve LBZ).

Considering DEGs p-value < 0.05, we found 545 DEGs (299 down-regulated and 246 up-regulated) in naïve LBZ (Figure 24.A) and 882 DEGs (430 down-regulated and 452 up-regulated) in stressed animals (Figure 24.B) compared to naïve HBZ. Also, stressed animals displayed 482 DEGs (257 down-regulated and 225 up-regulated) compared with naïve LBZ (Figure 24.C). After applying Benjamini–Hochberg method, DEGs padj < 0.1 were considered for further analysis. Therefore, we found 12 DEGs in naïve LBZ compared to naïve HBZ (Figure 24.D), while stressed vs. naïve HBZ comparison revealed 21 DEGs (Figure 24.E). In contrast, no DEGs (padj < 0.01) were found comparing stress and naïve LBZ groups. Table 1 summarizes the DESeq2 analysis of DEGs padj < 0.1.

Figure 24. Gene expression changes in the vHip of naïve LBZ and stressed animals
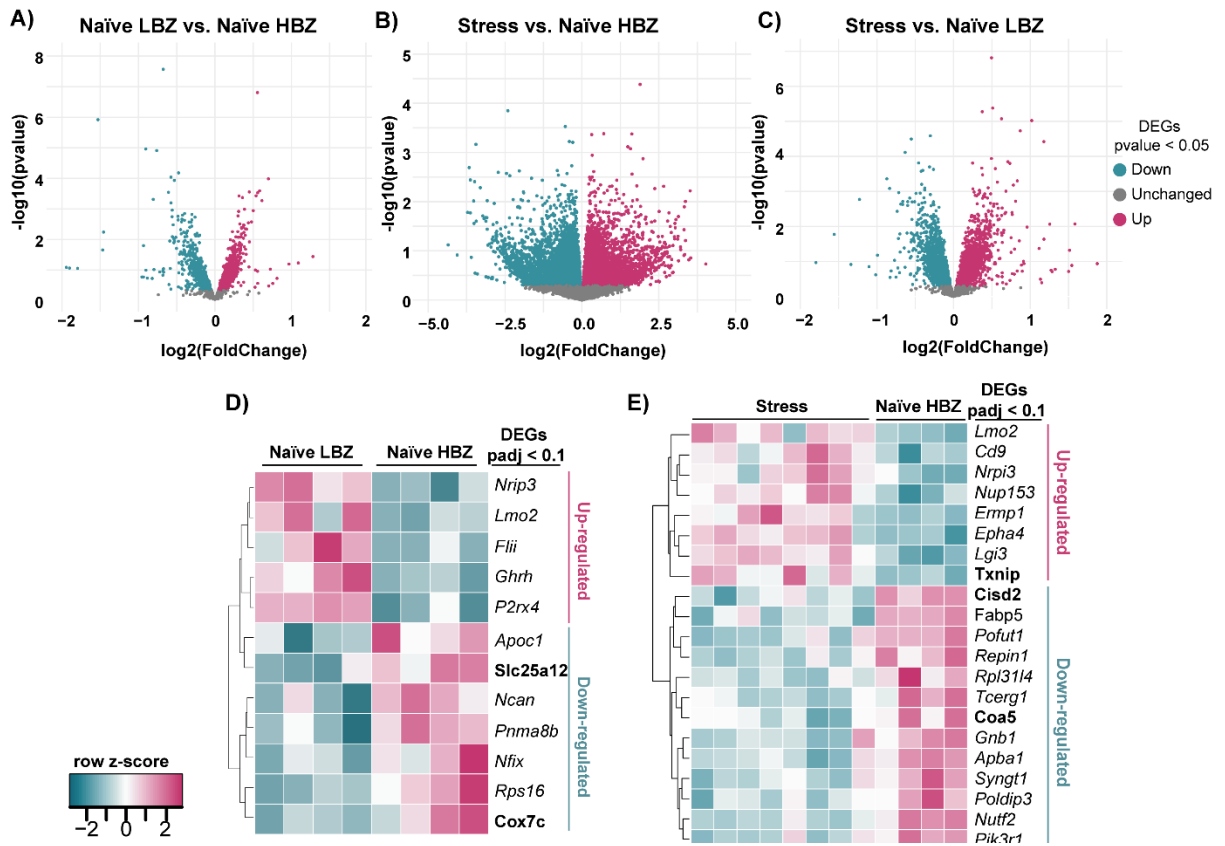
Volcano plot of DEGs (p-value < 0.05) in the vHip comparing **(A)** naïve LBZ vs. naïve HBZ, **(B)** stress vs. naïve HBZ and **(C)** stress vs. naïve LBZ. Heatmap of normalized mRNA DEGs (padj < 0.1) in the vHip comparing **(D)** naïve LBZ vs. naïve HBZ and **(E)** naïve HBZ vs. stressed animals. The DEGs up and down-regulated are described in their respective heatmaps. Mitochondria-associated DEGs are highlighted in black font. The dendrograms represent the hierarchical clustering of genes according to gene expression (Euclidean distance method).

Table 1. Results of the differential expression analysis using DESeq2 in the vHip of Naïve LBZ vs Naïve HBZ and Stressed vs. Naïve HBZ

DESeq2 analysis	Gene	baseMean	log2FC	lfcSE	stat	pvalue	padj
Naïve LBZ vs. Naïve HBZ	Ghrh	285.76	0.70	0.18	3.86	0.0001	0.0531
	Lmo2	134.90	0.59	0.16	3.63	0.0003	0.0972
	Flii	256.79	0.56	0.16	3.60	0.0003	0.0972
	Nrip3	1334.74	0.56	0.11	5.23	< 0.0001	0.0002
	P2rx4	253.81	0.45	0.12	3.61	0.0003	0.0972
	Rps16	1938.98	-0.48	0.12	-3.97	0.0001	0.0436
	Cox7c	430.45	-0.53	0.14	-3.83	0.0001	0.0539
	Nfix	754.82	-0.58	0.15	-3.89	0.0001	0.0528
	Ncan	343.18	-0.61	0.17	-3.60	0.0003	0.0972
	Apoc1	325.89	-0.76	0.18	-4.35	< 0.0001	0.0095
	Pnma8b	151.64	-0.90	0.21	-4.38	< 0.0001	0.0095
	Slc25a12	274.41	-1.53	0.32	-4.84	< 0.0001	0.0014
Stress vs. Naïve HBZ	Txnip	100.36	0.63	0.16	-3.95	0.0001	0.0609
	Lmo2	155.24	0.55	0.13	-4.16	< 0.0001	0.0316
	Ermp1	265.81	0.46	0.12	-3.78	0.0002	0.0837
	Nrip3	1463.43	0.42	0.12	-3.65	0.0003	0.1000
	Cd9	464.01	0.40	0.11	-3.66	0.0003	0.0996
	Nup153	437.05	0.31	0.08	-3.72	0.0002	0.0980
	Lgi3	418.44	0.30	0.07	-4.21	< 0.0001	0.0293
	Epha4	530.96	0.26	0.07	-3.68	0.0002	0.0982
	Rpl31l4	1045.43	-0.25	0.07	3.78	0.0002	0.0837
	Pik3r1	286.56	-0.37	0.10	3.70	0.0002	0.0980
	Fabp5	1009.62	-0.37	0.08	4.55	< 0.0001	0.0140
	Tcerg1	153.67	-0.49	0.13	3.86	0.0001	0.0828
	Cisd2	271.27	-0.49	0.09	5.25	< 0.0001	0.0012
	Syngr1	629.15	-0.51	0.11	4.60	< 0.0001	0.0140
	Gnb1	1150.77	-0.55	0.15	3.69	0.0002	0.0980
	Poldip3	294.84	-0.63	0.14	4.45	< 0.0001	0.0151
	Apba1	167.01	-0.71	0.19	3.81	0.0001	0.0837
	Nutf2	64.44	-0.73	0.19	3.78	0.0002	0.0837
	Coa8	58.94	-0.87	0.20	4.28	< 0.0001	0.0246
	Repin1	91.57	-1.02	0.23	4.43	< 0.0001	0.0151
	Pofut1	36.11	-1.18	0.29	4.12	< 0.0001	0.0334

Gene (ensemble gene symbol), baseMean (mean of normalized counts for all samples), log2F (log2 fold change), lfcSE (standard error of log2FC), stat (Wald test statistic), pvalue (p-value), padj (Benjamini- Hochberg adjusted p-values).

Next, we aimed to identify mitochondria-associated genes. By assessing functional gene annotation, we found 2 mitochondria-associated genes in naïve LBZ compared to naïve HBZ, that were down-regulated (*Slc25a12* and *Cox7c*). Comparison of stressed and naïve HBZ groups revealed 3 mitochondria-associated genes, in which *Cisd2* and *Coa5* were downregulated, and *Txnip* was up-regulated in stressed animals. Table 2 summarizes putative gene set enrichment, in which mitochondria-associated genes might contribute to biological processes and cellular components.

Table 2. Functional annotation of mitochondria-associated genes

Gene Symbol	Gene Ontology	Putative gene set enrichment
Slc25a12	BP	glutamate biosynthetic process (GO:0006537) positive regulation of glucose metabolic process (GO:0010907) neutral amino acid transport (GO:0015804) aspartate transport (GO:0015810) L-glutamate transport (GO:0015813) positive regulation of myelination (GO:0031643) response to calcium ion (GO0051592) negative regulation of glucose catabolic process to lactate via pyruvate (GO:1904024) positive regulation of ATP biosynthetic process (GO:2001171)
	CC	mitochondrion (GO:0005739) mitochondrial inner membrane (GO:0005743) membrane (GO:0016020)
Cox7c	BP	mitochondrial electron transport (GO:0006123)
	CC	mitochondrial respiratory chain complex IV (GO:0005751) integral component of membrane (GO:0016021) mitochondrial membrane (GO:0031966)
Coa5	BP	mitochondrial respiratory chain complex IV assembly (GO:0033617)
	CC	mitochondrion (GO:0005739)
Cisd2	BP	mitophagy (GO:0000422) multicellular organism aging (GO:0010259) regulation of autophagy (GO:0010506)
	CC	mitochondrial outer membrane (GO:0005741) endoplasmic reticulum membrane (GO:0005789)
Txnip	BP	response to oxidative stress (GO:0006979) response to hydrogen peroxide (GO:0042542) response to xenobiotic stimulus (GO:0009410) response to mechanical stimulus (GO:0009612) response to glucose (GO:0009749) protein import into nucleus (GO:0006606) protein transport (GO:0015031) keratinocyte differentiation (GO:0030216) response to estradiol (GO:0032355) response to progesterone (GO:0032570) regulation of cell proliferation (GO:0042127) positive regulation of apoptotic process (GO:0043065) response to calcium ion (GO:0051592) negative regulation of cell division (GO:0051782)
	CC	nucleus (GO:0005634) cytoplasm (GO:0005737) mitochondrial intermembrane space (GO:0005758)

GO = Gene Ontology; BP = Biological Process; CC = Cellular Component

6.11. Expression profiles of mitochondria-associated genes in the vHip relate to behavioral phenotypes

Next, we sought to understand whether distinct behavioral phenotypes are correlated to the expression of mitochondria-associated genes in the vHip (Figure 25.A). Positive correlations were observed for behavioral integrated z-score and *Coa8* and *Cisd2* encoding genes, as well as between *Coa8* and *Cisd2*. In contrast, behavioral performance was negatively correlated with *Txnip.*

In addition, we re-evaluated gene expression levels according to the behavioral phenotypes (Figure 25.B – F). Slc25a12 and Cox7c were significantly down-regulated in naïve LBZ (Figure 25.B and C). Although the expression of Coa8 and Cisd2 was not considered significantly altered in naïve LBZ, re-evaluating gene expression levels according to the behavioral phenotypes showed that both genes were significantly different among groups (Figure 25.D and E). Notably, *Txnip* gene expression levels were increased only in stressed animals (Figure 25.F). These results reinforce that specific changes in mitochondria-associated genes may be correlated to distinct behavioral phenotypes and stress responses.

Figure 25. Expression profiles of mitochondria-associated genes in the vHip in different adolescent behavioral phenotypes
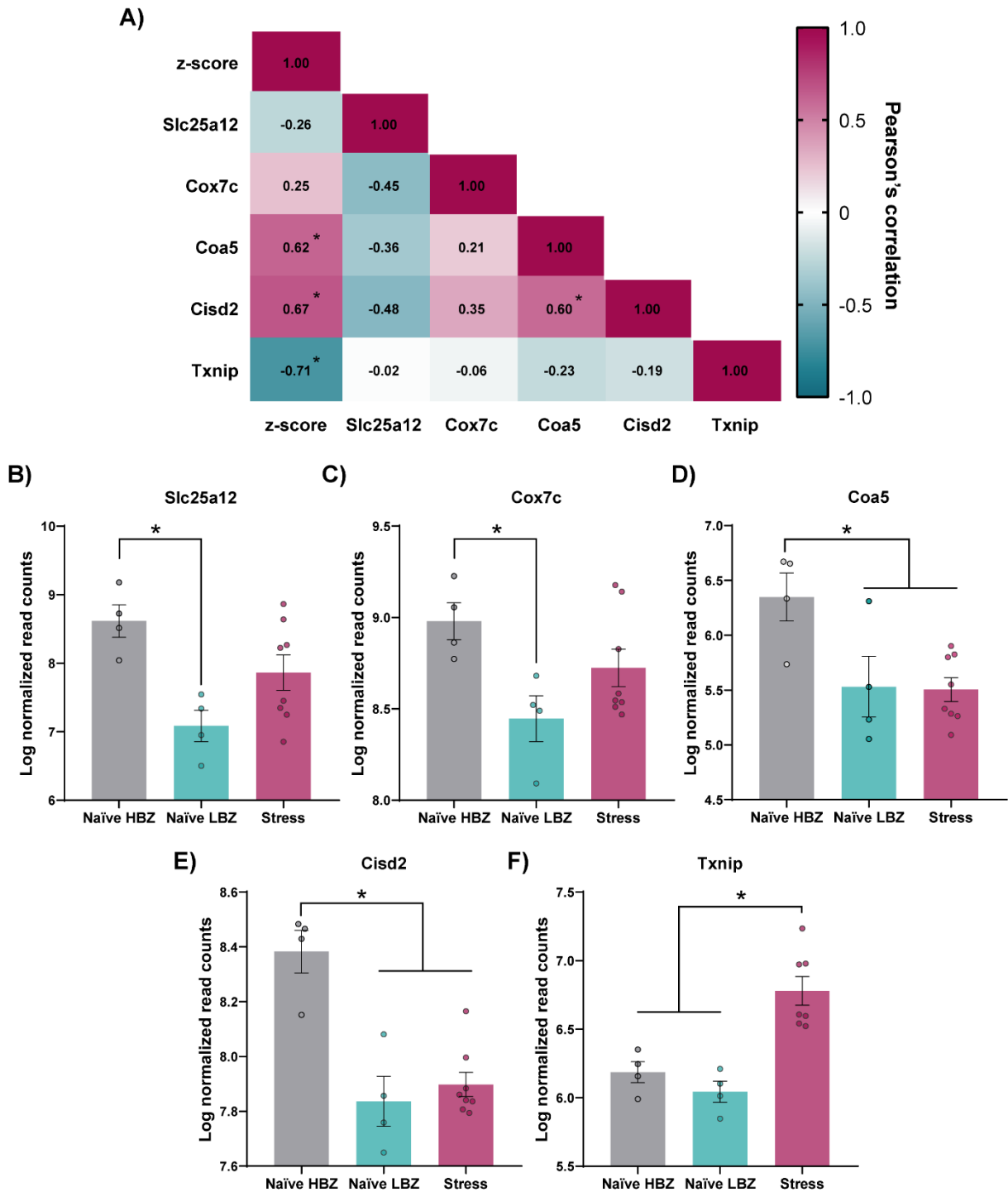
(A) A positive Pearson correlation was observed between the expression levels of complex IV genes (*Cox7c* and *Coa8*) and behavioral phenotype, while a negative correlation was found for *Txnip* expression level and z-score. Pearson values are described in the correlation matrix. Levels of gene expression from different OXPHOS complexes were significantly different among groups: **(B)** Slc25a12 ($F_{2,13} = 6.16$, $p = 0.01$); **(C)** Cox7c ($F_{2,13} = 25$, $p < 0.0001$); **(D)** Coa8 ($F_{2,13} = 19.4$, $p = 0.0001$); **(E)** Cisd2 ($F_{2,13} = 7.21$, $p = 0.008$); and **(F)** Txnip ($F_{2,13} = 25$, $p < 0.0001$). Data are shown as mean ± SEM. * $p < 0.05$; One-way ANOVA, followed by Tukey's multiple comparison test.

7. DISCUSSION

Given the importance of successful adolescent development for adequate sociability and cognitive performance in adulthood, identifying critical neurobiological underpinnings that moderate distinct behavioral phenotypes and stress responses can provide insights into mechanisms underlying the development of psychiatric disorders. Here, using rats, we showed that: 1) the exposure to adolescent stress led to marked behavioral changes, such as anxiety-like responses, loss of sociability, and cognitive impairment, and electrophysiological changes associated with in psychiatric disorders, such as schizophrenia; 2) adolescent stress induced mitochondrial respiratory dysfunction and redox dysregulation in the vHip, leading to oxidative damage in PV interneurons and other cells; 3) high levels of GSSG were found in the vHip and serum of adolescent stressed animals, indicating increases in oxidative stress; 4) differences in mitochondria-associated genes in the vHip correlated with the behavioral phenotypes, with most of the DEGs down-regulated in naïve LBZ and stressed animals compared to naïve HBZ. Overall, our findings unveil new molecular-based insights and strengthen the role of mitochondria in adolescent development, as well as brain abnormalities relate to anxiety, sociability, and cognition functions following stress exposure.

7.1. Adolescent stress leads to behavioral and electrophysiological changes and oxidative stress

Stress during critical neurodevelopmental periods may lead to a glutamatergic overdrive onto fast-spiking PV interneurons, potentially changing the balance of excitation and inhibition (E/I) in cortical and limbic circuits that support multiple behaviors (TZANOULINOU et al., 2014a, 2014b, 2016). Additionally, PV interneurons are highly vulnerable to stress, particularly during neurodevelopmental stages (GOMES; ZHU; GRACE, 2019b; RUDEN; DUGAN; KONRADI, 2020). Our previous findings have shown that adolescent stress leads to long-lasting behavioral changes in rats, marked by anxiety-like behavior, loss of sociability, cognitive impairment, and increased locomotor activity induced by amphetamine (CAVICHIOLI et al., 2023;

GOMES; ZHU; GRACE, 2019). In addition, adolescent stress exposure also caused long-lasting vHip hyperactivity and reduced the number of PV-positive cells at PND 51 and 75, including those surrounded by PNNs (GOMES; ZHU; GRACE, 2019a).Based on these findings, we evaluated social and cognitive performance one week after stress protocol, matching the late adolescent (PND 47 – 51), to further relate the changes in the behavioral performance with E/I balance. Animals exposed to stress markedly decreased social interaction and cognitive deficits. We also reproduced the hyperactivity of pyramidal neurons in the vHip and diminished levels of PV interneurons and their PNNs.

The abnormal PV interneuron activity is thought to lead to vHip hyperactivity, resulting in a hyperdopaminergic state (SONNENSCHEIN; GOMES; GRACE, 2020). This condition is highly consistent with clinical observations in schizophrenia (SCHOBEL et al., 2013; STONE et al., 2010). Additionally, abnormal levels of PV in the hippocampus are a robust finding in the postmortem brain of patients with schizophrenia (ZHANG; REYNOLDS, 2002). Dysregulation in the E/I balance may underlie the main symptoms of psychiatric disorders. For instance, abnormal PV expression in cortical regions is associated with cognitive impairment and abnormal emotional embodiment (MURRAY et al., 2015; ROSENKRANZ; GRACE, 2002). Dysfunction in hippocampal PV interneurons is accompanied by an augmented number of dopamine neurons firing spontaneously in the VTA, which consequently contributes to the emergence of psychosis (GRACE, 2016; LODGE; GRACE, 2007; SONNENSCHEIN; GOMES; GRACE, 2020). Our Pearson analyses revealed a positive correlation between behaviors (SIT and NOR) and the number of PV interneurons, reinforcing their importance in maintaining proper social and cognitive performance. In addition, an opposite correlation was observed when both behaviors were associated with vHip pyramidal neuron activity, showing that the hyperexcitability of vHip contributes negatively to sociability and cognition.

PV interneurons are fast-spiking interneurons and, due to their high firing rates, cause high metabolic demands, which generate ROS (DO; CUENOD; HENSCH, 2015). Therefore, they are particularly vulnerable to environmental and oxidative stress (STEULLET et al., 2010). During adolescence, PV interneurons are not completely mature, and the PNNs, which stabilize glutamatergic inputs onto the PV interneurons to end the plastic phase and protect them from oxidative damage, are not yet

completely formed (CABUNGCAL et al., 2013b; STEULLET et al., 2017). Thus, these dynamics of brain maturation make the developing brain highly vulnerable to environmental factors, for example, the deleterious effects of stress, that can lead to the emergence of psychiatric disorders (GOMES; ZHU; GRACE, 2019b). Studies with animal models confirm that environmental insults, such as maternal immune activation, post-weaning social isolation, pre and postnatal nutrition, and hypoxia, are associated with oxidative stress and neurodevelopmental disorders, such as schizophrenia (EYLES et al., 2007; NIATSETSKAYA et al., 2012; OSKVIG et al., 2012; SCHIAVONE et al., 2009). Here, we found that adolescent-stressed animals expressed higher levels of oxidative stress markers at PND 51, which was co-localized with the PV interneurons. Although many studies have observed oxidative stress associated with environmental risk factors for psychopathologies (MHILLAJ; MORGESE; TRABACE, 2015), little evidence has indicated that oxidative stress is pervasive in the PV interneuron population after early-life or juvenile insults, which have focused on the prefrontal cortex and dentate gyrus (CABUNGCAL et al., 2014; SOARES et al., 2020). Also, oxidative stress appears to be the proximate cause of neuronal dysfunction mediated by glutamate ionotropic receptor activation, a condition observed during stressful situations (FUCHS et al., 2007; MICHAELIS, 1998). Indeed, inducing NMDA receptor hypofunction during early life leads to oxidative stress in PV interneurons and abnormal cortical expression levels (HASAM-HENDERSON et al., 2018; WANG et al., 2007).

Increased oxidative damage is a consistent finding in persons with schizophrenia, including those who have never received antipsychotic medications and those meeting clinical psychosis high-risk criteria who subsequently developed psychosis (PERKINS et al., 2015; PERKINS; JEFFRIES; DO, 2020). Notably, SIT and NOR negatively correlated with oxidative stress markers, suggesting that animals performed worst in the behavioral test if they presented high levels of oxidative damage in the vHip. Aligned with that, higher concentrations of products of protein and lipid oxidation processes are associated with greater severity of psychopathological symptoms in schizophrenia (CHROBAK et al., 2023; FLATOW; BUCKLEY; MILLER, 2013).

7.2. Mitochondrial respiratory dysfunction and redox dysregulation in the vHip of adolescent stressed animals

Mitochondria play a critical role in supplying the brain's energy demands, and their dysfunction has been linked to the pathology of several psychiatric diseases (JOU; CHIU; LIU, 2022). Animal models have supported mitochondrial dysfunction in anxiety, depressive-like behavior, and aging (GRIMM; ECKERT, 2017; HOLLIS et al., 2015; WEGER et al., 2020). However, few studies have investigated mitochondrial respiratory function during postnatal neurodevelopment. Here, vHip of adolescent rats exhibited an increased leak and ETS one day after the stress. Proton leak is defined as when protons migrate to the matrix independent of ATP synthase, i.e., without generating ATP (JASTROCH et al., 2010). Although the lipid bilayer can significantly increase basal proton conductivity, about 5% of it is mediated by the mitochondrial inner membrane in normal conditions, and most of it correlates with adenine nucleotide translocase (BRAND et al., 2005; BROOKES; ROLFE; BRAND, 1997). This protein transports ADP into mitochondria and increases the capacity for oxidative phosphorylation by inducing proton leak. An animal model to study autism (*Fmr1* KO) exhibits forebrain proton leak, which, when blocked, synaptogenesis is restored, and behavioral phenotype in adulthood is normalized (GRIFFITHS et al., 2020). Under chronic stress, proton leak was also observed in cortical regions of *Nr4a1* knockout mice one-day after stress. Nr4a1 is a transcription factor involved in mitochondrial functions and synaptic activity under stress conditions (JEANNETEAU et al., 2018). Although we did not observe an improvement in oxidative phosphorylation capacity one-day after stress, we cannot discard that stress may improve mitochondrial function at earlier time points (DU et al., 2009; HUNTER et al., 2016).

It is estimated that 70 – 80% of the total energy spending of the brain is accounted for processes related to neuronal signaling, which highlights the crucial role of mitochondria-coupled respiration in sustaining brain function (HARRIS; JOLIVET; ATTWELL, 2012). The oxidative phosphorylation capacity decreased in the vHip of stressed animals at PND 51, indicating an impairment in the ADP-activated respiration in the presence of substrates. Accordingly, exposure of animals to stress from PND 28 – 42 decreased the mitochondrial respiratory capacity of the nucleus accumbens during adulthood, which was associated with loss of sociability (MORATÓ et al., 2022).

Diminished mitochondrial respiration in the prefrontal cortex and its association with depressive-like behaviors was also reported for chronic stress models applied during adulthood (GONG et al., 2011; GRIGORUŢĂ et al., 2020; MADRIGAL et al., 2001; WEGER et al., 2020). Impaired one of the mitochondrial respiratory chain complexes has also been linked with the emergence of abnormalities associated with brain disorders. For instance, the administration of rotenone, a complex I inhibitor, during the critical period of neurodevelopment (PND 5 – 11) induced hyperlocomotion, loss of sociability, and abnormal aversive memory in adult animals (SIENA et al., 2021).

As a product of oxidative phosphorylation by mitochondria, free radicals are formed and, in excess, can cause tissue damage. Indeed, mitochondria are a significant source of ROS in cells because this organelle consumes more than 90% of cellular oxygen (LAMBERT; BRAND, 2009). One day after stress, superoxide and hydrogen peroxide levels were elevated. However, ten days after stress, superoxide levels tend to decrease, and hydrogen peroxide maintains normal condition levels. These findings point to longitudinal changes in mitochondrial respiratory function. It has been proposed that proton leak and ROS generated from ETC in mitochondria are linked to each other since proton leak is the principal, but not the only, mechanism that incompletely couples substrate oxygen to ATP generation (BROOKES, 2005). Increased ROS generation activates mechanisms that promote proton leak, and the enhanced proton leak reduces ROS production as a feedback loop (BROOKES, 1998).

Aligned with the high amounts of ROS, peroxidase activity was elevated in the vHip at PND 41 and normalized with time (PND 51), revealing an antioxidant system activation to deal with the excessive free radicals. The enhanced peroxidase activity at PND 41 may explain no changes in the production rate of hydrogen peroxidase in the vHip of stressed animals. Interestingly, mice exposed to maternal separation (PND 2 – 15) showed decreased catalase activity in the hippocampus in adulthood (PND 60) (MALCON et al., 2020). On the other hand, evidence has shown increased activity of SOD and catalase in the hippocampus of adult rats exposed to long-term social isolation, immobilization stress, or cold stress (ŞAHIN; GÜMÜŞLÜ, 2004; SCHIAVONE et al., 2013). In humans, a meta-analysis of oxidative stress markers revealed that decreased plasma catalase in first-episode psychosis individuals seems to be a state-related marker for acute exacerbations of psychosis (FLATOW;

BUCKLEY; MILLER, 2013). In contrast, another meta-analysis did not find differences in catalase and GSH peroxidase in patients with schizophrenia (ZHANG et al., 2010).

Our findings reinforce the importance of investigating the impact of stress on the brain redox system in terms of longitudinal variations at the molecular level. Eventually, the dynamic and temporal changes in mitochondrial respiratory function and ROS abnormal levels after ten days of stress could represent responses to the "allostatic load" induced by the chronic stress protocol (BOBBA-ALVES; JUSTER; PICARD, 2022; MCEWEN, 2004; PICARD; JUSTER; MCEWEN, 2014). This term supports how the same mediators responsible for helping one adapt to stress can paradoxically become harmful when overused. Such a view would reconcile the reductions in PV interneurons in the vHip and long-lasting mitochondrial and redox changes observed in adolescent stressed animals. Indeed, the bioenergetic cost of chronic stress seems too high to be sustainable by PV interneurons. Nonetheless, more studies are needed to understand the link between mitochondrial respiratory function and E/I imbalance in adolescent stressed animals. In sum, our findings indicate that adolescent stress leads to dynamic and variable changes in the mitochondrial respiratory chain and redox system in the vHip, implying mitochondrial dysfunction in this brain region.

7.3.   GSH levels and adolescent stress

Among the antioxidant components (e.g., SOD, catalase, glutathione peroxidase), glutathione (GSH) is the most prominent antioxidant in the brain (AOYAMA, 2021), and aberrant levels have been identified in stress-related disorders (ZALACHORAS et al., 2020). GSH maintains the homeostasis of redox states in cells and prevents oxidative damage in the tissue. Two molecules of GSH are oxidized to produce one molecule of GSH disulfide (GSSG) to eliminate ROS. GSSG can be reduced to two GSH molecules via a reaction with GSH reductase (DRINGEN; HIRRLINGER, 2003). Here, we found that total GSH and GSSG forms tend to increase in the vHip of stressed animals at PND 51. Therefore in this brain region, the high levels of total GSH reflect the GSSG levels, evidencing a previous increase of ROS after adolescent stress. Indeed, our Pearson analysis showed a positive association between both measurements.

Aligned with our results, a significant increase in total GSH was found in the hippocampus of rats exposed to GBR 12909, a dopamine reuptake inhibitor, during early postnatal development (PND 5 – 16) (GÓRNY et al., 2020). On the other hand, 8-weeks of post-weaning social isolation decreased the cortical and striatal GSSG:GSH ratio in rats, suggesting a reduction in GSSG and an increase in reduced GSH in these brain regions (MÖLLER et al., 2011). In adult animals, studies have reported a link between exposure to psychogenic stress and decreased levels of GSH and GSH-related enzymes (ZALACHORAS et al., 2020). Indeed, glucocorticoid administration in rodents leads to decreased brain GSH levels (BEYTUT et al., 2018; ZAFIR; BANU, 2009). Similarly, studies that exposed adult animals to chronic stress found evidence for drastically decreased levels of GSH and related antioxidant enzymes in several brain regions, including the cortex, striatum, and hippocampus (SAMARGHANDIAN et al., 2017; SEO et al., 2012). Also, psychosocial stressors, such as social isolation and social defeat, have a negative impact on the GSH system in the hippocampus and prefrontal cortex (DJORDJEVIC et al., 2010; HERBET et al., 2017; SOLANKI et al., 2017).

In the serum of stressed animals, all forms were increased, i.e., total GSH, reduced GSH, and GSSG. An increase in GSH production is also suggestive of an increase in reductive stress, i.e. excessive accumulation of reducing equivalents, which could have similar deleterious effects (MÖLLER et al., 2011; RAJASEKARAN et al., 2007). Human findings have indicated decreased levels of reduced GSH and increased GSSG levels in plasma, erythrocytes, and cerebrospinal fluid in first-episode, nonmedicated, medicated, and chronic schizophrenia patients (DO et al., 2000; ERMAKOV et al., 2021; IWATA et al., 2021; LAVOIE et al., 2017; NUCIFORA et al., 2017; RAFFA et al., 2011; REDDY; KESHAVAN; YAO, 2003).

Recent evidence indicates a critical role for GSH in behavioral performance, such as aversively and appetitively motivated tasks (LAPIDUS et al., 2014; ZALACHORAS et al., 2022). For instance, downregulating GSH levels with an inhibitor (buthionine sulfoximine) in the nucleus accumbens impaired effort-based reward-incentivized performance (ZALACHORAS et al., 2022). Also, GSH depletion in the hippocampus disrupted short-term spatial recognition memory in a Y-maze test (CRUZ-AGUADO et al., 2001; DEAN et al., 2009). In humans, several psychopathological alterations, such as depression or schizophrenia, in which low

GSH levels have been reported are associated with motivational deficits, cognitive impartment, and psychosis (LAPIDUS et al., 2014; NUCIFORA et al., 2017; WANG et al., 2019; XIN et al., 2016). Here, we observed a negative correlation between SIT and total GSH or GSSG, i.e., animals with lower sociability have more GSSG, suggesting that ROS previously oxidized GSH in the tissue. In serum, low levels of total and reduced GSH and GSSG were associated with loss of sociability and cognitive dysfunction. Further studies are needed to reveal the potential role of GSH in adolescent stress-induced behavioral changes.

Although we have not investigated changes in GSH levels induced by adolescent stress and their directly associated with PV interneuron dysfunction in the vHip, antioxidant GSH has been suggested as a hub between redox dysregulation and excitatory and inhibitory circuit dysregulation in psychiatric disorders (DWIR et al., 2023). A transgenic mouse model of impaired synthesis of GSH (*Gclm* KO mice) has a 70% reduction in brain GSH levels and behavioral homologies to schizophrenia (DAS NEVES DUARTE et al., 2012; KULAK; CUENOD; DO, 2012). In *Gclm* KO mice, PV interneurons and PNNs deficits emerged in a spatiotemporal sequence that paralleled regional brain maturation, suggesting that GSH deficit delays the maturation of PV interneurons and their PNNs in the vHip, and lastly, the anterior cingulate cortex (CABUNGCAL et al., 2013a, 2013b). These changes correlated with oxidative DNA damage in these brain regions throughout development. Interestingly, PV interneurons, but not calbindin or calretinin interneurons, are vulnerable and prone to exhibit oxidative stress in this animal model (CABUNGCAL et al., 2013a; STEULLET et al., 2010, 2017). Additionally, administration of a specific inhibitor of the dopamine reuptake transporter, GBR-12909, in preweaning or pubertal but not in the young adult period reduces the number of PV interneurons in the anterior cingulate cortex in *Gclm* KO mice (CABUNGCAL et al., 2013a).

It is important to note that beyond the role in maintaining the intracellular antioxidant system, GSH also regulates cysteine transport/storage, cell signaling, regulation of some enzyme activities, gene expression, and cell differentiation and proliferation (AOYAMA, 2021). Therefore, modulating GSH levels in the brain by either increasing the availability of its precursors or the expression of GSH-regulating enzymes are promising therapeutic strategy for psychiatric disorders. It seems important to advance knowledge here, particularly focusing on GSH levels and its

modulation by adolescent stress, as it is amenable to modulation by nutritional interventions, such as N-acetylcysteine, which can be much easier and quicker implemented than drugs and can also be used as supplementation of available therapies.

7.4. Transcriptomic analysis reveals mitochondrial pathways associated with distinct adolescent behavioral phenotypes and stress response

It is well-established that both inbred and outbred adult rodents show individual differences in behavioral performance, but few studies have investigated this variability in adolescent naïve animals (CASTRO et al., 2012; MILNER; CRABBE, 2008; VAN DER GOOT et al., 2021). While no differences between the three behavioral clusters were observed in the EPM, the time spent in the light zone of LDB identified two distinct behaviors in naïve animals and the impact of stress during adolescence. Indeed, our group has demonstrated that the adolescent stress protocol applied induces anxiety-like behavior in adulthood (CAVICHIOLI et al., 2023).

Animals exposed to stress presented a marked decrease in social interaction and cognitive deficits in the NOR test and inter-individual differences in naïve rats. Adolescence is an adaptive period that shapes social and behavioral phenotypes based on individual differences, some insensitive to social contexts (SACHSER; HENNESSY; KAISER, 2018). Social behaviors acquired during childhood and adolescence, such as playing and dominance, are crucial for social organization, which impact later interactions with conspecifics and predict behavioral phenotypes and cognitive skills development (JONES; MONFILS, 2016). Our results align well with previous reports showing substantial inter-individual variation in sociability among adolescent animals (MOY et al., 2004).

Most reports emphasize individual variability in learning, risk-taking, and other cognitive processes during adolescence (CARAS; SANES, 2019; DEMIDENKO et al., 2020; LARSEN; LUNA, 2018; LUNA et al., 2015; SCHRIBER; GUYER, 2016). Corroborating with preclinical studies, higher-order cognition variations are associated

with human brain development (FOULKES; BLAKEMORE, 2018). Our results from the PCA defined a PC1 with significant contributions of the LDB and SIT variables, whereas PC2 has a considerable contribution of the NOR variable. Notably, when projecting the variables in a coordinate system, PC1 signs are all positive for cluster 3 (stressed animals) and all negative for clusters 1 (naïve HBZ) and 2 (naïve LBZ). PC2 signs are also opposite in clusters 1 and 2, all negative for the former and all positive for the latter. These findings indicate that stressed animals are more "anxious" and less sociable than naïve animals, and variability among naïve animals appears to be more prominently associated with cognitive performance.

Supporting the idea that vHip gene expression signatures are dynamic and affected by social experiences and stress exposure, we observed that animals with lower behavioral scores (naïve LBZ and stressed animals) exhibit down-regulated expression of genes directly linked to the mitochondrion cellular compartment. Both naïve LBZ and stressed animals down-regulated expression of genes encoded complex IV subunits, i.e., *Cox7c* and *Coa5*, respectively. Similar to our findings, a pharmacological animal model for SCZ, in which mice were exposed to NMDA receptor antagonism (PND 56 – 63), showed extensive perturbation in cortical co-expression patterns for mitochondrial respiratory chain complexes that were mainly downregulated (ZHAO et al., 2018). In contrast, an up-regulation in genes encoding for mitochondrial respiratory chain complex was identified in the cortex of adolescent isolated male rats and adult mice subjected to multimodal chronic restraint stress (WEGER et al., 2020; ZHAO et al., 2018).

Complex IV is the final complex in the electron transport chain, responsible for reducing molecular oxygen and forming water. Therefore, it is a critical regulatory point of oxidative phosphorylation (KADENBACH, 2021). Conditional knockout of *Cox10* or *Cox6a2*, isoforms of complex IV, in PV interneurons, results in abnormal gamma-oscillations in the prefrontal cortex and deficits in sensory-motor gating and sociability (INAN et al., 2016; SANZ-MORELLO et al., 2020). *In vitro* overexpression of complex IV subunits protect cortical and hippocampal neurons from oxidative stress, increasing the stability of the electron transport chain (YANG et al., 2019). In the prefrontal cortex and blood samples of *Gclm* KO animals associated with GBR, oxidative stress decreased Cox6a2 and exacerbated oxidative stress and PV interneurons impairment (KHADIMALLAH et al., 2022). Translating to early psychosis patients, blood Cox6a2

levels decreases, combined with mitophagy markers alterations (KHADIMALLAH et al., 2022).

The mitochondria-associated genes analysis revealed that Slc25a12 is specifically downregulated in adolescent naïve LBZ animals, reflecting their distinct behavioral phenotype. The *Slc25a12* gene encodes the Aralar/slc25a12/AGC1 protein, which is involved in the transport of aspartate from mitochondria to cytosol in exchange for glutamate and is a component of the malate-aspartate shuttle, essential to maintain glycolytic pyruvate supply to neuronal mitochondria (PUERTAS-FRÍAS et al., 2019). A recent study has identified Aralar/slc25a12/AGC1 as the mitochondrial transporter that sequesters GABA upon increased mitochondrial activity in Drosophila mutants of the human homolog CYFIP1, a protein that regulates cytoskeletal dynamics and translation and is linked to autism and schizophrenia (KANELLOPOULOS et al., 2020). Specifically, they showed that social deficits in mutant flies were causally related to defects in GABA signaling, as GABA accumulated in the mitochondria of mutants. These findings emphasize the importance of Aralar/slc25a12/AGC1 in modulating neuronal homeostasis and social behavior under pathological conditions. Nevertheless, the association of abnormal *Slc25a12* gene expression and mitochondrial dysfunction in distinct behavioral phenotypes requires more studies.

In stressed animals, we found downregulated expression of the *Cisd2* gene, encoding for CDGSH Iron Sulfur Domain 2. Cisd2 is localized on the endoplasmic reticulum and mitochondria-associated membranes. Therefore, it is crucial in regulating cytosolic Ca^{2+} homeostasis, endoplasmic reticulum integrity, and mitochondrial function (SHEN et al., 2021). Upregulation of *Cisd2* increases antioxidant capacity in response to elevated ROS levels, significantly correlated with stress response/redox signaling genes, such as glutathione peroxidase 3 (GPx-3) (LI et al., 2017). Indeed, the knockdown of *Cisd2* led to remarkable inflammation and mitochondrial dysfunction in neural cells (LIN, 2020). Specifically, *Cisd2* deficiency in mice causes mitochondrial fission, dysfunction accompanied by autophagic cell death, and behavioral phenotype suggestive of premature aging (CHEN et al., 2009). Also, overexpression of *Cisd2* reverses the age-related mitochondrial alterations in an animal model for Alzheimer's disease (CHEN et al., 2020). Given the important role of *Cisd2 in* mediating the intercommunication between the endoplasmic reticulum and mitochondria to regulate intracellular Ca^{2+} homeostasis and allow the maintenance of

properly functioning mitochondria, this gene is a potential target for better comprehension of adolescent stress-induced PV interneuron dysfunction.

Oxidative stress causes the oxidation of protein thiols to form disulfides, resulting in changes in cellular proteins and their biological activities and DNA damage (HERBET et al., 2017). Among the redox defense systems in mammalian cells, the thioredoxin (TRX) system reduces oxidized cysteine groups on proteins through an interaction with the redox-active center of TRX to form a disulfide bond (AHSAN et al., 2009). Thioredoxin-interacting protein (TXNIP) reduced TRX, inhibiting TRX function and increasing oxidative stress by the accumulation of intracellular ROS levels (NISHIYAMA et al., 1999). TXNIP expression is regulated by multiple factors, including high glucose, endoplasmic reticulum stress, and hypoxia (TSUBAKI; TOOYAMA; WALKER, 2020). Overexpression of TXNIP in Drosophila flies shortens lifespan due to elevated oxidative DNA damage, whereas downregulation of TXNIP enhances oxidative stress resistance and extends lifespan (OBERACKER et al., 2018). Therefore, TXNIP may induce a shift to a pro-oxidative cellular environment that facilitates DNA damage. We found that adolescent stressed animals exhibit upregulation of *Txnip* expression. Aligned with these transcriptomic findings, it is important to note the increased marker of DNA damage 8-OxoDg in the vHip of stressed animals. Importantly, our results evidence that high levels of *Txnip* expression were associated with lower behavioral performance in adolescent stress. Also, the different gene expression of *Txnip* was restricted to the stressed group and not affected in the naïve LBZ animals. It will be essential to investigate the role of *Txnip* in adolescent stress, given its potential contributions to the pathological mechanisms and emergence of behavioral alterations described in our findings.

In sum, our data provide behavioral correlations of distinct phenotypes with mitochondrial-associated genes in the vHip during late adolescence. Such similarities and differences in mitochondrial gene expression levels among groups may explain the variability in behavioral phenotypes described in this study. Future studies are needed to investigate the causal relationship of these correlations, unveiling possible neurobiological mechanisms of disorders associated with exposure to stressful events. Also, modulating mitochondria-associated genes may help to define potential targets to prevent the emergence of the neurodevelopmental disorders related with stressful environments.

8. CONCLUSION

Adolescent development outlines considerable learning, allowing individuals to acquire new knowledge and skills to transition to an independent adult role. Understanding the neurobiological underpinnings that lead to individual differences in adolescent behavioral phenotypes can help to predict vulnerability in healthy individuals. Likewise, uncovering the impact of stress on the sensitive period brings new strategies to ameliorate and counteract behavioral deficits after stress exposure. Most work on mitochondrial changes in response to stress has been done in early life or adulthood, and the relationship between environmental stress exposure during the post-natal period and long-term mitochondrial function has been less extensively studied. However, mitochondrial respiratory function and redox homeostasis have not been investigated in the vHip of animals exposed to stress during adolescence.

Under adolescent stress conditions, we showed that mitochondrial respiratory dysfunction shifted redox balance towards pro-oxidative states, marked by oxidative damage in the vHip. Hence, oxidative stress is a possible convergent point for behavioral abnormalities observed in the social and cognitive domains and the electrophysiological changes associated with psychiatric disorders. In addition, we also provided behavioral correlations of distinct phenotypes with mitochondria-associated genes in the developing vHip. Such similarities and differences in mitochondrial gene expression levels among groups may explain the variability in behavioral phenotypes described in this study (Figure 26).

Figure 26. Overall effects of adolescent stress on mitochondrial redox homeostasis and E/I balance
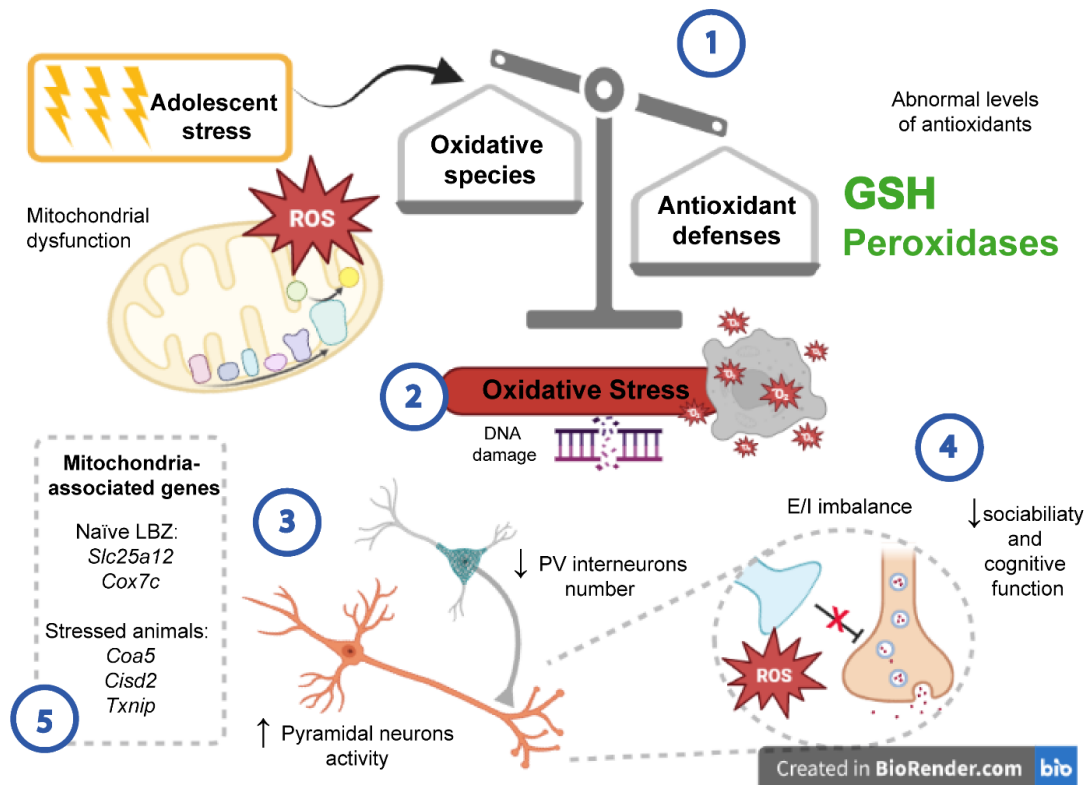
(1) Adolescent stress shifted the redox balance towards pro-oxidative states, marked by mitochondrial respiratory dysfunction, abnormal ROS levels, and dysregulation of the antioxidant system, including GSH levels and peroxidase activity. **(2)** Such imbalance led to oxidative stress, marked by DNA damage in the vHip. **(3)** PV interneurons seem to be affected by oxidative stress, given the reduction in PV-positive cell number and increased pyramidal neuron activity in the vHip. **(4)** Neuronal circuit deficits uncover an E/I imbalance in the vHip, associated with loss of sociability and cognitive impairment. **(5)** Transcriptomic findings identified mitochondrial genes associated with distinct adolescent behavioral phenotypes and stress responses.

In our progressively stressful world, adolescents have been suffering record stress levels. Also, the population reports mounting stress and anxiety levels due to terrorism and climate threats, which in the 2020s has further expanded to health and economic threats (TORALES et al., 2020). To date, we generated unique knowledge in a putative mechanism underlying the impact of adolescent stress. Further uncovering the causal relationship between emerging behavioral impairment and neuronal circuit deficits induced by stressful insults within the mitochondrial redox dysregulation will be of utmost importance. We hope these findings may guide approaches to prevent/reverse the deleterious impact of adolescent stress and, thus, contribute to ameliorating the behavioral deficits observed in many individuals with psychiatric disorders.

9. REFERENCES

AHSAN, M. K. et al. Redox regulation of cell survival by the thioredoxin superfamily: an implication of redox gene therapy in the heart. **Antioxidants & redox signaling**, v. 11, n. 11, p. 2741–2758, 1 nov. 2009.

ALPERN, D. et al. BRB-seq: ultra-affordable high-throughput transcriptomics enabled by bulk RNA barcoding and sequencing. **Genome Biology**, v. 20, n. 1, p. 1–15, 19 abr. 2019.

ANNESLEY, S. J.; FISHER, P. R. Mitochondria in Health and Disease. **Cells 2019, Vol. 8, Page 680**, v. 8, n. 7, p. 680, 5 jul. 2019.

AOKI, C.; ROMEO, R. D.; SMITH, S. S. Adolescence as a Critical Period for Developmental Plasticity. **Brain Research**, v. 1654, p. 85–86, 1 jan. 2017.

AOYAMA, K. Glutathione in the Brain. **International Journal of Molecular Sciences 2021, Vol. 22, Page 5010**, v. 22, n. 9, p. 5010, 9 maio 2021.

APONTE, Y.; BISCHOFBERGER, J.; JONAS, P. Efficient Ca2+ buffering in fast-spiking basket cells of rat hippocampus. **The Journal of Physiology**, v. 586, n. Pt 8, p. 2061, 4 abr. 2008.

BACKES, E. P.; BONNIE, R. J. Adolescent Development. Em: **The Promise of Adolescence: Realizing Opportunity for All Youth.** [s.l.] National Academies Press (US), 2019.

BALABAN, R. S.; NEMOTO, S.; FINKEL, T. Mitochondria, Oxidants, and Aging. **Cell**, v. 120, n. 4, p. 483–495, 25 fev. 2005.

BALMER, T. S. Neuronal Excitability Perineuronal Nets Enhance the Excitability of Fast-Spiking Neurons. 2016.

BAXTER, P. S.; HARDINGHAM, G. E. Adaptive regulation of the brain's antioxidant defences by neurons and astrocytes. **Free radical biology & medicine**, v. 100, p. 147–152, 1 nov. 2016.

BÉLANGER, M.; ALLAMAN, I.; MAGISTRETTI, P. J. Brain Energy Metabolism: Focus on Astrocyte-Neuron Metabolic Cooperation. **Cell Metabolism**, v. 14, n. 6, p. 724–738, 7 dez. 2011.

BENJAMINI, Y.; HOCHBERG, Y. Controlling the False Discovery Rate: A Practical and Powerful Approach to Multiple Testing. **Journal of the Royal Statistical Society: Series B (Methodological)**, v. 57, n. 1, p. 289–300, 1 jan. 1995.

BEYTUT, E. et al. The possible protective effects of vitamin E and selenium administration in oxidative stress caused by high doses of glucocorticoid administration in the brain of rats. **Journal of trace elements in medicine and biology : organ of the Society for Minerals and Trace Elements (GMS)**, v. 45, p. 131–135, 1 jan. 2018.

BICKS, L. K. et al. An Adolescent Sensitive Period for Social Dominance Hierarchy Plasticity Is Regulated by Cortical Plasticity Modulators in Mice. **Frontiers in Neural Circuits**, v. 15, p. 1–9, 12 maio 2021.

BIJLSMA, A. et al. Social Play Behavior Is Critical for the Development of Prefrontal Inhibitory Synapses and Cognitive Flexibility in Rats. **The Journal of neuroscience : the official journal of the Society for Neuroscience**, v. 42, n. 46, p. 8716–8728, 16 nov. 2022.

BOBBA-ALVES, N.; JUSTER, R. P.; PICARD, M. The energetic cost of allostasis and allostatic load. **Psychoneuroendocrinology**, v. 146, p. 105951, 1 dez. 2022.

BRAND, M. D. et al. The basal proton conductance of mitochondria depends on adenine nucleotide translocase content. **Biochemical Journal**, v. 392, n. Pt 2, p. 353, 12 dez. 2005.

BRENHOUSE, H. C.; ANDERSEN, S. L. Nonsteroidal anti-inflammatory treatment prevents delayed effects of early life stress in rats. **Biological Psychiatry**, v. 70, n. 5, p. 434–440, 1 set. 2011.

BROOKES, P. S. 32 Mitochondrial proton leak and superoxide generation: an hypothesis. **Biochemical Society Transactions**, v. 26, n. 4, p. S331–S331, 1 nov. 1998.

BROOKES, P. S. Mitochondrial H+ leak and ROS generation: An odd couple. **Free Radical Biology and Medicine**, v. 38, n. 1, p. 12–23, 1 jan. 2005.

BROOKES, P. S.; ROLFE, D. F. S.; BRAND, M. D. The proton permeability of liposomes made from mitochondrial inner membrane phospholipids: Comparison with isolated mitochondria. **Journal of Membrane Biology**, v. 155, n. 2, p. 167–174, 1997.

CABALLERO, A. et al. Downregulation of parvalbumin expression in the prefrontal cortex during adolescence causes enduring prefrontal disinhibition in adulthood. **Neuropsychopharmacology**, v. 45, n. 9, p. 1527, 1 ago. 2020.

CABALLERO, A.; DIAH, K. C.; TSENG, K. Y. Region-specific upregulation of parvalbumin-, but not calretinin-positive cells in the ventral hippocampus during adolescence. **Hippocampus**, v. 23, n. 12, p. 1331–1336, 1 dez. 2013.

CABALLERO, A.; TSENG, K. Y. GABAergic Function as a Limiting Factor for Prefrontal Maturation during Adolescence. **Trends in Neurosciences**, v. 39, n. 7, p. 441–448, 1 jul. 2016.

CABUNGCAL, J. H. et al. Early-life insults impair parvalbumin interneurons via oxidative stress: Reversal by N-acetylcysteine. **Biological Psychiatry**, v. 73, n. 6, p. 574–582, 15 mar. 2013a.

CABUNGCAL, J. H. et al. Perineuronal nets protect fast-spiking interneurons against oxidative stress. **Proceedings of the National Academy of Sciences of the United States of America**, v. 110, n. 22, p. 9130–9135, 28 maio 2013b.

CABUNGCAL, J.-H. et al. Juvenile Antioxidant Treatment Prevents Adult Deficits in a Developmental Model of Schizophrenia. **Neuron**, v. 83, p. 1073–1084, 2014.

CARAS, M. L.; SANES, D. H. Neural Variability Limits Adolescent Skill Learning. **Journal of Neuroscience**, v. 39, n. 15, p. 2889–2902, 10 abr. 2019.

CARLSON, G. C. et al. Dysbindin-1 mutant mice implicate reduced fast-phasic inhibition as a final common disease mechanism in schizophrenia. **Proceedings of the National Academy of Sciences of the United States of America**, v. 108, n. 43, p. E962–E970, 25 out. 2011.

CASTRO, J. E. et al. Personality traits in rats predict vulnerability and resilience to developing stress-induced depression-like behaviors, HPA axis hyper-reactivity and brain changes in pERK1/2 activity. **Psychoneuroendocrinology**, v. 37, n. 8, p. 1209–1223, 1 ago. 2012.

CAVICHIOLI, A. M. et al. Levetiracetam Attenuates Adolescent Stress-induced Behavioral and Electrophysiological Changes Associated With Schizophrenia in Adult Rats. **Schizophrenia Bulletin**, v. 49, n. 1, p. 68–77, 3 jan. 2023.

CEMBROWSKI, M. S. et al. The subiculum is a patchwork of discrete subregions. **eLife**, v. 7, p. 1–21, 1 out. 2018.

CHAVAN, V. et al. Central Presynaptic Terminals Are Enriched in ATP but the Majority Lack Mitochondria. **PLoS ONE**, v. 10, n. 4, p. e0125185, 1 abr. 2015.

CHEN, Y. F. et al. Cisd2 deficiency drives premature aging and causes mitochondria-mediated defects in mice. **Genes & Development**, v. 23, n. 10, p. 1183–1194, 15 maio 2009.

CHEN, Y. F. et al. Upregulation of Cisd2 attenuates Alzheimer's-related neuronal loss in mice. **Journal of Pathology**, v. 250, n. 3, p. 299–311, 1 mar. 2020.

CHROBAK, A. A. et al. Oxidative Stress Biomarkers among Schizophrenia Inpatients. **Brain Sciences 2023, Vol. 13, Page 490**, v. 13, n. 3, p. 490, 14 mar. 2023.

COHEN, A. O. et al. When Is an Adolescent an Adult? Assessing Cognitive Control in Emotional and Nonemotional Contexts. **Psychological Science**, v. 27, n. 4, p. 549–562, 24 fev. 2016.

COLASANTI, A. et al. Primary mitochondrial diseases increase susceptibility to bipolar affective disorder. **Journal of Neurology, Neurosurgery & Psychiatry**, v. 91, n. 8, p. 892–894, 1 ago. 2020.

CRONE, E. A.; DAHL, R. E. Understanding adolescence as a period of social–affective engagement and goal flexibility. 2012.

CRUZ-AGUADO, R. et al. Behavioral and biochemical effects of glutathione depletion in the rat brain. **Brain research bulletin**, v. 55, n. 3, p. 327–333, 2001.

DAHL, R. E.; ALLEN, N. B.; WILBRECHT, L. Importance of investing in adolescence from a developmental science perspective. **Nature**, v. 554, p. 441–460, 2018.

DANIELS, T. E.; OLSEN, E. M.; TYRKA, A. R. Stress and Psychiatric Disorders: The Role of Mitochondria. **Annual review of clinical psychology**, v. 16, p. 165, 5 maio 2020.

DAS NEVES DUARTE, J. M. et al. N-Acetylcysteine Normalizes Neurochemical Changes in the Glutathione-Deficient Schizophrenia Mouse Model During Development. **Biological Psychiatry**, v. 71, n. 11, p. 1006–1014, 1 jun. 2012.

DE ALMEIDA, A. J. P. O. et al. ROS: Basic Concepts, Sources, Cellular Signaling, and its Implications in Aging Pathways. **Oxidative medicine and cellular longevity**, v. 2022, 2022.

DEAN, O. et al. Glutathione depletion in the brain disrupts short-term spatial memory in the Y-maze in rats and mice. **Behavioural brain research**, v. 198, n. 1, p. 258–262, 2 mar. 2009.

DEMIDENKO, M. I. et al. Cortical and subcortical response to the anticipation of reward in high and average/low risk-taking adolescents. **Developmental Cognitive Neuroscience**, v. 44, 1 ago. 2020.

DJAFARZADEH, S.; JAKOB, S. M. High-resolution Respirometry to Assess Mitochondrial Function in Permeabilized and Intact Cells. **Journal of Visualized Experiments : JoVE**, v. 2017, n. 120, 8 fev. 2017.

DJORDJEVIC, J. et al. Chronic social isolation compromises the activity of both glutathione peroxidase and catalase in hippocampus of male wistar rats. **Cellular and molecular neurobiology**, v. 30, n. 5, p. 693–700, jul. 2010.

DO, K. Q. et al. Redox dysregulation, neurodevelopment, and schizophrenia. **Current Opinion in Neurobiology**, v. 19, n. 2, p. 220–230, 1 abr. 2009.

DO, K. Q.; CUENOD, M.; HENSCH, T. K. Targeting Oxidative Stress and Aberrant Critical Period Plasticity in the Developmental Trajectory to Schizophrenia. **Schizophrenia Bulletin**, v. 41, n. 4, p. 835–846, 1 jul. 2015.

DRINGEN, R. Metabolism and functions of glutathione in brain. **Progress in Neurobiology**, v. 62, p. 649–671, 2000.

DRINGEN, R.; HIRRLINGER, J. Glutathione pathways in the brain. **Biological Chemistry**, v. 384, n. 4, p. 505–516, 1 abr. 2003.

DU, J. et al. Dynamic regulation of mitochondrial function by glucocorticoids. **Proceedings of the National Academy of Sciences of the United States of America**, v. 106, n. 9, p. 3543–3548, 3 mar. 2009.

DWIR, D. et al. Redox and Immune Signaling in Schizophrenia: New Therapeutic Potential. **International Journal of Neuropsychopharmacology**, v. XX, p. 1–13, 28 mar. 2023.

EOM, S.; LEE, Y. M. Long-term developmental trends of pediatric mitochondrial diseases: The five stages of developmental decline. **Frontiers in Neurology**, v. 8, n. MAY, p. 208, 17 maio 2017.

EYLES, D. et al. Developmental vitamin D deficiency alters the expression of genes encoding mitochondrial, cytoskeletal and synaptic proteins in the adult rat brain. **The Journal of steroid biochemistry and molecular biology**, v. 103, n. 3–5, p. 538–545, mar. 2007.

FANSELOW, M. S.; DONG, H. W. Are the Dorsal and Ventral Hippocampus Functionally Distinct Structures? **Neuron**, v. 65, n. 1, p. 7–19, 14 jan. 2010.

FAWCETT, J. W.; OOHASHI, T.; PIZZORUSSO, T. The roles of perineuronal nets and the perinodal extracellular matrix in neuronal function. **Nature Reviews Neuroscience**, v. 20, n. 8, p. 451–465, 1 ago. 2019.

FLATOW, J.; BUCKLEY, P.; MILLER, B. J. Meta-Analysis of Oxidative Stress in Schizophrenia. **Biological psychiatry**, v. 74, n. 6, p. 400, 9 set. 2013.

FOULKES, L.; BLAKEMORE, S. J. Studying individual differences in human adolescent brain development. **Nature Neuroscience 2018 21:3**, v. 21, n. 3, p. 315–323, 5 fev. 2018.

FUCHS, E. C. et al. Recruitment of Parvalbumin-Positive Interneurons Determines Hippocampal Function and Associated Behavior. **Neuron**, v. 53, n. 4, p. 591–604, 15 fev. 2007.

GALTREY, C. M.; FAWCETT, J. W. The role of chondroitin sulfate proteoglycans in regeneration and plasticity in the central nervous system. **Brain Research Reviews**, v. 54, n. 1, p. 1–18, 1 abr. 2007.

GERGUES, M. M. et al. Circuit and molecular architecture of a ventral hippocampal network. **Nature neuroscience**, v. 23, n. 11, p. 1444, 1 nov. 2020.

GOKHALE, A. et al. Quantitative Proteomic and Genetic Analyses of the Schizophrenia Susceptibility Factor Dysbindin Identify Novel Roles of the Biogenesis of Lysosome-Related Organelles Complex 1. **Journal of Neuroscience**, v. 32, n. 11, p. 3697–3711, 14 mar. 2012.

GOLDENBERG, D. et al. Greater response variability in adolescents is associated with increased white matter development. **Social Cognitive and Affective Neuroscience**, v. 12, n. 3, p. 436, 1 mar. 2017.

GOMES, F. V.; GRACE, A. A. Adolescent Stress as a Driving Factor for Schizophrenia Development—A Basic Science Perspective. **Schizophrenia Bulletin**, v. 43, n. 3, p. 486, 1 maio 2017a.

GOMES, F. V.; GRACE, A. A. Prefrontal Cortex Dysfunction Increases Susceptibility to Schizophrenia-Like Changes Induced by Adolescent Stress Exposure. **Schizophrenia Bulletin**, v. 43, n. 3, p. 592–600, 1 maio 2017b.

GOMES, F. V.; RINCÓN-CORTÉS, M.; GRACE, A. A. Adolescence as a period of vulnerability and intervention in schizophrenia: Insights from the MAM model. **Neuroscience & Biobehavioral Reviews**, v. 70, p. 260–270, 1 nov. 2016.

GOMES, F. V.; ZHU, X.; GRACE, A. A. The pathophysiological impact of stress on the dopamine system is dependent on the state of the critical period of vulnerability. **Molecular Psychiatry 2019 25:12**, v. 25, n. 12, p. 3278–3291, 5 set. 2019a.

GOMES, F. V.; ZHU, X.; GRACE, A. A. Stress during critical periods of development and risk for schizophrenia. **Schizophrenia Research**, v. 213, p. 107–113, 1 nov. 2019b.

GONG, Y. et al. Chronic mild stress damages mitochondrial ultrastructure and function in mouse brain. **Neuroscience Letters**, v. 488, n. 1, p. 76–80, 13 jan. 2011.

GÓRNY, M. et al. Alterations in the Antioxidant Enzyme Activities in the Neurodevelopmental Rat Model of Schizophrenia Induced by Glutathione Deficiency during Early Postnatal Life. **Antioxidants**, v. 9, n. 6, p. 1–25, 1 jun. 2020.

GRACE, A. A. Dysregulation of the dopamine system in the pathophysiology of schizophrenia and depression. **Nature Reviews Neuroscience**, v. 176, n. 8, p. 139–148, 2016.

GREEN, D. E.; ODA, T. On the unit of mitochondrial structure and function. **Journal of Biochemistry**, v. 49, n. 6, p. 742–757, 1 jun. 1961.

GRIFFITHS, K. K. et al. Inefficient Thermogenic Mitochondrial Respiration Due to Futile Proton Leak in a Mouse Model of Fragile X Syndrome. **FASEB journal : official publication of the Federation of American Societies for Experimental Biology**, v. 34, n. 6, p. 7404, 1 jun. 2020.

GRIGORUȚĂ, M. et al. Psychological stress phenocopies brain mitochondrial dysfunction and motor deficits as observed in a Parkinsonian rat model. **Molecular neurobiology**, v. 57, n. 4, p. 1781, 1 abr. 2020.

GRIMM, A.; ECKERT, A. Brain aging and neurodegeneration: from a mitochondrial point of view. **Journal of Neurochemistry**, v. 143, n. 4, p. 418–431, 1 nov. 2017.

GUILLOUX, J. P. et al. Integrated behavioral z-scoring increases the sensitivity and reliability of behavioral phenotyping in mice: Relevance to emotionality and sex. **Journal of Neuroscience Methods**, v. 197, n. 1, p. 21–31, 2011.

GULYÁS, A. I. et al. Populations of hippocampal inhibitory neurons express different levels of cytochrome c. **European Journal of Neuroscience**, v. 23, n. 10, p. 2581–2594, maio 2006.

HAHM, J. Y. et al. 8-Oxoguanine: from oxidative damage to epigenetic and epitranscriptional modification. **Experimental & Molecular Medicine 2022 54:10**, v. 54, n. 10, p. 1626–1642, 21 out. 2022.

HARA, Y. et al. From the Cover: Presynaptic mitochondrial morphology in monkey prefrontal cortex correlates with working memory and is improved with estrogen treatment. **Proceedings of the National Academy of Sciences of the United States of America**, v. 111, n. 1, p. 486, 1 jan. 2014.

HARRIS, J. J.; JOLIVET, R.; ATTWELL, D. Synaptic Energy Use and Supply. **Neuron**, v. 75, n. 5, p. 762–777, 6 set. 2012.

HASAM-HENDERSON, L. A. et al. NMDA-receptor inhibition and oxidative stress during hippocampal maturation differentially alter parvalbumin expression and gamma-band activity. **Scientific Reports**, v. 8, n. 1, p. 1–15, 1 dez. 2018.

HAWES, M. T. et al. Increases in depression and anxiety symptoms in adolescents and young adults during the COVID-19 pandemic. **Psychological Medicine**, v. 52, n. 14, p. 1, 13 out. 2022.

HENSCH, T. K. Critical period plasticity in local cortical circuits. **Nature Reviews Neuroscience 2005 6:11**, v. 6, n. 11, p. 877–888, nov. 2005.

HERBET, M. et al. Chronic Variable Stress Is Responsible for Lipid and DNA Oxidative Disorders and Activation of Oxidative Stress Response Genes in the Brain of Rats. **Oxidative medicine and cellular longevity**, v. 2017, p. 1–10, 2017.

HOLLIS, F. et al. Mitochondrial function in the brain links anxiety with social subordination. **Proceedings of the National Academy of Sciences of the United States of America**, v. 112, n. 50, p. 15486–15491, 15 dez. 2015.

HUNTER, R. G. et al. Stress and corticosteroids regulate rat hippocampal mitochondrial DNA gene expression via the glucocorticoid receptor. **Proceedings of the National Academy of Sciences of the United States of America**, v. 113, n. 32, p. 9099–9104, 9 ago. 2016.

INAN, M. et al. Energy deficit in parvalbumin neurons leads to circuit dysfunction, impaired sensory gating and social disability. **Neurobiology of Disease**, v. 93, p. 35–46, 1 set. 2016.

JASTROCH, M. et al. Mitochondrial proton and electron leaks. **Essays in biochemistry**, v. 47, p. 53, 2010.

JEANNETEAU, F. et al. The Stress-Induced Transcription Factor NR4A1 Adjusts Mitochondrial Function and Synapse Number in Prefrontal Cortex. **The Journal of Neuroscience**, v. 38, n. 6, p. 1335, 2 fev. 2018.

JONES, C. E.; MONFILS, M. H. Dominance status predicts social fear transmission in laboratory rats. **Animal Cognition**, v. 19, n. 6, p. 1051, 1 nov. 2016.

JOU, S. H.; CHIU, N. Y.; LIU, C. S. Mitochondrial dysfunction in psychiatric disorders. **Schizophrenia Research**, v. 32, n. 4, p. 370–379, 27 set. 2022.

KADENBACH, B. Complex IV – The regulatory center of mitochondrial oxidative phosphorylation. **Mitochondrion**, v. 58, p. 296–302, 1 maio 2021.

KANELLOPOULOS, A. K. et al. Aralar Sequesters GABA into Hyperactive Mitochondria, Causing Social Behavior Deficits. **Cell**, v. 180, n. 6, p. 1178- 1197.e20, 19 mar. 2020.

KANN, O. et al. Gamma oscillations in the hippocampus require high complex I gene expression and strong functional performance of mitochondria. **Brain**, v. 134, n. 2, p. 345–358, 1 fev. 2011.

KANN, O.; PAPAGEORGIOU, I. E.; DRAGUHN, A. Highly energized inhibitory interneurons are a central element for information processing in cortical networks. **Journal of Cerebral Blood Flow and Metabolism**, v. 34, n. 8, p. 1270–1282, 4 jun. 2014.

KAUSAR, S.; WANG, F.; CUI, H. The role of mitochondria in reactive oxygen species generation and its implications for neurodegenerative diseases. **Cells**, v. 7, n. 12, p. 1–19, 1 dez. 2018.

KESSLER, R. C. et al. Age of onset of mental disorders: A review of recent literature. **Current Opinion in Psychiatry**, v. 20, n. 4, p. 359–364, jul. 2007.

KHADIMALLAH, I. et al. Mitochondrial, exosomal miR137-COX6A2 and gamma synchrony as biomarkers of parvalbumin interneurons, psychopathology, and neurocognition in schizophrenia. **Molecular Psychiatry**, v. 27, n. 2, p. 1192, 1 fev. 2022.

KLINGER, K. et al. Female rats are resistant to the long-lasting neurobehavioral changes induced by adolescent stress exposure. **European Neuropsychopharmacology**, v. 29, n. 10, p. 1127–1137, 2019.

KONRAD, K.; FIRK, C.; UHLHAAS, P. J. Brain Development During Adolescence Neuroscientific Insights Into This Developmental Period. **Medicine**, v. 110, n. 25, p. 425–431, 2013.

KULAK, A.; CUENOD, M.; DO, K. Q. Behavioral phenotyping of glutathione-deficient mice: Relevance to schizophrenia and bipolar disorder. **Behavioural Brain Research**, v. 226, n. 2, p. 563–570, 15 jan. 2012.

LAMBERT, A. J.; BRAND, M. D. Reactive oxygen species production by mitochondria. **Methods in molecular biology (Clifton, N.J.)**, v. 554, p. 165–181, 2009.

LAPIDUS, K. A. B. et al. In vivo 1H MRS study of potential associations between glutathione, oxidative stress and anhedonia in major depressive disorder. **Neuroscience letters**, v. 569, p. 74, 5 maio 2014.

LARRIEU, T. et al. Hierarchical Status Predicts Behavioral Vulnerability and Nucleus Accumbens Metabolic Profile Following Chronic Social Defeat Stress. **Current Biology**, v. 27, n. 14, p. 2202- 2210.e4, 24 jul. 2017.

LARSEN, B.; LUNA, B. Adolescence as a neurobiological critical period for the development of higher-order cognition. **Neuroscience & Biobehavioral Reviews**, v. 94, p. 179–195, 1 nov. 2018.

LEHNINGER, A. L. **Principles of Biochemistry** . 5. ed. [s.l.] Worth Publishers, 2008.

LENSJØ, K. K. et al. Differential Expression and Cell-Type Specificity of Perineuronal Nets in Hippocampus, Medial Entorhinal Cortex, and Visual Cortex Examined in the Rat and Mouse. **eNeuro**, v. 4, n. 3, p. 379–395, 2017.

LI, S. M. et al. Upregulation of CISD2 augments ROS homeostasis and contributes to tumorigenesis and poor prognosis of lung adenocarcinoma. **Scientific Reports 2017 7:1**, v. 7, n. 1, p. 1–13, 19 set. 2017.

LIN, M. S. CISD2 Attenuates Inflammation and Regulates Microglia Polarization in EOC Microglial Cells—As a Potential Therapeutic Target for Neurodegenerative Dementia. **Frontiers in Aging Neuroscience**, v. 12, p. 260, 26 ago. 2020.

LODGE, D. J.; GRACE, A A. Aberrant hippocampal regulation of dopamine neuron responsivity in an animal model of schizophrenia. **Schizophrenia bulletin**, v. 33, n. 2, p. 407, 2007.

LOVE, M. I.; HUBER, W.; ANDERS, S. Moderated estimation of fold change and dispersion for RNA-seq data with DESeq2. **Genome Biology**, v. 15, n. 12, p. 1–15, 5 dez. 2014.

LUNA, B. et al. An Integrative Model of the Maturation of Cognitive Control. **Annual review of neuroscience**, v. 38, p. 151, 7 jul. 2015.

LYNCH, K. M. et al. Hippocampal Shape Maturation in Childhood and Adolescence. **Cerebral Cortex (New York, NY)**, v. 29, n. 9, p. 3651, 1 set. 2019.

MADRIGAL, J. L. M. et al. Glutathione Depletion, Lipid Peroxidation and Mitochondrial Dysfunction Are Induced by Chronic Stress in Rat Brain. **Neuropsychopharmacology 2000 24:4**, v. 24, n. 4, p. 420–429, 2001.

MALCON, L. M. C. et al. Maternal separation induces long-term oxidative stress alterations and increases anxiety-like behavior of male Balb/cJ mice. **Experimental Brain Research**, v. 238, n. 9, p. 2097–2107, 1 set. 2020.

MANNELLA, C. A. Structure and dynamics of the mitochondrial inner membrane cristae. **Biochimica et Biophysica Acta (BBA) - Molecular Cell Research**, v. 1763, n. 5–6, p. 542–548, 1 maio 2006.

MAURITZ, M. W. et al. Prevalence of interpersonal trauma exposure and trauma-related disorders in severe mental illness. **European Journal of Psychotraumatology**, v. 4, p. 1–15, 2013.

MCEWEN, B. S. Protection and Damage from Acute and Chronic Stress: Allostasis and Allostatic Overload and Relevance to the Pathophysiology of Psychiatric Disorders. **Annals of the New York Academy of Sciences**, v. 1032, n. 1, p. 1–7, 1 dez. 2004.

MHILLAJ, E.; MORGESE, M.; TRABACE, L. Early Life and Oxidative Stress in Psychiatric Disorders: What Can we Learn From Animal Models? **Current Pharmaceutical Design**, v. 21, n. 11, p. 1396–1403, 9 jan. 2015.

MICHAELIS, E. K. Molecular biology of glutamate receptors in the central nervous system and their role in excitotoxicity, oxidative stress and aging. **Progress in Neurobiology**, v. 54, n. 4, p. 369–415, 2 mar. 1998.

MILLS, K. L. et al. Structural brain development between childhood and adulthood: Convergence across four longitudinal samples. **NeuroImage**, v. 141, p. 273–281, 1 nov. 2016.

MILNER, L. C.; CRABBE, J. C. Three murine anxiety models: results from multiple inbred strain comparisons. **Genes, Brain and Behavior**, v. 7, n. 4, p. 496–505, 1 jun. 2008.

MODINOS, G. et al. Translating the MAM model of psychosis to humans. **Trends in Neurosciences**, v. 38, n. 3, p. 129–138, 1 mar. 2015.

MÖLLER, M. et al. Isolation rearing-induced deficits in sensorimotor gating and social interaction in rats are related to cortico-striatal oxidative stress, and reversed by sub-chronic clozapine administration. **European neuropsychopharmacology : the journal of the European College of Neuropsychopharmacology**, v. 21, n. 6, p. 471–483, jun. 2011.

MORATÓ, L. et al. eNAMPT actions through nucleus accumbens NAD+/SIRT1 link increased adiposity with sociability deficits programmed by peripuberty stress. **Science Advances**, v. 8, n. 9, p. 9109, 1 mar. 2022.

MOY, S. S. et al. Sociability and preference for social novelty in five inbred strains: an approach to assess autistic-like behavior in mice. **Genes, Brain and Behavior**, v. 3, n. 5, p. 287–302, 1 out. 2004.

MURRAY, A. J. et al. Parvalbumin-positive interneurons of the prefrontal cortex support working memory and cognitive flexibility. **Scientific Reports**, v. 5, n. November, p. 1–14, 2015.

MURRAY, A. J. et al. Oxidative Stress and the Pathophysiology and Symptom Profile of Schizophrenia Spectrum Disorders. **Frontiers in Psychiatry**, v. 12, p. 1235, 22 jul. 2021.

NIATSETSKAYA, Z. V. et al. The oxygen free radicals originating from mitochondrial complex I contribute to oxidative brain injury following hypoxia-ischemia in neonatal mice. **The Journal of neuroscience : the official journal of the Society for Neuroscience**, v. 32, n. 9, p. 3235–3244, 29 fev. 2012.

NISHIYAMA, A. et al. Identification of thioredoxin-binding protein-2/vitamin D(3) up-regulated protein 1 as a negative regulator of thioredoxin function and expression. **The Journal of biological chemistry**, v. 274, n. 31, p. 21645–21650, 30 jul. 1999.

NOLFI-DONEGAN, D.; BRAGANZA, A.; SHIVA, S. Mitochondrial electron transport chain: Oxidative phosphorylation, oxidant production, and methods of measurement. **Redox Biology**, v. 37, p. 101674, 1 out. 2020.

NUCIFORA, L. G. et al. Reduction of plasma glutathione in psychosis associated with schizophrenia and bipolar disorder in translational psychiatry. **Translational Psychiatry**, v. 7, n. 8, p. e1215, 2017.

OBERACKER, T. et al. Enhanced expression of thioredoxin-interacting-protein regulates oxidative DNA damage and aging. **Febs Letters**, v. 592, n. 13, p. 2297, 1 jul. 2018.

O'MARA, S. The subiculum: what it does, what it might do, and what neuroanatomy has yet to tell us. **Journal of Anatomy**, v. 207, n. 3, p. 271–282, 1 set. 2005.

OSKVIG, D. B. et al. Maternal immune activation by LPS selectively alters specific gene expression profiles of interneuron migration and oxidative stress in the fetus without triggering a fetal immune response. **Brain, behavior, and immunity**, v. 26, n. 4, p. 623–634, maio 2012.

ØSTBY, Y. et al. Heterogeneity in Subcortical Brain Development: A Structural Magnetic Resonance Imaging Study of Brain Maturation from 8 to 30 Years. **Journal of Neuroscience**, v. 29, n. 38, p. 11772–11782, 23 set. 2009.

PALANIYAPPAN, L. et al. Is There a Glutathione Centered Redox Dysregulation Subtype of Schizophrenia? **Antioxidants (Basel, Switzerland)**, v. 10, n. 11, p. 1–19, 1 nov. 2021.

PELKEY, K. A. et al. Hippocampal GABAergic Inhibitory Interneurons. **Physiological Reviews**, v. 97, n. 4, p. 1619, 10 out. 2017.

PERKINS, D. O. et al. Towards a Psychosis Risk Blood Diagnostic for Persons Experiencing High-Risk Symptoms: Preliminary Results From the NAPLS Project. **Schizophrenia Bulletin**, v. 41, n. 2, p. 419, 1 mar. 2015.

PERKINS, D. O.; JEFFRIES, C. D.; DO, K. Q. Potential Roles of Redox Dysregulation in the Development of Schizophrenia. **Biological Psychiatry**, v. 88, n. 4, p. 326–336, 15 ago. 2020.

PFANNER, N.; WARSCHEID, B.; WIEDEMANN, N. Mitochondrial proteins: from biogenesis to functional networks. **Nature Reviews Molecular Cell Biology 2018 20:5**, v. 20, n. 5, p. 267–284, 9 jan. 2019.

PICARD, M. et al. An energetic view of stress: Focus on mitochondria. **Frontiers in Neuroendocrinology**, v. 49, p. 72–85, 1 abr. 2018.

PICARD, M.; JUSTER, R. P.; MCEWEN, B. S. Mitochondrial allostatic load puts the "gluc" back in glucocorticoids. **Nature Reviews Endocrinology 2014 10:5**, v. 10, n. 5, p. 303–310, 25 mar. 2014.

PICARD, M.; SHIRIHAI, O. S. Mitochondrial signal transduction. **Cell Metabolism**, v. 34, n. 11, p. 1620–1653, 1 nov. 2022.

PUERTAS-FRÍAS, G. et al. Mitochondrial movement in Aralar/Slc25a12/AGC1 deficient cortical neurons. **Neurochemistry international**, v. 131, p. 1–15, 1 dez. 2019.

RAJASEKARAN, N. S. et al. Human αB-Crystallin Mutation Causes Oxido-Reductive Stress and Protein Aggregation Cardiomyopathy in Mice. **Cell**, v. 130, n. 3, p. 427–439, 10 ago. 2007.

REICHELT, A. C. et al. Perineuronal Nets: Plasticity, Protection, and Therapeutic Potential. **Trends in Neurosciences**, v. 42, n. 7, p. 458–470, 1 jul. 2019.

ROBERTS, R. C. Mitochondrial dysfunction in schizophrenia: with a focus on postmortem studies. **Mitochondrion**, v. 56, p. 91, 1 jan. 2021.

ROMEO, R. D. The Teenage Brain: The Stress Response and the Adolescent Brain. **Current Directions in Psychological Science**, v. 22, n. 2, p. 140–145, 2013.

ROSENKRANZ, J. A.; GRACE, A. A. Cellular Mechanisms of Infralimbic and Prelimbic Prefrontal Cortical Inhibition and Dopaminergic Modulation of Basolateral Amygdala Neurons In Vivo. **The Journal of Neuroscience**, v. 22, n. 1, p. 324–337, 2002.

RUDEN, J. B.; DUGAN, L. L.; KONRADI, C. Parvalbumin interneuron vulnerability and brain disorders. **Neuropsychopharmacology 2020 46:2**, v. 46, n. 2, p. 279–287, 28 jul. 2020.

SACHSER, N.; HENNESSY, M. B.; KAISER, S. The adaptive shaping of social behavioural phenotypes during adolescence. **Biology Letters**, v. 14, n. 11, p. 1–7, 30 nov. 2018.

ŞAHIN, E.; GÜMÜŞLÜ, S. Alterations in brain antioxidant status, protein oxidation and lipid peroxidation in response to different stress models. **Behavioural Brain Research**, v. 155, n. 2, p. 241–248, 6 dez. 2004.

SALIM, S. Oxidative Stress and the Central Nervous System. **The Journal of Pharmacology and Experimental Therapeutics**, v. 360, n. 1, p. 201, 1 jan. 2017.

SAMARGHANDIAN, S. et al. Protective effects of carnosol against oxidative stress induced brain damage by chronic stress in rats. **BMC Complementary and Alternative Medicine**, v. 17, n. 1, p. 1–7, 4 maio 2017.

SANZ-MORELLO, B. et al. Complex IV subunit isoform COX6A2 protects fast-spiking interneurons from oxidative stress and supports their function. **The EMBO Journal**, v. 39, n. 18, 9 set. 2020.

SCHENKEL, L. C.; BAKOVIC, M. Formation and Regulation of Mitochondrial Membranes. **International Journal of Cell Biology**, v. 2014, p. 1–13, 2014.

SCHIAVONE, S. et al. Involvement of NOX2 in the development of behavioral and pathologic alterations in isolated rats. **Biological psychiatry**, v. 66, n. 4, p. 384–392, 15 ago. 2009.

SCHIAVONE, S. et al. Severe Life Stress and Oxidative Stress in the Brain: From Animal Models to Human Pathology. **Antioxidants & Redox Signaling**, v. 18, n. 12, p. 1475, 4 abr. 2013.

SCHOBEL, S. A. et al. Imaging Patients with Psychosis and a Mouse Model Establishes a Spreading Pattern of Hippocampal Dysfunction and Implicates Glutamate as a Driver. **Neuron**, v. 78, n. 1, p. 81–93, 10 abr. 2013.

SCHRIBER, R. A.; GUYER, A. E. Adolescent neurobiological susceptibility to social context. **Developmental Cognitive Neuroscience**, v. 19, p. 1, 1 jun. 2016.

SEO, J. S. et al. NADPH Oxidase Mediates Depressive Behavior Induced by Chronic Stress in Mice. **The Journal of Neuroscience**, v. 32, n. 28, p. 9690, 7 jul. 2012.

SHEN, Z. Q. et al. CISD2 maintains cellular homeostasis. **Biochimica et Biophysica Acta (BBA) - Molecular Cell Research**, v. 1868, n. 4, p. 118954, 1 abr. 2021.

SHERMAN, B. T. et al. DAVID: a web server for functional enrichment analysis and functional annotation of gene lists (2021 update). **Nucleic Acids Research**, v. 50, n. W1, p. W216, 7 jul. 2022.

SHONKOFF, J. P. et al. The Lifelong Effects of Early Childhood Adversity and Toxic Stress. **Pediatrics**, v. 129, n. 1, p. e232–e246, 1 jan. 2012.

SIENA, A. et al. Neonatal Rotenone Administration Induces Psychiatric Disorder-Like Behavior and Changes in Mitochondrial Biogenesis and Synaptic Proteins in Adulthood. **Molecular Neurobiology 2021 58:7**, v. 58, n. 7, p. 3015–3030, 19 fev. 2021.

SISK, C. L.; FOSTER, D. L. The neural basis of puberty and adolescence. **Nature neuroscience**, v. 7, n. 10, p. 1040–1047, out. 2004.

SOARES, A. R. et al. Region-specific effects of maternal separation on oxidative stress accumulation in parvalbumin neurons of male and female rats. **Behavioural Brain Research**, v. 388, p. 112658, 18 jun. 2020.

SOLANKI, N. et al. Modulating Oxidative Stress Relieves Stress-Induced Behavioral and Cognitive Impairments in Rats. **International Journal of Neuropsychopharmacology**, v. 20, n. 7, p. 550, 1 jul. 2017.

SOLMI, M. et al. Age at onset of mental disorders worldwide: large-scale meta-analysis of 192 epidemiological studies. **Molecular Psychiatry 2021 27:1**, v. 27, n. 1, p. 281–295, 2 jun. 2021.

SONNENSCHEIN, S. F.; GOMES, F. V.; GRACE, A. A. Dysregulation of Midbrain Dopamine System and the Pathophysiology of Schizophrenia. **Frontiers in Psychiatry**, v. 11, 30 jun. 2020.

SPEAR, L. P. Neurobehavioral changes in adolescence. **Current Directions in Psychological Science**, v. 9, n. 4, p. 111–114, 2000.

STANIKA, R. I. et al. Coupling diverse routes of calcium entry to mitochondrial dysfunction and glutamate excitotoxicity. **Proceedings of the National Academy of Sciences of the United States of America**, v. 106, n. 24, p. 9854–9859, 16 jun. 2009.

STEULLET, P. et al. Redox Dysregulation Affects the Ventral But Not Dorsal Hippocampus: Impairment of Parvalbumin Neurons, Gamma Oscillations, and Related Behaviors. **The Journal of Neuroscience**, v. 30, n. 7, p. 2547, 2 fev. 2010.

STEULLET, P. et al. Oxidative stress-driven parvalbumin interneuron impairment as a common mechanism in models of schizophrenia. **Molecular Psychiatry 2017 22:7**, v. 22, n. 7, p. 936–943, 21 mar. 2017.

STEVENS, H. E. et al. Prenatal stress delays inhibitory neuron progenitor migration in the developing neocortex. **Psychoneuroendocrinology**, v. 38, n. 4, p. 509–521, 1 abr. 2013.

STOJKOVIĆ, T. et al. Risperidone reverses phencyclidine induced decrease in glutathione levels and alterations of antioxidant defense in rat brain. **Progress in**

Neuro-Psychopharmacology and Biological Psychiatry, v. 39, n. 1, p. 192–199, 1 out. 2012.

STONE, J. M. et al. Altered relationship between hippocampal glutamate levels and striatal dopamine function in subjects at ultra high risk of psychosis. **Biological Psychiatry**, v. 68, n. 7, p. 599–602, 1 out. 2010.

TSUBAKI, H.; TOOYAMA, I.; WALKER, D. G. Thioredoxin-Interacting Protein (TXNIP) with Focus on Brain and Neurodegenerative Diseases. **International Journal of Molecular Sciences 2020, Vol. 21, Page 9357**, v. 21, n. 24, p. 9357, 8 dez. 2020.

TZANOULINOU, S. et al. Long-Term Behavioral Programming Induced by Peripuberty Stress in Rats Is Accompanied by GABAergic-Related Alterations in the Amygdala. **PLOS ONE**, v. 9, n. 4, p. e94666, 15 abr. 2014a.

TZANOULINOU, S. et al. Peripubertal stress-induced behavioral changes are associated with altered expression of genes involved in excitation and inhibition in the amygdala. **Translational Psychiatry 2014 4:7**, v. 4, n. 7, p. e410–e410, 8 jul. 2014b.

TZANOULINOU, S. et al. Neuroligin-2 Expression in the Prefrontal Cortex is Involved in Attention Deficits Induced by Peripubertal Stress. **Neuropsychopharmacology**, v. 41, n. 3, p. 751, 1 fev. 2016.

ÜLGEN, D. H.; RUIGROK, S. R.; SANDI, C. Powering the social brain: Mitochondria in social behaviour. **Current Opinion in Neurobiology**, v. 79, p. 102675, 1 abr. 2023.

VAN DER GOOT, M. H. et al. Inter-individual variability in habituation of anxiety-related responses within three mouse inbred strains. **Physiology & Behavior**, v. 239, p. 113503, 1 out. 2021.

VÁZQUEZ, D. M.; AKIL, H. Pituitary-Adrenal Response to Ether Vapor in the Weanling Animal: Characterization of the Inhibitory Effect of Glucocorticoids on Adrenocorticotropin Secretion. **Pediatric Research 1993 34:5**, v. 34, n. 5, p. 646–653, 1993.

VOTYAKOVA, T. V.; REYNOLDS, I. J. ΔΨm-Dependent and -independent production of reactive oxygen species by rat brain mitochondria. **Journal of Neurochemistry**, v. 79, n. 2, p. 266–277, 15 out. 2001.

WALF, A. A.; FRYE, C. A. The use of the elevated plus maze as an assay of anxiety-related behavior in rodents. **Nature Protocols 2007 2:2**, v. 2, n. 2, p. 322–328, 1 mar. 2007.

WALKER, E. F. et al. Cortisol levels and risk for psychosis: Initial findings from the North American Prodrome Longitudinal Study. **Biological Psychiatry**, v. 74, n. 6, p. 410–417, 15 set. 2013.

WANG, A. M. et al. Assessing Brain Metabolism With 7-T Proton Magnetic Resonance Spectroscopy in Patients With First-Episode Psychosis. **JAMA psychiatry**, v. 76, n. 3, p. 314–323, 1 mar. 2019.

WANG, C. Z. et al. Postnatal Phencyclidine Administration Selectively Reduces Adult Cortical Parvalbumin-Containing Interneurons. **Neuropsychopharmacology 2008 33:10**, v. 33, n. 10, p. 2442–2455, 5 dez. 2007.

WEGER, M. et al. Mitochondrial gene signature in the prefrontal cortex for differential susceptibility to chronic stress. **Scientific Reports 2020 10:1**, v. 10, n. 1, p. 1–15, 27 out. 2020.

WILSON, C.; MUÑOZ-PALMA, E.; GONZÁLEZ-BILLAULT, C. From birth to death: A role for reactive oxygen species in neuronal development. **Seminars in Cell & Developmental Biology**, v. 80, p. 43–49, 1 ago. 2018.

XIN, L. et al. Genetic Polymorphism Associated Prefrontal Glutathione and Its Coupling With Brain Glutamate and Peripheral Redox Status in Early Psychosis. **Schizophrenia Bulletin**, v. 42, n. 5, p. 1185, 1 set. 2016.

YANG, H. Y.; LEE, T. H. Antioxidant enzymes as redox-based biomarkers: a brief review. **BMB reports**, v. 48, n. 4, p. 200–208, 2015.

YANG, S. et al. Overexpression of COX6B1 protects against I/R-induced neuronal injury in rat hippocampal neurons. **Molecular Medicine Reports**, v. 19, n. 6, p. 4852, 1 jun. 2019.

YARDENI, T. et al. An mtDNA mutant mouse demonstrates that mitochondrial deficiency can result in autism endophenotypes. **Proceedings of the National**

Academy of Sciences of the United States of America, v. 118, n. 6, p. e2021429118, 9 fev. 2021.

ZAFIR, A.; BANU, N. Modulation of in vivo oxidative status by exogenous corticosterone and restraint stress in rats. **Stress**, v. 12, n. 2, p. 167–177, mar. 2009.

ZALACHORAS, I. et al. Therapeutic potential of glutathione-enhancers in stress-related psychopathologies. **Neuroscience & Biobehavioral Reviews**, v. 114, p. 134–155, 1 jul. 2020.

ZALACHORAS, I. et al. Glutathione in the nucleus accumbens regulates motivation to exert reward-incentivized effort. **eLife**, v. 11, p. 77791, 2022.

ZHANG, H. et al. Reactive Oxygen Species-mediated Loss of Phenotype of Parvalbumin Interneurons Contributes to Long-term Cognitive Impairments After Repeated Neonatal Ketamine Exposures. **Neurotoxicity Research**, v. 30, n. 4, p. 593–605, 1 nov. 2016.

ZHANG, M. et al. A meta-analysis of oxidative stress markers in schizophrenia. **Science China Life Sciences**, v. 53, n. 1, p. 112–124, 12 fev. 2010.

ZHAO, J. et al. Abnormalities in Prefrontal Cortical Gene Expression Profiles Relevant to Schizophrenia in MK-801-Exposed C57BL/6 Mice. **Neuroscience**, v. 390, p. 60–78, 15 out. 2018.

10. ATTACHMENT

UNIVERSIDADE DE SÃO PAULO
FACULDADE DE MEDICINA DE RIBEIRÃO PRETO
COMISSÃO DE ÉTICA NO USO DE ANIMAIS

FMRP
65 anos USP

A U T O R I Z A Ç Ã O

A CEUA-FMRP autoriza a execução do projeto intitulado: *"Estudo do estresse na adolescência como fator de risco para esquizofrenia: envolvimento da desregulação da metaloproteinase de matriz 9"*, registrado com o número de protocolo **248/2019**, sob a responsabilidade do **Prof. Dr. Felipe Villela Gomes**, envolvendo a produção, manutenção ou utilização de animais pertencentes ao *filo Chordata, subfilo Vertebrata* (exceto humanos) para fins de pesquisa científica (ou ensino), encontra-se de acordo com os preceitos da Lei nº 11.794 de 8 de outubro de 2008, do Decreto nº 6.899 de 15 de julho de 2009 e com as normas editadas pelo Conselho Nacional de Controle de Experimentação Animal (CONCEA). O Protocolo foi **APROVADO** pela Comissão de Ética no Uso de Animais da Faculdade de Medicina de Ribeirão Preto da Universidade de São Paulo, em reunião de 27 de janeiro de 2020.
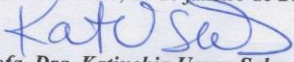
Colaboradores: Thamyris Santos Silva
Prof. Dr. Francisco Silveira Guimarães

Lembramos da obrigatoriedade de apresentação do Relatório Final, em modelo da CEUA, para emissão do Certificado, como disposto nas Resoluções Normativas do CONCEA.

Finalidade				() Ensino (X) Pesquisa Científica	
Vigência da autorização				27/01/2020 a 01/03/2024	
Espécie/Linhagem	Nº de Animais	Peso/Idade	Sexo	Origem	
	14	300g / 60 dias	Macho	Serviço de Biotério	
	28	250g / 60 dias	Fêmea		
	12	60g / 21 dias	Macho	Biotério de Manutenção e Experimentação do Departamento de Fisiologia	
	662	100g / 31 dias	Macho		
Rato / Sprague Dawley	12	150g / 41 dias	Macho		
	12	225g / 51 dias	Macho		
	36	275g / 65 dias	Macho		
	12	330g / 75 dias	Macho		
	12	360g / 85 dias	Macho		
	12	400g / 110 dias	Macho		

Ribeirão Preto, 27 de janeiro de 2020

Profa. Dra. Katiuchia Uzzun Sales
Coordenadora da CEUA–FMRP–USP

UNIVERSIDADE DE SÃO PAULO
FACULDADE DE MEDICINA DE RIBEIRÃO PRETO
COMISSÃO DE ÉTICA NO USO DE ANIMAIS

FMRP
65 anos USP

CEUA
FMRP-USP
Comissão de Ética no Uso de Animais
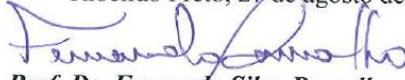Replacement|Reduction|Refinement

CERTIFICADO

Certificamos que o Protocolo intitulado *"O impacto do estresse sobre o sistema dopaminérgico é determinado pelo período crítico de plasticidade - implicações para a depressão e a esquizofrenia"*, registrado com o número **155/2018**, sob a responsabilidade do **Prof. Dr. Felipe Villela Gomes,** envolvendo a produção, manutenção ou utilização de animais pertencentes ao *filo Chordata, subfilo Vertebrata* (exceto humanos) para fins de pesquisa científica, encontra-se de acordo com os preceitos da Lei nº 11.794 de 8 de outubro de 2008, do Decreto nº 6.899 de 15 de julho de 2009 e com as normas editadas pelo Conselho Nacional de Controle de Experimentação Animal (CONCEA), e foi **APROVADO** pela Comissão de Ética no Uso de Animais da Faculdade de Medicina de Ribeirão Preto da Universidade de São Paulo em reunião de 27 de agosto de 2018.

Este Protocolo prevê a utilização de 457 ratos Sprague Dawley machos pesando 60g e 964 ratos Sprague Dawley machos pesando 280g oriundos do Serviço de Biotério da Prefeitura do *Campus* de Ribeirão Preto da Universidade de São Paulo. Vigência da autorização: 27/08/2018 a 28/04/2024.

We certify that the Protocol *nº* **155/2018**, entitled *"The impact of stress on the dopamine system depends on the state of the critical period of neuroplasticity - implications for depression and schizophrenia"*, is in accordance with the Ethical Principles in Animal Research adopted by the National Council for Control of Animal Experimentation (CONCEA) and was approved by the Local Animal Ethical Committee from Ribeirão Preto Medical School of the University of São Paulo in *08/27/2018*. This protocol involves the production, maintenance or use of animals from *phylumChordata, subphylumVertebrata* (except humans) for research purposes, and includes the use of 457 male Sprague Dawley rats weighing 60g and 964 male Sprague Dawley rats weighing 280g from the Central Animal House of Ribeirão Preto Medical School, University of São Paulo. This certificate is valid until 04/28/2024.

Ribeirão Preto, 27 de agosto de 2018

Prof. Dr. Fernando Silva Ramalho
Coordenador da CEUA–FMRP – USP